

UNIVERSITÀ
DEGLI STUDI
DI PADOVA



**DIPARTIMENTO DI INGEGNERIA INDUSTRIALE
CORSO DI LAUREA MAGISTRALE IN
INGEGNERIA DELL'ENERGIA ELETTRICA**

**TESI DI LAUREA MAGISTRALE IN
INGEGNERIA DELL'ENERGIA ELETTRICA**

MODELLING OF “EXTENDED-DELTA” TRANSFORMERS FOR POWER CONVERTERS

RELATORE: Prof. Roberto Turri, DII

CORRELATORE: Ing. Ivone Benfatto, ITER Organization

LAUREANDO: Francesco Campostrini

ANNO ACCADEMICO 2015-16

Disclaimer: The views and opinions expressed herein do not necessarily reflect those of the ITER Organization.

The ITER Organization is an intergovernmental organization among: the People's Republic of China, the European Atomic Energy Community (Euratom), the Republic of India, Japan, the Republic of Korea, the Russian Federation, and the United States of America.

The ITER Project (www.iter.org) is under construction in St Paul Lez Durance, France.

Index

I.	Sommario.....	1
II.	Abstract.....	2
1.	Introduction.....	3
2.	Extended-delta Winding Connection.....	6
2.1	Calculation of the voltage magnitude	8
2.1.1	Number of turns and partial voltages with 15° shift ($\delta=\pm 15^\circ$).....	8
2.2	From grid voltage V to phasors B.....	10
2.2.1	Negative values of phase-shift	11
3.	Simscape Power Systems™ overview	13
3.1	Simscape Power Systems™ Specialized Technology	14
3.1.1	Transformers block	14
3.1.2	Three-Phase Transformer block.....	15
3.2	Simscape Components & Foundation Library.....	17
3.2.1	Phase splitter block	17
3.2.2	Electromagnetic Converter Block.....	17
3.2.3	Controlled magnetomotive source	18
3.3	Block Mask Editor	19
4.	Extended-delta/delta SPS Specialized Technology model	21
4.1	ITER Coil Correction Side converter-transformer datasheet.....	22
4.2	Structure of the model.....	25
4.2.1	Edited mask and parameters of the extended-delta/delta subsystem	25
4.2.2	B former transformer subsystem.....	27
4.2.3	Delta/delta Three-Phase Transformer	31
4.2.4	Extended-delta/delta subsystem.....	33
4.3	Real extended-delta/delta transformer's model	35
4.3.1	Model in per units	35
4.3.2	Needed parameters' script.....	36
4.3.3	Model of core saturation	40
5.	Model's first validation: comparison with actual datasheets	44
5.1	Verification circuit	45
5.2	Phase shift measurement.....	47
5.3	No load simulation.....	48

5.4	Short circuit simulation	49
5.5	On load simulation	51
5.6	Results comparison in brief.....	54
6.	Model's second validation: a different approach	55
6.1	SPS Simscape Components model.....	56
6.1.1	Turns of electromagnetic converter blocks	58
6.1.2	Electrical Circuit.....	59
6.1.3	Magnetic circuit.....	59
6.1.4	Subsystem mask	61
6.2	Validation of two models	64
6.2.1	SPS Simscape Components verification circuit	64
6.2.2	Phase-shift and no-load verifications	65
6.2.3	Short Circuit verification.....	66
6.2.4	On load verification.....	66
6.2.5	In-rush current comparison.....	69
6.3	Specific verifications for ITER	72
6.3.1	Zero-sequence verification	72
6.3.2	DC fault among two phases.....	75
6.3.3	Phase-to-phase fault verification	83
7.	Conclusions	87
	Acknowledgments	89
	References	90
	Figures.....	92

I. Sommario

La presente tesi riguarda la realizzazione di un modello originale per la simulazione al calcolatore del comportamento elettrico di trasformatori con avvolgimenti a delta esteso.

Questo genere di trasformatore, non molto diffuso e di cui è disponibile scarsa letteratura, è usato principalmente per alimentare convertitori statici di potenza multi-impulso, in una configurazione che prevede il parallelo di più trasformatori di questo tipo. Infatti, in questa configurazione lo sfasamento desiderato tra le tensioni che alimentano il convertitore, permette di non immettere in rete determinate armoniche di corrente prodotte dai convertitori. Inoltre, vengono mantenuti i vantaggi usuali della connessione a triangolo.

Tale tipologia di trasformatori, tuttavia, non è ancora presente come elemento della libreria “*Specialized Technology*” di *Simscape Power Systems*TM (*MatLab/Simulink*®), software largamente utilizzato nella simulazione di circuiti elettrici complessi. Questa tesi intende primariamente contribuire a sopperire a tale mancanza.

L’analisi dei fasori effettuata sugli avvolgimenti a delta esteso ha permesso di individuare la relazione tra la tensione di rete e quella che cade sugli avvolgimenti di una colonna, in fase con il flusso magnetico nella stessa. Questa relazione è stata utilizzata per la modellazione del trasformatore a delta esteso in un “blocco” di *Simscape Power Systems*TM – *Specialized Technology*, effettuata mediante l’assemblaggio opportuno di blocchi già esistenti nella stessa libreria.

Il nuovo blocco sviluppato tiene conto anche della caratteristica di magnetizzazione del nucleo ed è in grado di simulare il comportamento elettrico del trasformatore in uno spettro assai esteso di condizioni operative. La sua funzionalità è stata infatti verificata con carichi diversi, paragonando i risultati ottenuti dalle simulazioni con quelli dei test di un trasformatore di questo tipo utilizzato per il progetto ITER sulla fusione nucleare.

Al fine di validare ulteriormente il modello proposto e verificarne la robustezza, è stato realizzato un altro modello che include il circuito magnetico dello stesso trasformatore, utilizzando gli elementi della libreria “*Simscape Components*” dello stesso software *Simscape Power Systems*TM.

I risultati ottenuti dalle numerose prove di simulazione qui presentate comprovano la validità e la robustezza del modello realizzato, che potrebbe essere valido anche per altri tipi di trasformatore.

Il ragionamento adottato è generale e pertanto applicabile anche ad altri software di calcolo.

II. Abstract

The present thesis addresses the realisation of an original model for the computer simulation of a transformer with windings in an extended-delta configuration.

This kind of transformer, not widely diffused and with scarce literature available, is mainly used to supply multi-pulse power static converters, in a configuration that foresees a parallel of these transformers. In fact, in this configuration, the required phase displacement between the voltages feeding the converter allows for not-injecting into the grid some specific harmonic components produced by the converters. In addition, the usual advantages of delta configurations are maintained.

However, this kind of transformers is not present yet as element of the library “*Specialized Technology*” of *Simscape Power Systems*TM (MatLab/Simulink®), a software broadly used in complex electrical circuit simulations. The main aim of this thesis is to contribute to fill this gap.

A phasor analysis, performed on extended-delta windings, allowed to describe the relationship between the grid voltage and the voltage applied in a transformer’s column winding, in phase with the magnetic flux in the same column. This relationship has been used to model the delta-extended transformer as a “block” of *Simscape Power Systems*TM – *Specialized Technology*, by means of a proper assembling of already existing blocks of the same library.

The newly developed block considers also the actual magnetic characteristic of the core and is able to simulate the electrical behaviour of the transformer in a broad range of operative conditions. In fact, its functionality has been verified using several working loads, comparing the simulations’ results with the tests data of a transformer of this kind used in the ITER project on nuclear fusion.

In order to provide a further validation of the proposed model and to verify its robustness, another model which includes the magnetic circuit of the transformer has been realized, using the elements of the library “*Simscape Components*” of the same software *Simscape Power Systems*TM.

The results obtained in the numerous simulations performed and here presented, proof the validity and the robustness of the proposed model, that can be valid also for other types of transformer.

The proposed approach is general and therefore applicable in other simulation software, too.

1. Introduction

This thesis has been realized with the collaboration of the Electric Power Systems group of the Industrial Engineering Department, University of Padua, and the Electrical Engineering Division of ITER Organization.

ITER (International Thermonuclear Experimental Reactor) is presently under assembling in Cadarache (FR), by a Consortium of several States, which includes the EU. It will be the world’s largest tokamak and it is one of the most ambitious energy projects in the world today. ITER will be the first fusion device to produce net energy and to maintain fusion reactions for long periods of time. ITER will test also the integrated technologies, materials and physics regimes necessary for the commercial production of fusion-based electricity [1].

The ITER Coil Power Supply and Distribution System (CPSDS) will be installed to receive power from the French 400 kV transmission grid and to provide controlled DC power to the superconducting tokamak magnets for plasma operation. The Coil Power Supply System (CPSS) consists of AC/DC converter units connected in series with Switching Network Units (SNU) and Fast Discharge Units (FDU) to provide the controlled DC for plasma initiation, current, shape and position control, error field correction, as well as superconductive magnet quench protection. The installed power of the ITER CPSS is nearly 2 GVA. [2]

Each AC/DC converter of CPSS is supplied by a converter transformer [3]. In order to use high power converters and maintain at the same time a high power quality, it is necessary to reduce the harmonic disturbance injected in the grid. For this reason, the AC/DC converters used in ITER are 12-pulse bridge and the only harmonic currents injected are of the h-order, where:

$$h = 12 \cdot k \pm 1 \quad k = 1, 2, 3, \dots$$

A 12-pulse power converter is realized placing in parallel two 6-pulse converters and supplying them with two voltage triplets shifted by 30° [4]. A conventional way for producing this configuration, shown in the Figure 1.1, is to provide a transformer with two secondary windings [5], one in delta-connection and the other in wye-connection: in this way, the two secondary voltage triplets are shifted 30° respectively.

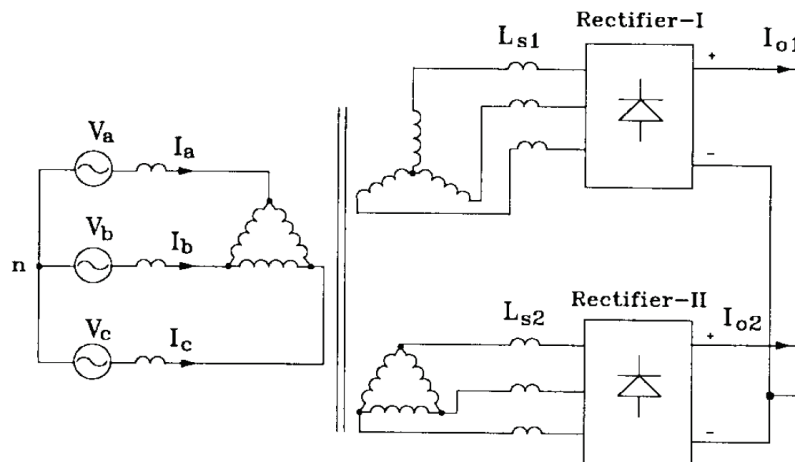


Figure 1.1: Conventional 12-pulse system

However, in a conventional 12-pulse the two secondary Δ -Y has unequal leakage reactances due to the different number of turns. Therefore, the two converters see the grid with different short circuit power and thus they can be differently loaded [5]. In order to overcome this issue, the ITER Electrical Engineering Division decided to supply the 12-pulse bridges by transformers with an extended-delta winding connection at the primary and a delta winding connection at the secondary (ED-d). These specific transformers realize, as it will be exposed later, a phase shifting of $\pm 15^\circ$ to the secondary voltage triplets, realising the desired 30° shift.

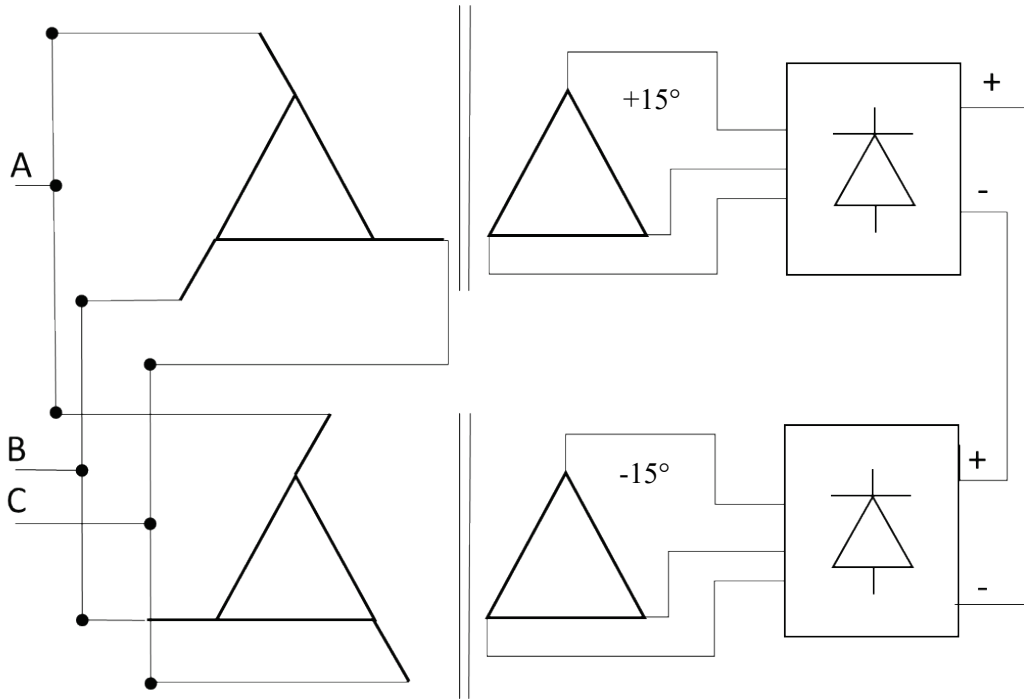


Figure 1.2: Scheme of a 12-pulse converter with ED-d transformer

In order to perform circuit calculations, the ITER Electrical Engineering Division team is extensively using the tool *Simscape Power Systems™ - Specialized Technology* (SPS ST), which is a toolbox of the Matlab/Simulink® software. This software has a good library of basic electrical components. Nevertheless, it does not include yet the extended-delta transformer used in the ITER CPSS.

Therefore, the main aim of this thesis is to realise a model of a transformer with an extended-delta winding connection, to be integrated in the SPS ST toolbox.

The actual ITER transformer, considered a reference for model validation, has a 3 column iron core, a primary winding with extended-delta connection and secondary winding delta connected. The model should take into consideration the actual magnetic characteristic of the core and the non-linearity related to saturation. The model proposed in this thesis has been built to be used as a SPS ST block, also in order to integrate the thesis work done by Marco Olivier at ITER [6].

In fact, the ITER Electrical Engineering Division needs to study the electrical behaviour of the CPSDS, including possible fault conditions, by means of extensive circuit simulations. Some fault conditions might produce a direct current component on the secondary winding of the transformer, which will induce a saturation of the transformer magnetic core.

In order to validate the functionality of proposed SPS ST model under these conditions, another model has been built, using *Simscape Power Systems*TM - *Simscape Components* (SPS SC) tool, which allow a proper modelling of the magnetic circuit of the transformer. Beside the validation of the SPS ST model, the evaluation of the SPS SC tool for this kind of application became an ancillary result of the present thesis.

The available literature on extended-delta winding connection transformer is scarce. Indeed, this winding configuration is used almost exclusively with high power converters and also in this field it is not so widespread yet. For this reason, while some descriptions of the extended-delta winding connection can be found in literature, nothing is present on its mathematical representation or on single-phase equivalent electrical circuits. On the other hand, detailed descriptions on how to model transformers with many other winding connections are available. Finally, the literature (manual guides and others) on how to build custom transformer blocks using SPS ST is not quite detailed.

Therefore, the modelling of the extended-delta transformers started substantially from scratch, i.e. from the analysis of the actual functioning scheme of this kind of devices.

The general description of extended-delta transformers and the phasor analysis of the voltages on the winding is reported in Chapter 2. In particular, here is shown a way to build a phasor triplet in phase with the three magnetic fluxes into the transformer's columns. Starting from these results, after an overview of the SPS software tools performed in Chapter 3, -the model of the extended-delta/delta transformer realized with SPS ST blocks is presented in Chapter 4. In Chapter 5 a first validation of the model is presented, comparing the simulation results with datasheet received by the transformer manufacturer. In Chapter 6, a second model validation is presented: it is based on the comparison with another model newly developed, built according to a different approach and with another library of the same Simscape software. In addition, some specific fault conditions interesting to ITER application, have been tested using both models, providing a substantial robustness verification.

Finally, the conclusions (Chapter 7) includes some proposals for a future work development.

The validity of the SPS ST model proposed has been proved, with several verifications presented. Moreover, the initial analysis performed has a general validity. Therefore, also other kinds of transformer with other non-common windings configuration could be modelled using the same paradigm here exposed.

2. Extended-delta Winding Connection

The extended-delta winding connection, which derives from the delta connection, is used in one of the transformer’s winding (primary or secondary), while generally the other winding is connected in a conventional wye or delta configuration. This connection scheme is used to realise a customised phase displacement between the primary and secondary voltages and it can also provide the necessary circulating pathway for any zero-sequence component [7]. Therefore, the zero-sequence impedance of the transformers with an extended-delta connection is very high. These aspects assume a central importance when using this kind of transformer to supply multi-pulse power converters: same possible sub-harmonic components (like the third harmonic) produced by the converter in unbalanced case can be passively deleted.

In this thesis, as paradigmatic example, a three-limb core transformer with the primary windings in extended-delta connection and with the secondary windings in delta connection (ED/d [8]) it is considered. This transformer provides a nominal phase-shift of 15° and it is used, in parallel with another identical transformer (phase-shift -15°), to supply a 12-pulse bridge AC/DC converter. The results here presented can also be applied to many other kinds of transformer’s cores, providing that one winding is configured in extended-delta connection.

In general, in the extended-delta winding connection, each primary is composed of two windings, the *main winding*, and the *extended winding*. The three main windings are delta-connected and the extended windings are connected to the terminals of the triangle. (Figure 2.1)

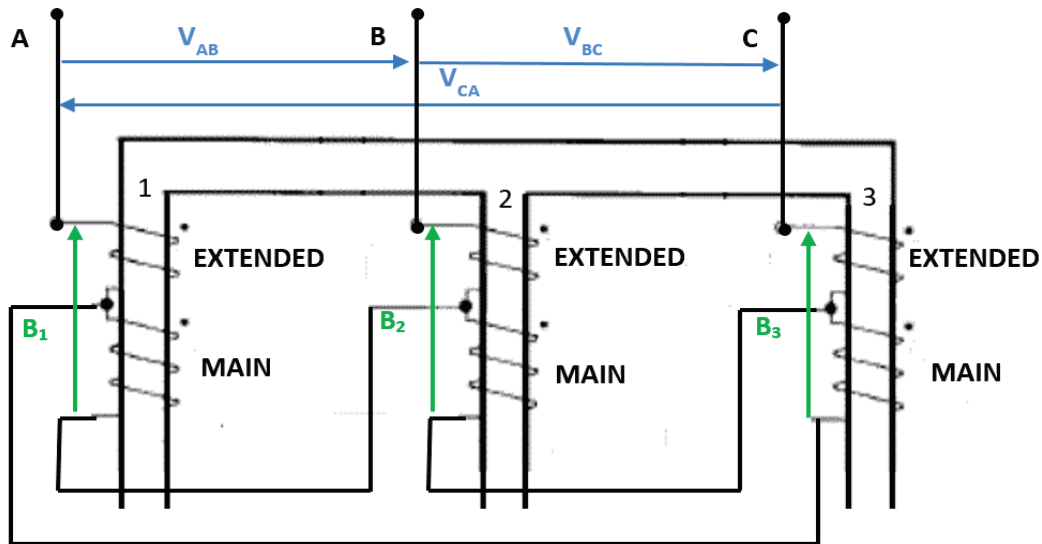


Figure 2.1: Extended-delta windings on a three-limb transformer

In this scheme, the grid provides the phase-to-phase voltages V to the primary side of the transformer but, due to the extended-delta connection, the voltage on the primary windings is different (here named $B_1 B_2 B_3$) [9]. The voltage B is proportional to the flux in each limb of the transformer’s magnetic core, so the voltage V' on the delta connected secondary windings is in phase with B (Figure 2.2).

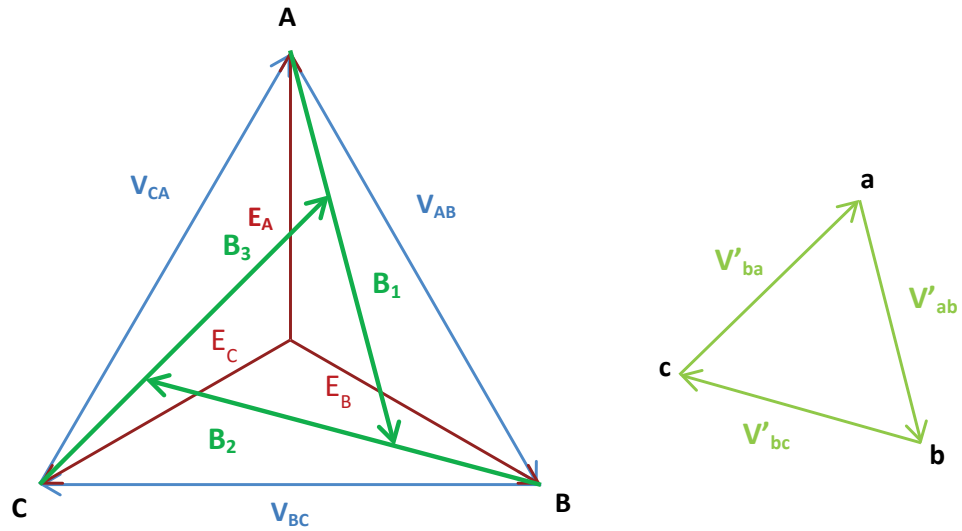


Figure 2.2: Phasor voltage diagram

Due to the extended-delta connection, the phasor **B** has a phase shift compared to the primary phase-to-phase voltage **V** and therefore the same shift occurs for the secondary voltage phase-to-phase **V'**.

Once established the grid phase-to-phase voltage, the phase and the magnitude of the voltage **B** depends on the number of turns of the extended-delta windings. It is possible to change the number of these turns to induce the desired phase shift of the transformer.

2.1 Calculation of the voltage magnitude

The voltage magnitude on the transformer windings is a fundamental information to size the electrical insulation, but it can be useful also for a phasor analysis, allowing the calculation of the phase shift in this kind of transformers.

In fact, with reference to the shifted phasor diagram in Figure 2.3, the magnitude of the phasor **B** is the sum of the voltages **A** and **B'** that drop on the extended and on the main winding of the primary, respectively [10].

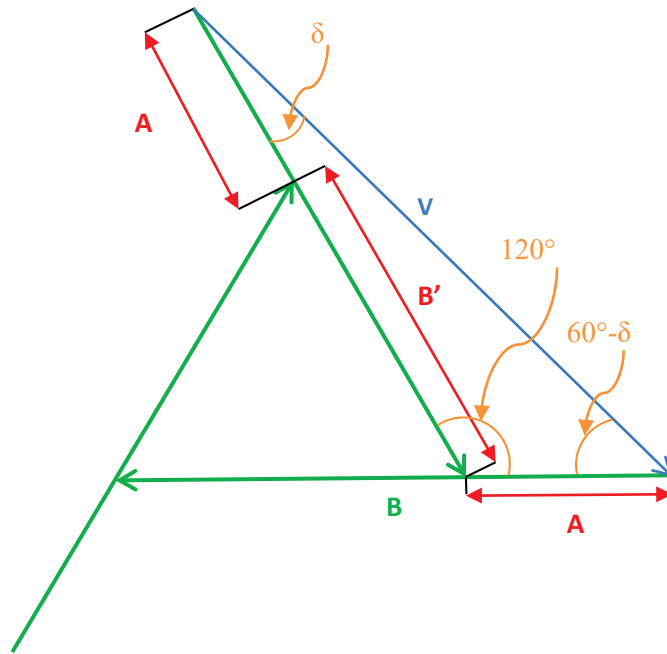


Figure 2.3: Shifted primary phasor diagram

Calling δ the desired phase shift, in degrees, it can be noticed that:

$$\frac{A}{\sin|\delta|} = \frac{V}{\sin(120^\circ)} = \frac{B}{\sin(60^\circ - |\delta|)}$$

Therefore, the magnitude of the phasor **B** can be calculated as:

$$B = V \cdot \frac{\sin(60^\circ - |\delta|)}{\sin(120^\circ)}$$

In other words, for each primary voltage **V**, the magnitude of phasor **B** is uniquely determined once the transformer's phase shift δ is established.

2.1.1 Number of turns and partial voltages with 15° shift ($\delta = \pm 15^\circ$)

As reported in the literature [9], being:

- N_E : number of turns of the extended windings;
- N_T : number of turns of the main windings;
- N_2 : number of turns of the delta connected secondary windings.

with reference to Figure 2.2 and Figure 2.3 for the meaning of **A**, **B**, **δ**, **V** and **V'**, the following relationships occur:

$$\begin{cases} \frac{N_E}{N_E + N_T} = \frac{A}{B} = \frac{\sin(|\delta|)}{\sin(60^\circ - |\delta|)} \\ \frac{N_2}{N_E + N_T} = \frac{V'}{B} = \frac{V'}{V} \cdot \frac{\sin(120^\circ)}{\sin(60^\circ - |\delta|)} \end{cases}$$

In order to generate a phase shift $\delta = \pm 15^\circ$, the number of turns of the windings are determined by the following formulas [9]:

$$N_T = \left(\frac{\sin 45^\circ}{\sin 15^\circ} - 1 \right) \cdot N_E = \sqrt{3} \cdot N_E$$

$$N_2 = \frac{V' \sin 120^\circ}{V \sin 15^\circ} \cdot N_E = \frac{V'}{V} \frac{2 \cdot \sqrt{3}}{\sqrt{3} \cdot \sqrt{2} + \sqrt{2}} \cdot N_E = \frac{V'}{V} \frac{2}{\sqrt{3} \cdot \sqrt{2} + \sqrt{2}} \cdot N_T$$

Setting $K = V/V'$, the same relations can be expressed as:

$$N_T \cong 1,73205 \cdot N_E \quad N_2 \cong \frac{3,34606}{K} \cdot N_E$$

While the voltage magnitudes are:

$$A = V \cdot \frac{\sin 15^\circ}{\sin 120^\circ}$$

$$B = V \cdot \frac{\sin 45^\circ}{\sin 120^\circ} \rightarrow B' = B - A = V \cdot \frac{(\sin 45^\circ - \sin 15^\circ)}{\sin 120^\circ}$$

These formulas will be used in the following for building the transformer model.

2.2 From grid voltage V to phasors B

In order to build a model of the extended-delta/delta transformer, the adopted strategy is to realize a three-phase grid with B voltage as a phase-to-phase voltage and then transform that triplet in the secondary voltage triplet. This Chapter presents how the B phasors voltages can be obtained by voltages in phase with primary phase-to-phase voltages.

The phasor diagram in the Figure 2.4 below shows how the phasor B can be formed by a sum of two phasors E and D , in phase with two phase-to-phase voltages V .

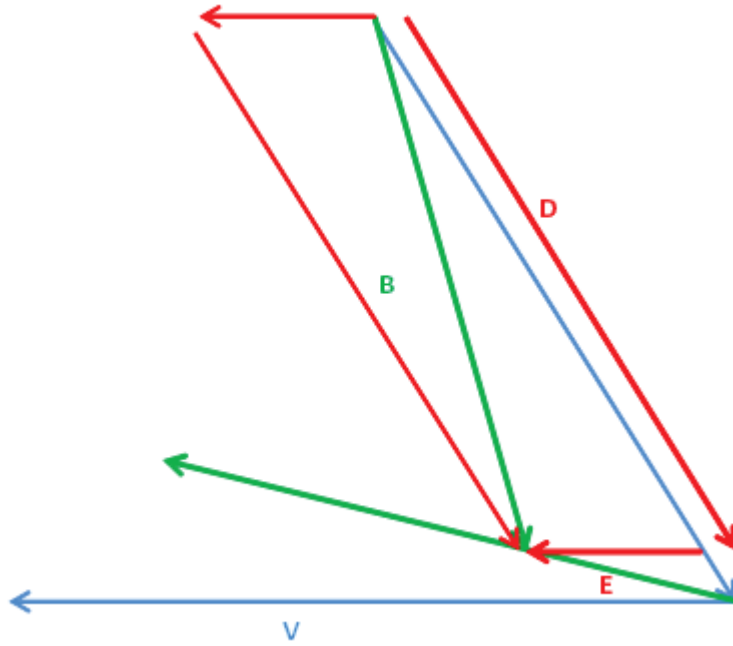


Figure 2.4: B phasor as sum of phasors D and E

In particular:

$$\bar{B} = \bar{D} + \bar{E}$$

The phase of the D and E are evident; the magnitudes respect the law of sines:

$$\frac{B}{\sin 60^\circ} = \frac{D}{\sin(180^\circ - 60^\circ - \delta)} = \frac{E}{\sin(|\delta|)}$$

Since the magnitude of B (for a given V) is fixed by the δ shift, the two phasors D and E are uniquely defined.

In the case of $\delta = \pm 15^\circ$ the law of sines is:

$$\frac{B}{\sin 60^\circ} = \frac{D}{\sin 105^\circ} = \frac{E}{\sin 15^\circ} = \frac{V \cdot \sin 45^\circ}{\sin 120^\circ} \frac{1}{\sin 60^\circ} = \frac{4}{3} \cdot V \cdot \sin 45^\circ$$

Therefore:

$$D = \frac{4}{3} \cdot V \cdot \frac{\sin 45^\circ}{\sin 105^\circ};$$

$$E = \frac{4}{3} \cdot V \cdot \frac{\sin 45^\circ}{\sin 15^\circ}$$

It is clearly understandable that using a phase-to-phase voltage, transformed in magnitude, it is possible to create phasor **D**. Similarly, using the subsequent phase-to-phase voltage, still transformed in magnitude, it is possible to generate the phasor **E**. Summing phasors **D** and **E** we can obtain phasor **B**.

Repeating this procedure in sequence, for each couple V_{AB} , V_{BC} and V_{CA} , the three voltages **B**₁, **B**₂ and **B**₃ are obtained. These voltages, as mentioned before and well discussed in [5] and [9], are proportional to the flux in each limb of the transformer and to the transformer’s secondary voltages. Then, a three-phase transformer of group 0 can be used to transform the three-phase voltages **B** to the established **V**’ secondary voltage triplet.

These considerations are true independently to the value of the phase displacement. For example, they are valid also for an extended-delta/delta transformer used for 24-pulse converters, that have 4 transformers with 7,5° of phase shift in parallel. Furthermore, this kind of approach has a general validity at steady state: building a voltage phasor triplet in phase with the flux in the transformer’s core limbs starting from the primary voltages allows to model transformers (with two windings) with any kind of winding connections.

2.2.1 Negative values of phase-shift

When the phase-shift δ is negative, the phasor diagram becomes as in Figure 2.5.

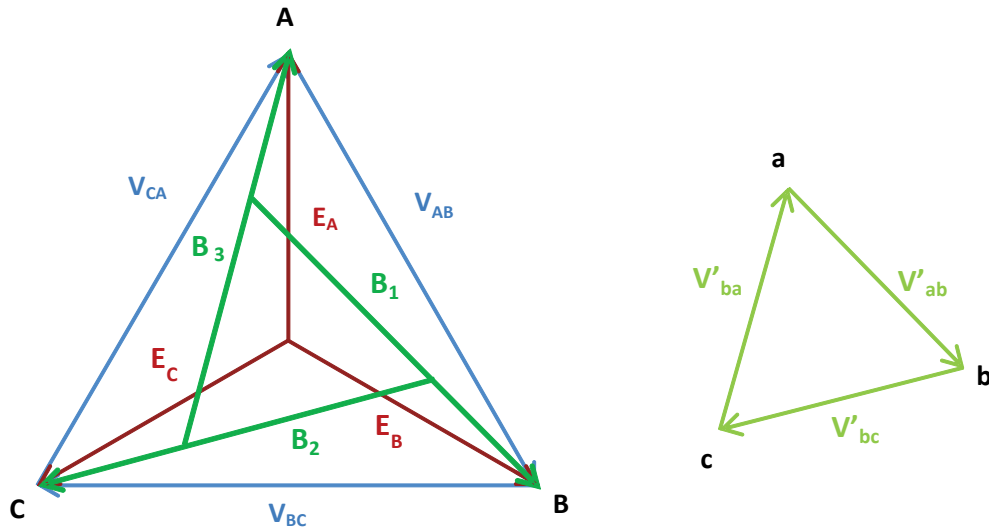


Figure 2.5: Negative phase-shift phasor diagram

A way to proceed with a negative phase shift value is to use the same transformer configuration of the positive phase shift value, supplying it with the inverse voltage triplet V_{AB}^i , V_{BC}^i and V_{CA}^i which is specular to the direct one. A common way to do this, used for example in delta/wye transformers [9], is to make a phase transposition. In particular, this can be done swapping two transformer terminals, for example the connection of phase **B** and **C**.

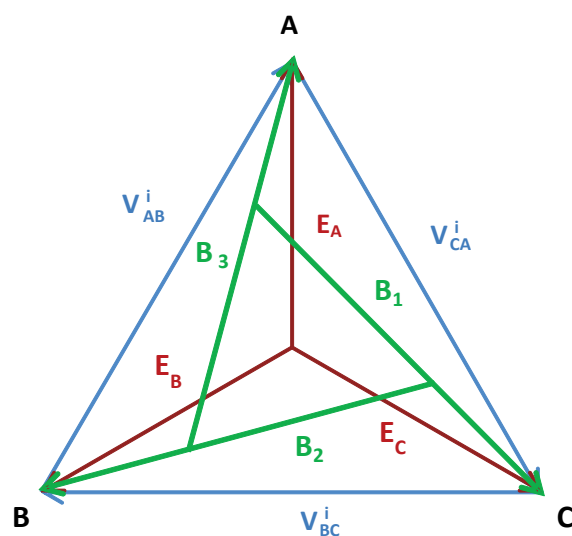


Figure 2.6: Phasor diagram with phase connection exchanging

The result is shown in Figure 2.6.

3. Simscape Power Systems™ overview

Simscape Power Systems™ (SPS) is a toolbox of MatLab/Simulink® software, used for electrical system simulations. In the last release of MatLab (2016a), SPS is divided into two libraries [11]:

1. Simscape Components (SC): it contains Simscape blocks developed to work with multiphase electrical domains. With the blocks in this library, using the Simscape language, it is possible to develop custom three-phase blocks and to connect them to other Simscape blocks from the Simscape Foundation Library (SFL).
2. Specialized Technology (ST): it contains typical power equipments, such as transformers, lines, machines, etc. The validity of these blocks is based on the experience of many testing laboratories all over the world. Even if this is a good library of basic electrical components, it does not have phase shifting transformer.

It is possible to create and simulate complex electrical systems either using a single library or using a model containing components from both libraries. However, in order to connect blocks from the two different libraries it is necessary a converter block and this generally slows significantly the simulation.

Since the SPS ST library is the most frequently used and it is used also in ITER electrical division, blocks from this library have been used in this thesis to build a subsystem able to simulate the electrical behaviour of the extended-delta/delta transformer. Subsequently, a physical model of the same transformer was built with SPS SC to validate the first model.

3.1 Simscape Power Systems™ Specialized Technology

In this Chapter the main blocks from the SPS ST library used to build a SPS ST model are described. The basic Simulink® or SPS ST blocks (as resistance, inductance, scopes, ect) will not be described in this thesis (see the reference [12] for more details).

3.1.1 Transformers block

In order to simulate a transformer with Simscape Power Systems™ Specialized Technology there are some parameters to be set (Figure 3.1 and Figure 3.2), regardless the kind of transformer [12].

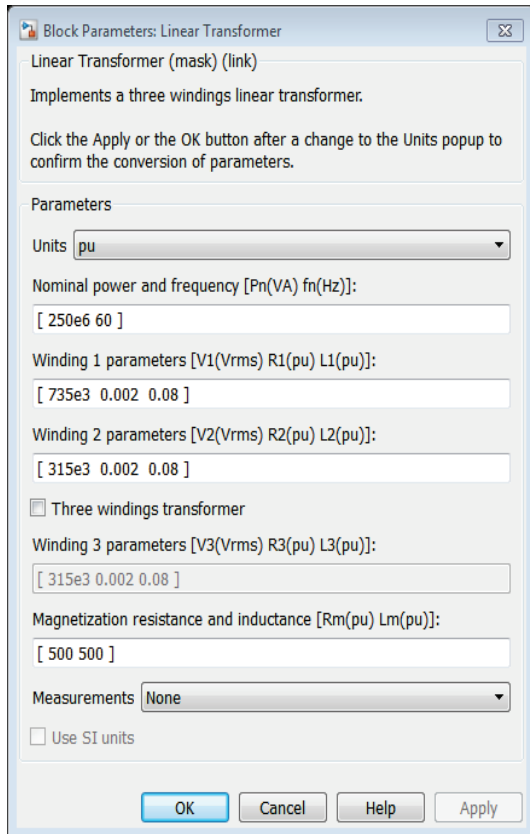


Figure 3.1: Linear Transformer block parameters

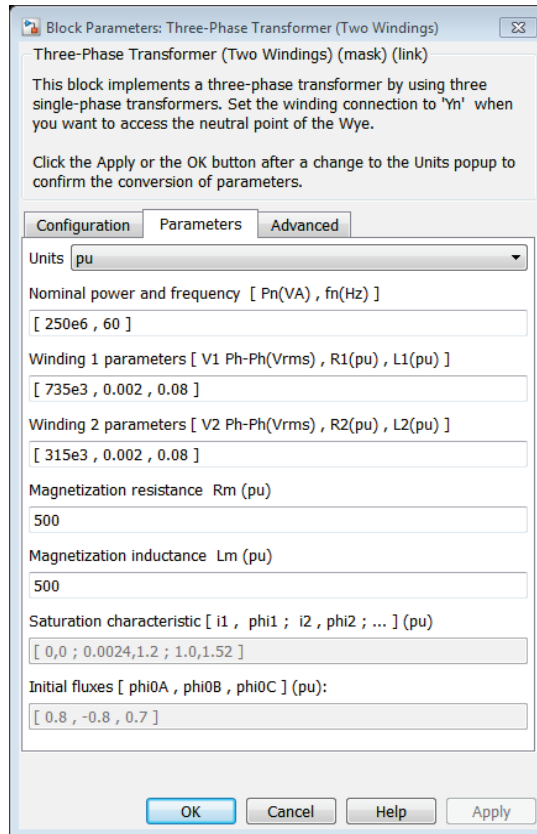


Figure 3.2: Three-Phase Transformer block parameters

These parameters are:

- Nominal Power in Volt-Ampere [VA];
- Nominal frequency in Hertz [Hz];
- Nominal primary and secondary RMS voltage in Volt [V];
- Primary and secondary winding resistance;
- Primary and secondary winding leakage inductance;
- Magnetization resistance and inductance.

The parameters can be set in per-units (*p.u.*) or in international system units (*SI*) and are based on the mono-phase equivalent electric circuit [13] in Figure 3.3.

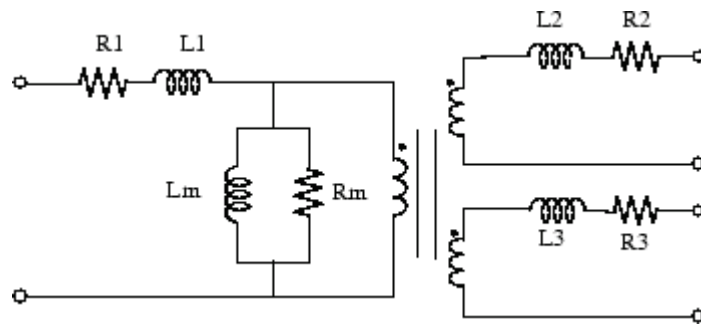


Figure 3.3: mono-phase equivalent electric circuit of a transformer (with two secondary)

In SPS ST it is not necessary to set the number of turns or to establish the ratio of transformation of a transformer, but just to set the nominal voltages at primary and secondary.

3.1.1.1 Ideal transformers and convergence problems

To implement an ideal transformer model in SPS ST, it is sufficient to set the windings resistances and inductances to 0 and the magnetization resistance and inductance (R_m L_m) to inf^1 [12].

However, connecting two ideal transformers can create a loop, thus a convergence problem of the model (Figure 3.4).

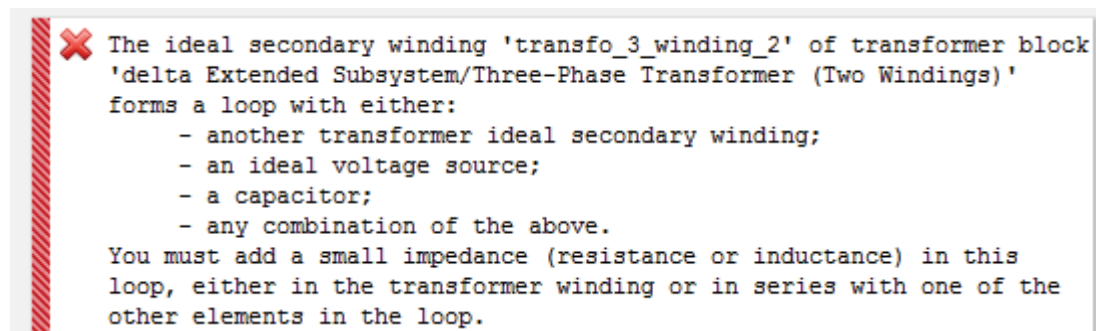


Figure 3.4: Error with 2 ideal transformer connected together

To solve this kind of problem it is possible to set the winding resistances and inductances to a small value but not 0. In this case however magnetic resistance and inductance cannot be infinite. Otherwise a small resistance in the connections between ideal transformers can be placed.

3.1.2 Three-Phase Transformer block

The *Three-Phase Transformer (two windings)* SPS ST block implements a three-phase transformer using three single-phase transformers [12]. When the leakage inductance and resistance of each winding are given in *p.u.*, they are based on the transformer nominal power Pn^2 and on the nominal voltage of the winding.

The connection of the two windings of the three-phase transformer is configurable, but not customizable, so it is possible to choose among the standard connection solutions (Figure 3.5).

¹ In MatLab *inf* returns the IEEE arithmetic representation for positive infinity [12].

² In SimPowerSystem the machine base power is the mono-phase power, so for a three-phase machine: $P_b = P_n/3$

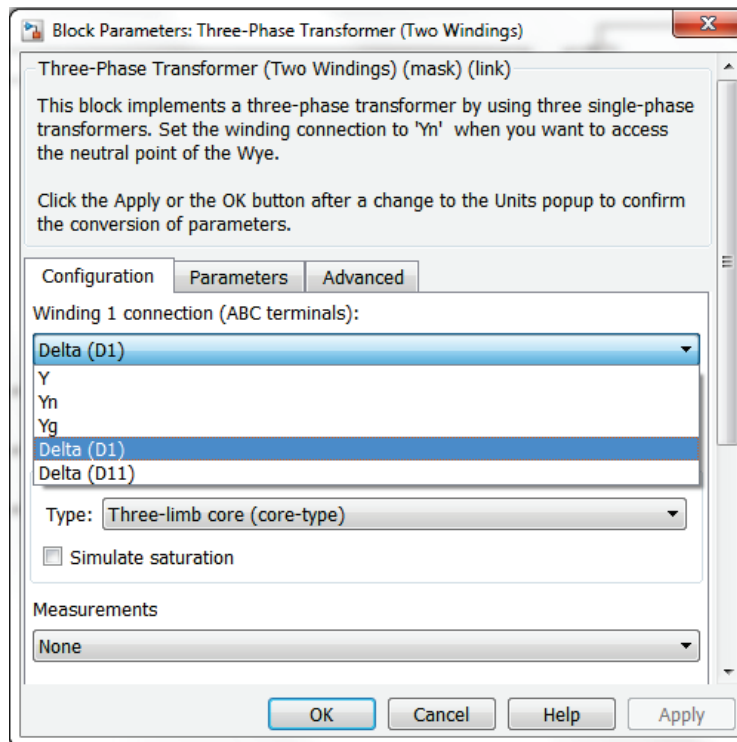


Figure 3.5: Configuration tab of Three-Phase Transformer block

Starting from the 2015a MatLab release, the Three-Phase Transformers blocks has the possibility to choose the type of transformer's core. In this way it is possible to define the zero-sequence inductance of the transformer and to simulate the saturation and the hysteresis of a three-phase transformer.

These last features are useless in an ideal model, but will be fundamental in real study.

3.2 Simscape Components & Foundation Library

In the SPS Simscape Components library almost all the three-phase elements that are modelled in the SPS ST library can be found, but here they are modelled in Simscape language. Therefore, they can be connected to the Simscape Foundation Library blocks. It is consequently possible to use the blocks from electrical and magnetic SFL to build custom transformer and to connect it to SPS SC blocks.

In this Chapter are presented the main blocks used to build the physical model described in later Chapters.

3.2.1 Phase splitter block

One of the most important block used is the *Phase Splitter* SPS SC block. Indeed, even if all the SPS SC block can be set to expand three-phase line ports, the common and default use is to have the connection in single-line diagrams to make the work easier.

The *Phase Splitter* block simply separates a single-line electrical connection into the three lines of the three-phase system and vice versa, so it is possible, for example, to connect a single-phase load to a three-phase system.

3.2.2 Electromagnetic Converter Block

The *Electromagnetic Converter* SFL block is an interface between the electrical and the magnetic systems of Simscape. It has two sides with two terminals each: one side is connectable to an electrical circuit, the other to a magnetic circuit.

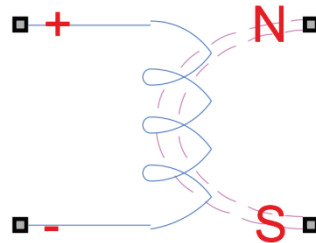


Figure 3.6: Simscape Foundation Library Electromagnetic Converter block

When a current and a voltage is recorded at the electrical side, a flux and a magneto motive force (mmf) are produced at the magnetic side and vice versa, following the well-known laws:

$$\begin{cases} mmf = N \cdot I \\ V = -N \cdot \frac{\delta\phi}{\delta t} \end{cases}$$

Where N is the number of turns that has to be set in the block parameters dialog box.

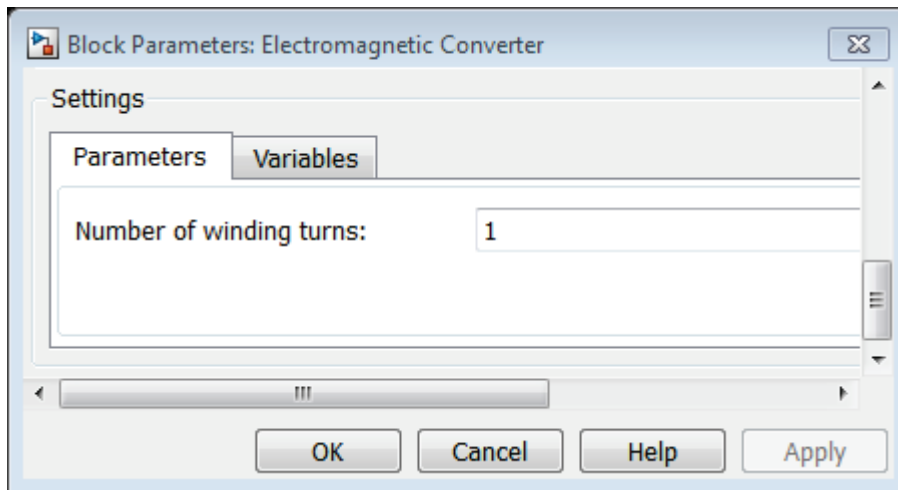


Figure 3.7: Electromagnetic converter dialog box

3.2.3 Controlled magnetomotive source

The *Controlled Magnetomotive Source* SFL block represents, in Simscape language, an ideal magneto-motive generator that maintains the mmf input specified by the Simscape signal.

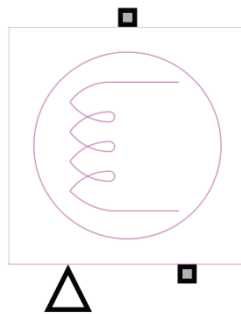


Figure 3.8: Simscape Foundation Library Controlled MMF Source

To control the block with a Simulink® signal a converter block is necessary. Another way to control it is having some kind of Simscape signal source, so that no Simulink® block is strictly required. Obviously this block has only two magnetic ports and can be only connected to a magnetic circuit.

3.3 Block Mask Editor

Simulink® gives the possibility to create custom interfaces that can be applied to the blocks. These interfaces are called *Mask* and can mask also Simscape Power Systems™ blocks. A mask hides the user interface of a block (Figure 3.9) and in its place it displays a custom dialog control box for specific parameters of the masked block (Figure 3.10) called *mask parameters*.

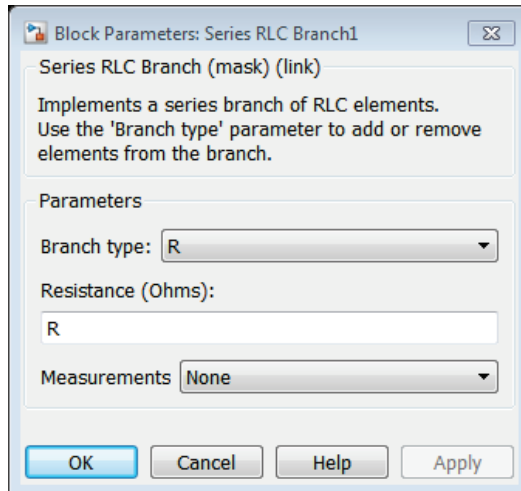


Figure 3.9: Un-masked resistance dialog control

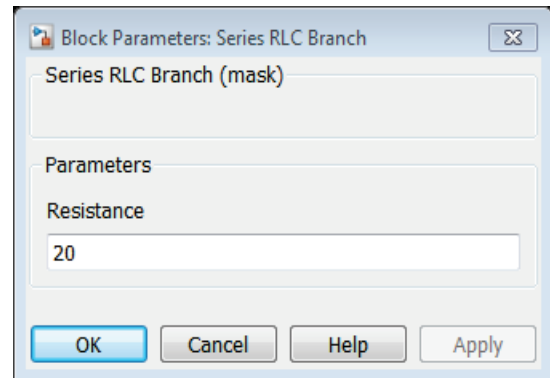


Figure 3.10: Masked resistance with custom dialog control

Mask parameters are the links to the underlying block parameters. In order to edit a mask of a block, the mask parameter names have to be defined. The names have to be the same of those set for the corresponding block parameters. For example, in Figure 3.11 the name of the defined parameter “Resistance” is “R” as in Figure 3.9.

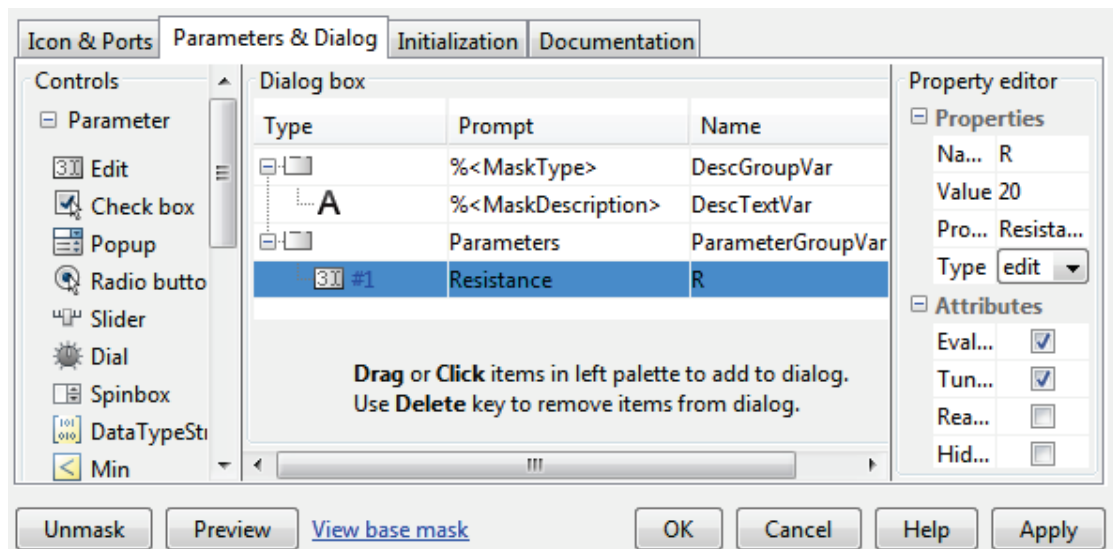


Figure 3.11: Parameters Mask Editor

A mask can be also used for subsystems of blocks and this gives the possibility to build custom parameter dialog box, to create the desired block icon and to place this new block in a personal library [11].

In the case of masking a subsystem, it is useful to distinguish whether the mask is edited. In case of an edited mask, double clicking on the mask opens a dialog box and it is possible to change the parameters of interest within the blocks of the subsystem [14]. Otherwise, double clicking on an unedited mask shows the blocks and their connections under the subsystem’s mask.

Another important feature of an edited mask is the initialization of the parameters. It is possible to calculate some mask parameters from those defined by the user (Figure 3.12).

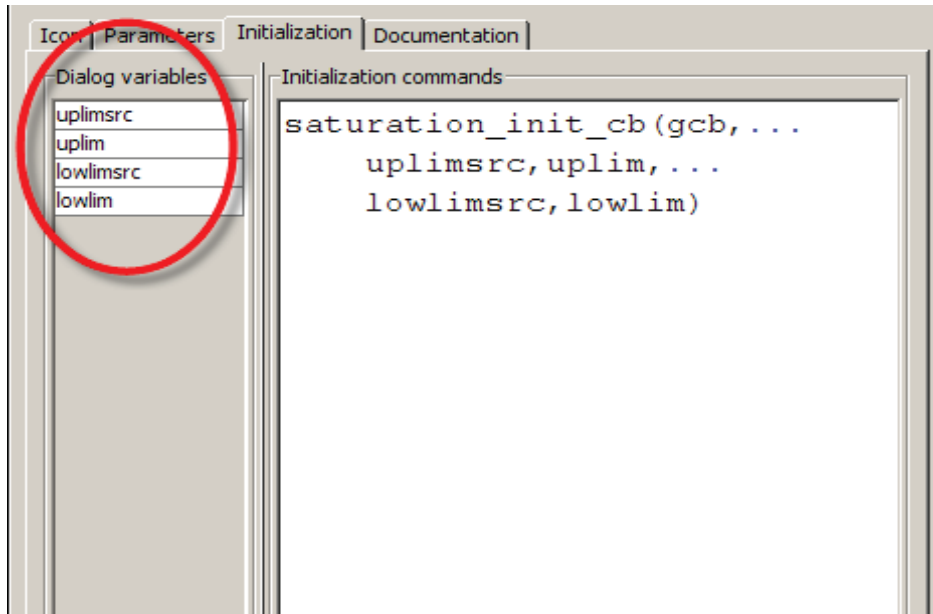


Figure 3.12: Initialization parameters in Mask Editor

4. Extended-delta/delta SPS Specialized Technology model

Using the blocks of SPS ST library, a subsystem called *extended-delta/delta subsystem* has been built. This subsystem behaves like a block that represents the transformer considered and it is masked in order to be totally similar to the SPS ST transformer blocks. Therefore, the transformer parameters (voltages, phase shift degrees, etc.) can be easily set.

This model represents properly an extended-delta/delta transformer with all possible phase-shift, transformation rate and power losses, that are to be set. Moreover, following the procedure presented in this Chapter and in Chapter 2.2 to obtain the voltage on the windings, it could be possible to model many kind of transformer with SPS ST, surely when there's only direct sequence components.

As input parameters, the datasheet parameters of a particular ITER converter-transformer (used for the alimentation of AC/DC converter for the correction coil) has been used.

4.1 ITER Coil Correction Side converter-transformer datasheet

The ITER Coil Power Supply System includes several systems to supply with controlled voltage and currents the magnet coils of the tokamak. One group of coils is the Correction Coils Side (CCS) that are supply by an AC/DC converter unit. This in turn is supplied by a rectifier-transformer with the extended-delta/delta windings connection [3].

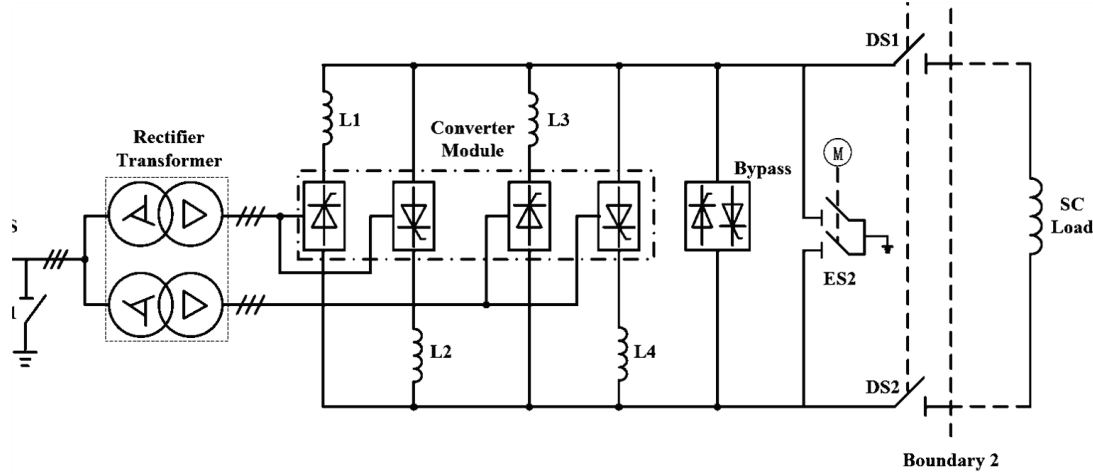


Figure 4.1: Simplified circuit scheme of Correction Coil supply system

The converter-transformer is actually composed of two transformer units, each giving a 15° shift: one gives $+15^\circ$ and the other -15° , so the two secondary are reciprocally shifted of 30° . The desired harmonic cancellation thus occurs at the primary side. Since this transformer supplies the CCS coils, it is commonly called CCS converter-transformer or simply CCS transformer.

The CCS transformer is produced by a Korean manufacturer that provided several information in its datasheet. Some of the electrical and magnetic data are reported in Table 1.

Rated Power	2 X 2.209	MVA
Rated Primary Voltage	22	kV
Rated Secondary Voltage	0.327	kV
DC Current	5	kA
HV Line Current	63	A
LV Line Current	4082.5	A
No-Load Loss	5.6	kW
Load loss@50Hz	79.2	kW
harmonic loss	15	kW
Total Loss	99.8	kW
% impedance voltage	16	%
Flux density @rated voltage	1.65	T
No-Load current	1.23	%

Table 1: CCS transformer datasheet electrical parameters, courtesy of the Hyosung Corporation (A Korean company supplying products to the ITER Project.)

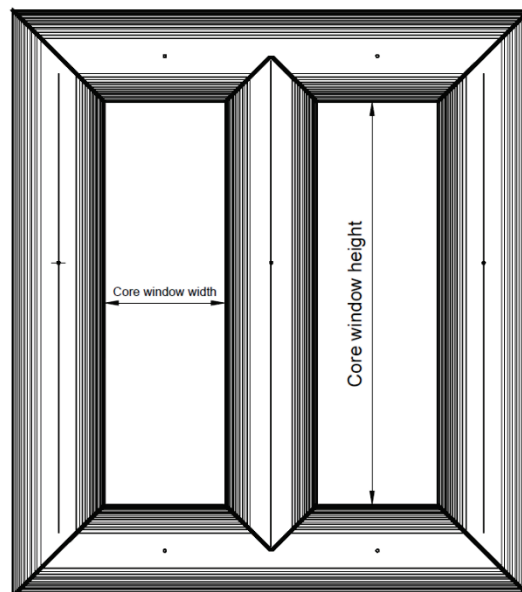
The manufacturer gave also some geometrical data of transformer’s windings and core that are reported in Table 2 and Table 3.

Winding ³	HVe	HVm	LV
Phase Voltage (kV)	6.6	11.4	0.337
Phase Current (A)	63	36.4	2357
Number of turns	332	574	17

Table 2: Windings' data

Core diameter (mm)	298
Core effective area (cm ²)	591.2
Core window height (mm)	695
Core window width (mm)	434

Table 3: Transformer's core geometry



Courtesy of the Hyosung Corporation (A Korean company supplying products to the ITER Project.)

Finally, the manufacturer provided the magnetization characteristic B-H of Figure 4.2.

³ HVe: extended winding of the primary winding;
 HVm: main winding of the primary winding;
 LV: secondary winding.

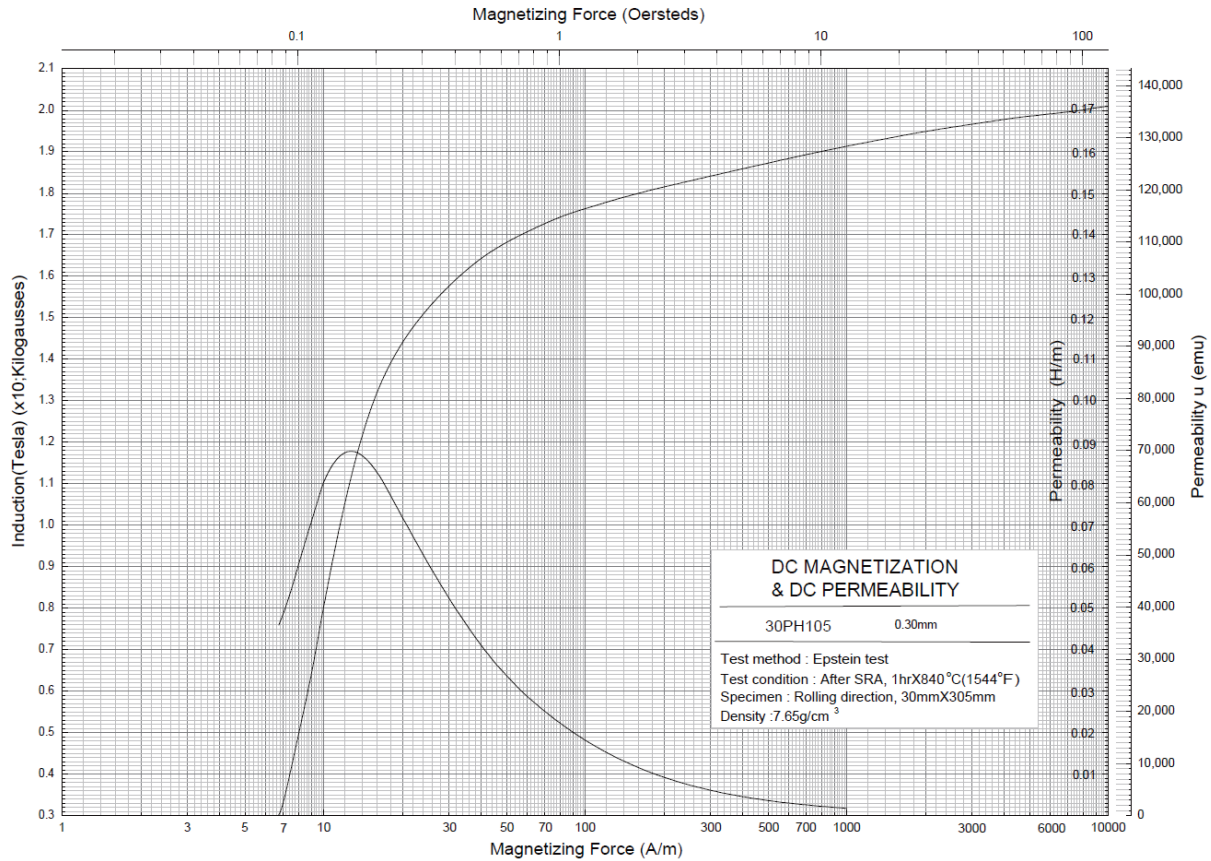


Figure 4.2: Magnetizing characteristic of CCS transformer as given by the manufacturer, courtesy of the Hyosung Corporation (A Korean company supplying products to the ITER Project.)

It has to be underlined, as reported in [6], that this magnetic characteristic is not so precise and complete. For this reason, some discrepancies between the numerical results reported in the present thesis and in possible future measurements on the real machine might occur.

The electrical and magnetic parameters for the SPS ST model of the transformer have been calculated through the elaboration of many of the above mentioned data.

4.2 Structure of the model

The two main components of SPS ST library used for the construction of the model of an extended-delta/delta transformer are:

- *Linear Transformer* block, used to build a subsystem called *B former transformer* that creates each **B** voltage as described in Chapter 2.2. Since there are three **B** phasors, three *B former transformer* subsystems are needed: these three subsystems are grouped in a subsystem called *ideal phase-shifter* subsystem.
- *Three-Phase Transformer (Two Windings)* block, used to provide the chosen ratio of transformation between primary and secondary windings.

This Chapter describes the SPS ST subsystem that can represent the extended-delta/delta transformer and how it has been created.

4.2.1 Edited mask and parameters of the extended-delta/delta subsystem

The extended-delta/delta subsystem has an edited mask and so, in the dialog box, the parameters similar to those described in Chapter 3.1.1 (Figure 4.3) for a transformer block can be defined. Other parameters are calculated in the mask parameters initialization.

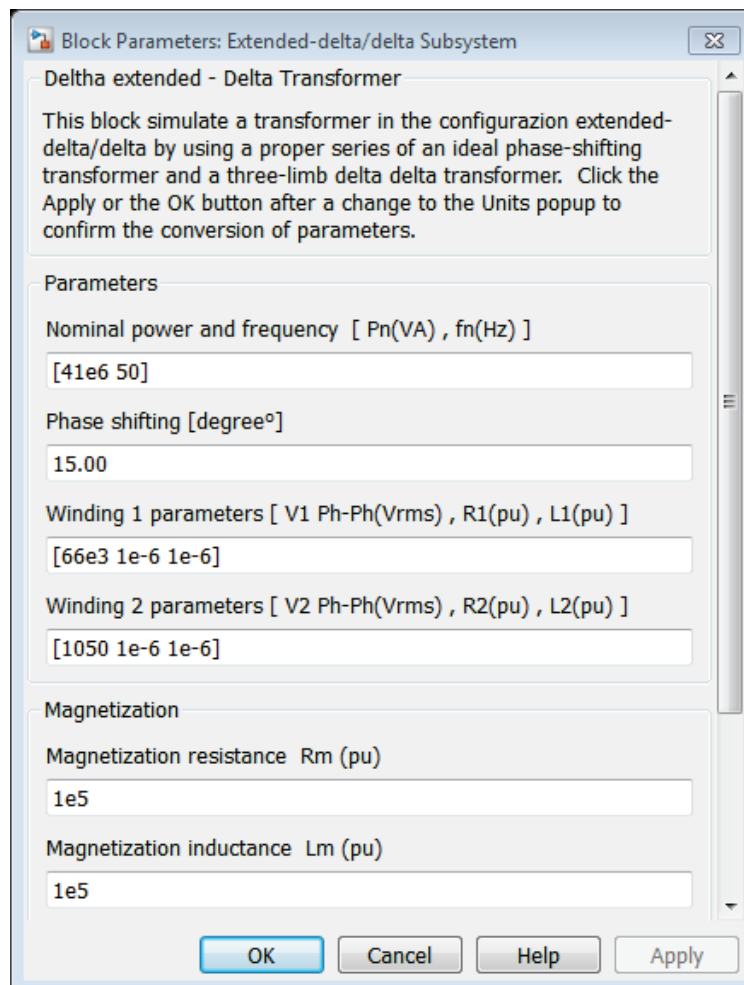


Figure 4.3: Extended-delta/delta subsystem dialog control parameters (illustrative values)

As can be seen in Figure 4.3, in addition to the typical parameters of a transformer block, there is the *Phase shift* parameter that is the chosen phase-shift between the primary and secondary voltages of the extended-delta/delta transformer (δ in the notation of Chapter 2.1).

The names of the mask parameters are (Figure 4.4):

- *Powerfreq*: nominal power and frequency vector;
- *s*: required phase shift value;
- *Winding1*: primary voltage, winding resistance and inductance vector;
- *Winding2*: secondary voltage, winding resistance and inductance vector;
- *Rm*: magnetic resistance;
- *Lm*: magnetic inductance;
- *sat*: the saturation vector;
- *L0*: inductance of zero-sequence.

Parameters	ParameterElectrical
Nominal power and frequency [Pn(VA) , fn(Hz)]	Powerfreq
Phase shifting [degree°]	s
Winding 1 parameters [V1 Ph-Ph(Vrms) , R1(pu) , L1(pu)]	Winding1
Winding 2 parameters [V2 Ph-Ph(Vrms) , R2(pu) , L2(pu)]	Winding2
Magnetization	ParameterMagnetization
Magnetization resistance Rm (pu)	Rm
Magnetization inductance Lm (pu)	Lm
Saturation characteristic [i1 , phi1 ; i2 , phi2 ; ...] (pu)	sat
Inductance L0 of zero-sequence flux path return (pu)	L0

Figure 4.4: Mask parameters name of extended-delta/delta subsystem

Notably, the resistance and the leakage inductance of the windings have to be different from 0 because of the convergence problem described in Chapter 3.1.1.1. In order to build an ideal model, it is necessary to set them to a very little value, for example $1e-6$ [p.u.]. In this situation, since the windings' impedances are not 0, magnetization impedance cannot be infinite [12], so, to give an ideal approximation, it has to be set to a very high value, such as $1e5$ [p.u.].

In the mask edition it is possible to change the icon. For the extended-delta/delta subsystem the same icon of the three-phase transformer block has been copied.

4.2.1.1 Other parameter calculation

In the parameters initialization of the edited mask the following parameters (defined in Chapter 2.2) are automatically calculated to ease the user compilation:

- V: primary voltage **V** magnitude;
- R1: primary winding resistance;
- L1: primary winding inductance;
- VB: voltage **B** magnitude;
- VD: voltage **D** magnitude;
- VE: voltage **E** magnitude.

Figure 4.5 shows the used syntax.

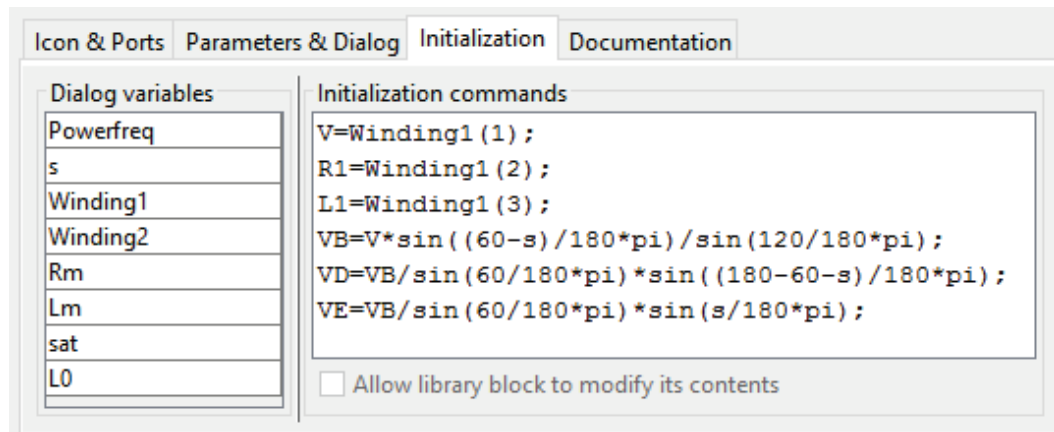


Figure 4.5: Parameter initialization syntax in extended-delta/delta subsystem

4.2.2 B former transformer subsystem

As shown in Chapter 2.2, transforming two consecutive phase-to-phase voltages in **D** and **E** voltages allows to create the voltage **B**. Repeating this operation with all the couples of consecutive voltages, the triplet of voltages **B**₁, **B**₂ and **B**₃ are obtained.

To create a **B** phasor in SPS ST two Linear Transformer in the ideal configuration (Chapter 3.1.1.1) has been used: one to form the component **D** of the **B** phasor and the other to form the component **E** (Figure 4.6). Then, connecting properly the secondary terminals of the two linear transformer, the components **D** and **E** are summed together and the **B** voltage is created.

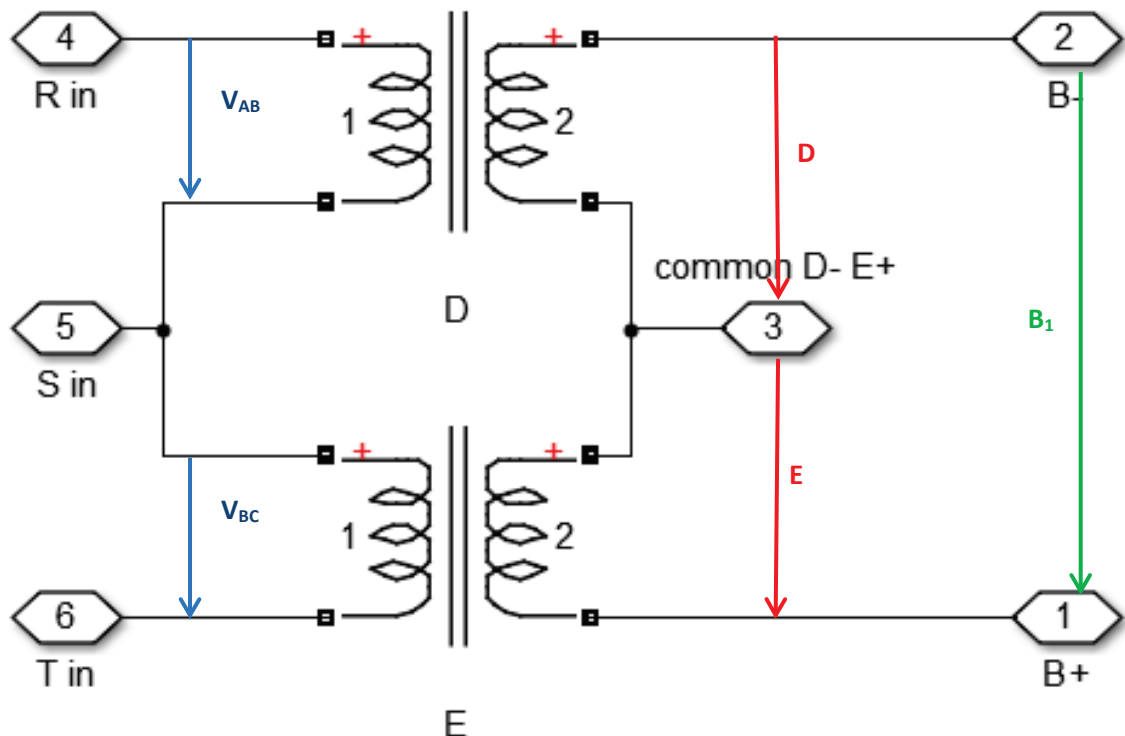


Figure 4.6: Mono-phase ideal B former transformer

The parameters of the two transformers are expressed in SI units, so that are not referred to the transformer nominal power, which becomes a useless datum ignored by SPS ST.

The Figure 4.7 shows the transformer D parameters:

- The nominal power (which is ignored) and frequency is *Powerfreq*;
- The primary nominal voltage is V as defined by user in the extended-delta/delta subsystem dialog box;
- The secondary nominal voltage is VD as calculated in initialization (Chapter 4.2.1.1);
- All other parameters are set to make the transformer ideal (Chapter 3.1.1.1).

Block Parameters: D

Linear Transformer (mask) (link)

Implements a three windings linear transformer.

Click the Apply or the OK button after a change to the Units popup to confirm the conversion of parameters.

Parameters

Units: SI

Nominal power and frequency [Pn(VA) fn(Hz)]:

Powerfreq

Winding 1 parameters [V1(Vrms) R1(ohm) L1(H)]:

[V 0 0]

Winding 2 parameters [V2(Vrms) R2(ohm) L2(H)]:

[VD 0 0]

☐ Three windings transformer

Winding 3 parameters [V3(Vrms) R3(ohm) L3(H)]:

[3.15e+05 4.8402 0.61628]

Magnetization resistance and inductance [Rm(ohm) Lm(H)]:

[Inf Inf]

Measurements: None

☒ Use SI units

OK Cancel Help Apply

Figure 4.7: Transformer D parameters

Similarly, transformer E parameters are shown in the Figure 4.8: nominal power and frequency, primary nominal voltage and transformer’s ideal settings are the same of those in the Figure 4.7. The difference is the secondary voltage that here is VE as calculated in initialization (Chapter 4.2.1.1).

Block Parameters: E

Linear Transformer (mask) (link)

Implements a three windings linear transformer.

Click the Apply or the OK button after a change to the Units popup to confirm the conversion of parameters.

Parameters

Units: SI

Nominal power and frequency [Pn(VA) fn(Hz)]:

Powerfreq

Winding 1 parameters [V1(Vrms) R1(ohm) L1(H)]:

[V 0 0]

Winding 2 parameters [V2(Vrms) R2(ohm) L2(H)]:

[VE 0 0]

☒ Three windings transformer

Winding 3 parameters [V3(Vrms) R3(ohm) L3(H)]:

[3.15e+05 4.8402 0.61628]

Magnetization resistance and inductance [Rm(ohm) Lm(H)]:

[Inf Inf]

Measurements: None

☒ Use SI units

OK Cancel Help Apply

Figure 4.8: Transformer E parameters

The two transformers of the B former transformer, with the described connection, are masked under a subsystem block (Figure 4.9). It has as input the three line voltages and as output the positive and negative terminals of **B** voltage. Moreover it has one more output for the measurements that is the common terminal of the secondary of the E and D transformers.

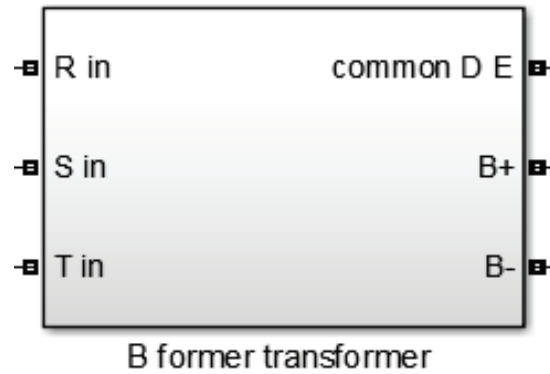


Figure 4.9: B former transformer subsystem

4.2.2.1 Ideal phase-shifter subsystem

Supplying three B former transformers shown in the Figure 4.6 with different couple of phase-to-phase voltages, it is possible to create the triplet of voltages B_1 , B_2 and B_3 as the scheme in Figure 4.10:

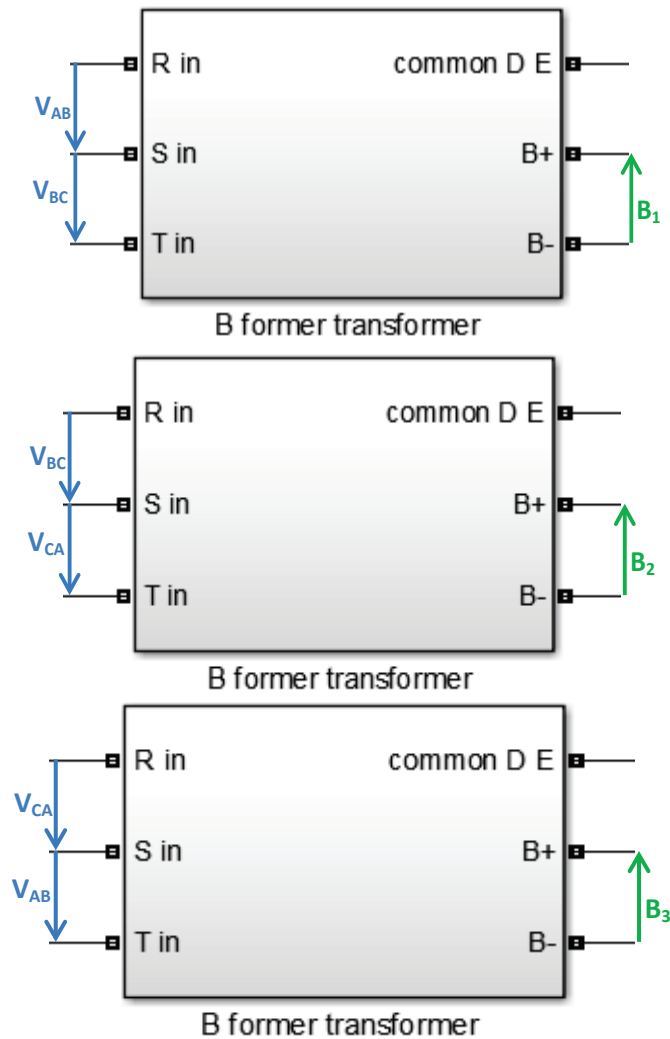
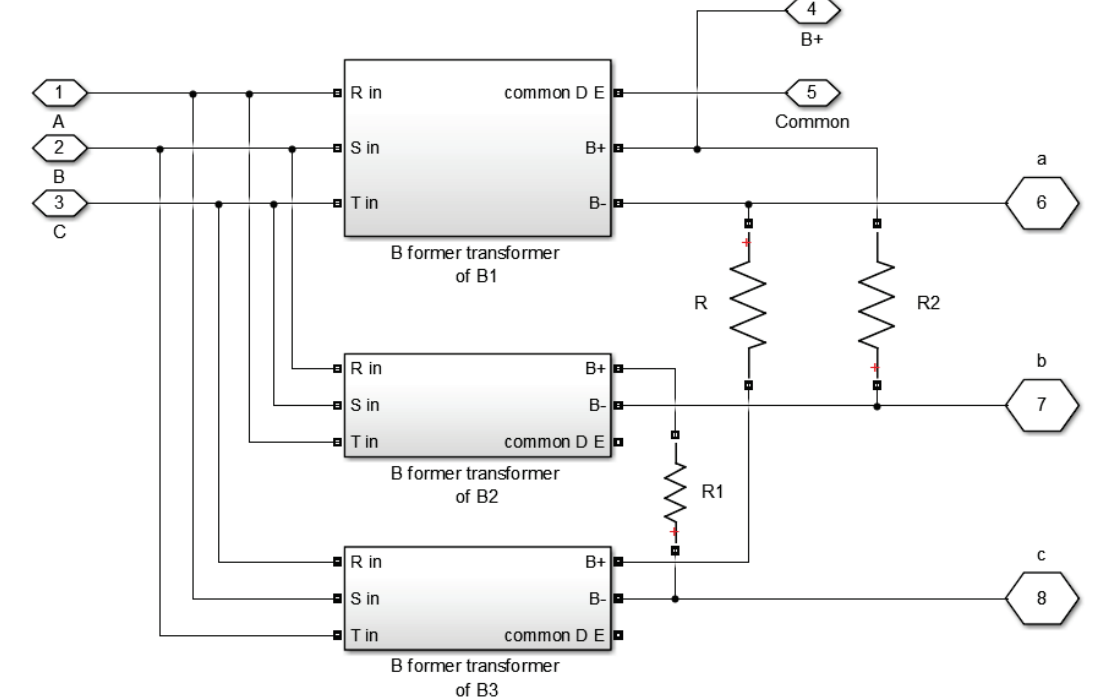
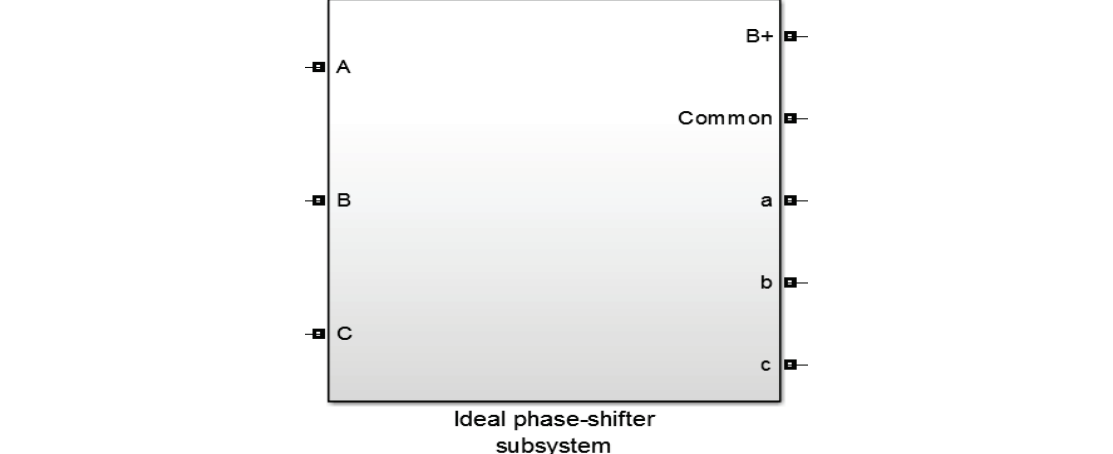


Figure 4.10: Three B former transformers


$$A_{11}(1) = 1, \quad A_{12}(1) = 0, \quad A_{13}(1) = 1, \quad A_{14}(1) = 0, \quad A_{15}(1) = 1, \quad A_{16}(1) = 0, \quad A_{17}(1) = 1, \quad A_{18}(1) = 0, \quad A_{19}(1) = 1, \quad A_{20}(1) = 0, \quad A_{21}(1) = 1, \quad A_{22}(1) = 0, \quad A_{23}(1) = 1, \quad A_{24}(1) = 0, \quad A_{25}(1) = 1, \quad A_{26}(1) = 0, \quad A_{27}(1) = 1, \quad A_{28}(1) = 0, \quad A_{29}(1) = 1, \quad A_{30}(1) = 0, \quad A_{31}(1) = 1, \quad A_{32}(1) = 0, \quad A_{33}(1) = 1, \quad A_{34}(1) = 0, \quad A_{35}(1) = 1, \quad A_{36}(1) = 0, \quad A_{37}(1) = 1, \quad A_{38}(1) = 0, \quad A_{39}(1) = 1, \quad A_{40}(1) = 0, \quad A_{41}(1) = 1, \quad A_{42}(1) = 0, \quad A_{43}(1) = 1, \quad A_{44}(1) = 0, \quad A_{45}(1) = 1, \quad A_{46}(1) = 0, \quad A_{47}(1) = 1, \quad A_{48}(1) = 0, \quad A_{49}(1) = 1, \quad A_{50}(1) = 0, \quad A_{51}(1) = 1, \quad A_{52}(1) = 0, \quad A_{53}(1) = 1, \quad A_{54}(1) = 0, \quad A_{55}(1) = 1, \quad A_{56}(1) = 0, \quad A_{57}(1) = 1, \quad A_{58}(1) = 0, \quad A_{59}(1) = 1, \quad A_{60}(1) = 0, \quad A_{61}(1) = 1, \quad A_{62}(1) = 0, \quad A_{63}(1) = 1, \quad A_{64}(1) = 0, \quad A_{65}(1) = 1, \quad A_{66}(1) = 0, \quad A_{67}(1) = 1, \quad A_{68}(1) = 0, \quad A_{69}(1) = 1, \quad A_{70}(1) = 0, \quad A_{71}(1) = 1, \quad A_{72}(1) = 0, \quad A_{73}(1) = 1, \quad A_{74}(1) = 0, \quad A_{75}(1) = 1, \quad A_{76}(1) = 0, \quad A_{77}(1) = 1, \quad A_{78}(1) = 0, \quad A_{79}(1) = 1, \quad A_{80}(1) = 0, \quad A_{81}(1) = 1, \quad A_{82}(1) = 0, \quad A_{83}(1) = 1, \quad A_{84}(1) = 0, \quad A_{85}(1) = 1, \quad A_{86}(1) = 0, \quad A_{87}(1) = 1, \quad A_{88}(1) = 0, \quad A_{89}(1) = 1, \quad A_{90}(1) = 0, \quad A_{91}(1) = 1, \quad A_{92}(1) = 0, \quad A_{93}(1) = 1, \quad A_{94}(1) = 0, \quad A_{95}(1) = 1, \quad A_{96}(1) = 0, \quad A_{97}(1) = 1, \quad A_{98}(1) = 0, \quad A_{99}(1) = 1, \quad A_{100}(1) = 0.$$


The three-phase transformer used in the model has the task to transform in magnitude the

any phase displacement between the primary and the secondary voltages. The secondary winding of the transformer under analysis is in delta connection. For this reason, the Delta (D1) winding connection was chosen for the primary and secondary windings in the dialog box of the transformer block (Figure 4.13). Thus this block represents a Dd0 transformer [8].

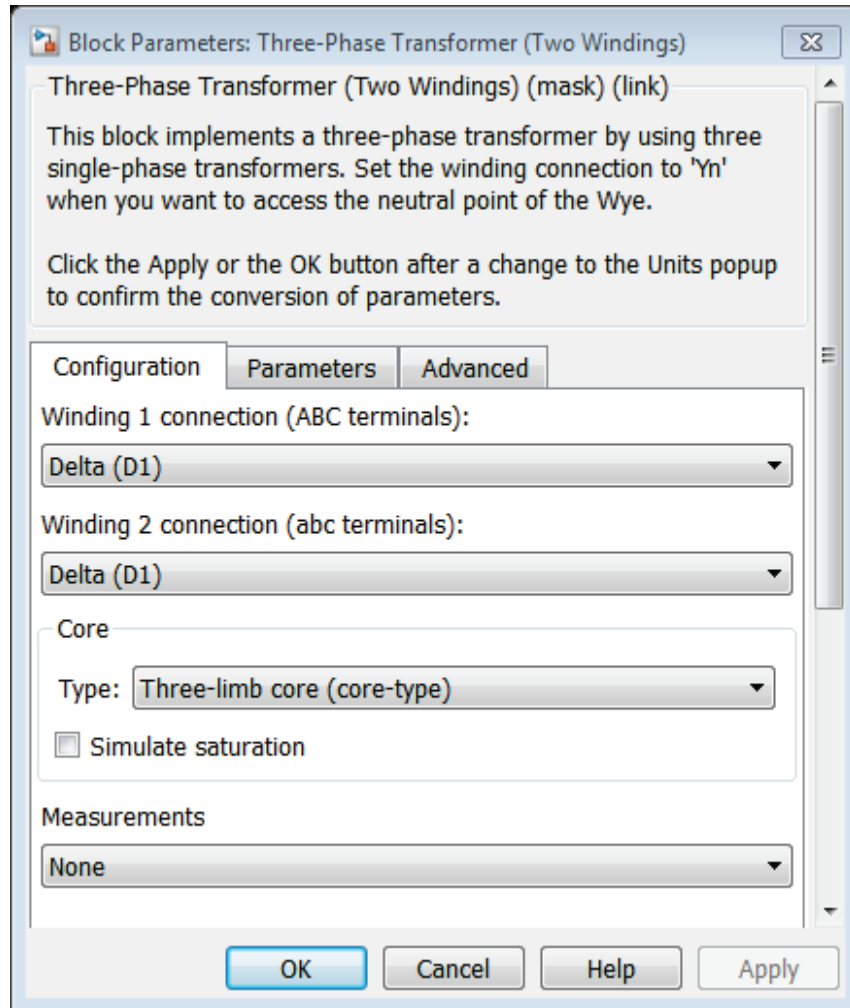


Figure 4.13: Delta/delta configuration of three-phase transformer block

The examined extended-delta/delta transformer has a three-limb magnetic core: in the present model this is simulated by choosing the three-limb core type of the three-phase transformer block. This will be better explained in a later Chapter.

The parameters of this transformer are expressed in p.u., as can be observed in the Figure 4.14, and they are based on the parameters discussed in Chapter 4.2.1. In particular, it should be noted that:

- The nominal power and frequency is *Powerfreq* vector;
- The primary nominal voltage is *VB* as calculated in initialization (Chapter 4.2.1.1);
- *R1* and *L1* are the second and the third element of the *Winding1* vector, as calculated in the initialization.
- The secondary nominal voltage, resistance and inductance of winding are expressed in the vector *Winding2* defined by the user in the extended-delta/delta subsystem dialog box;

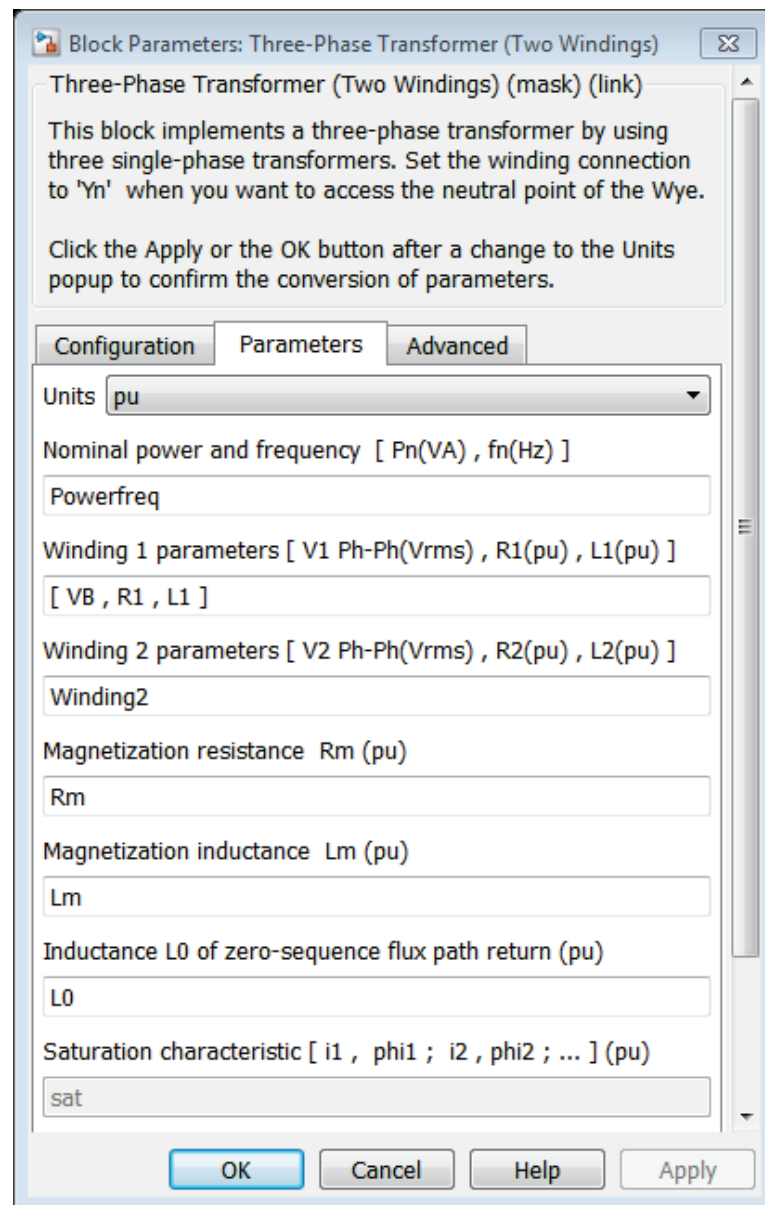


Figure 4.14: Delta/delta transformer block parameters

As can be observed in the Figure 4.14, all the primary impedance of the extended-delta/delta transformer is attributed to the primary winding of the Delta/delta transformer block. Although in an ideal representation this is not relevant, this is significant when considering a real transformer (this will be discussed in later Chapters).

4.2.4 Extended-delta/delta subsystem

The ideal phase-shifter subsystem and the delta/delta three-phase transformer described in Chapters 4.2.2.1 and 4.2.3 are connected together to form the extended-delta/delta subsystem (Figure 4.15). In the subsystem are present some *Three-Phase VI Measurement* blocks that provide the phase-to-phase voltages and line currents of the branch they are connected to.

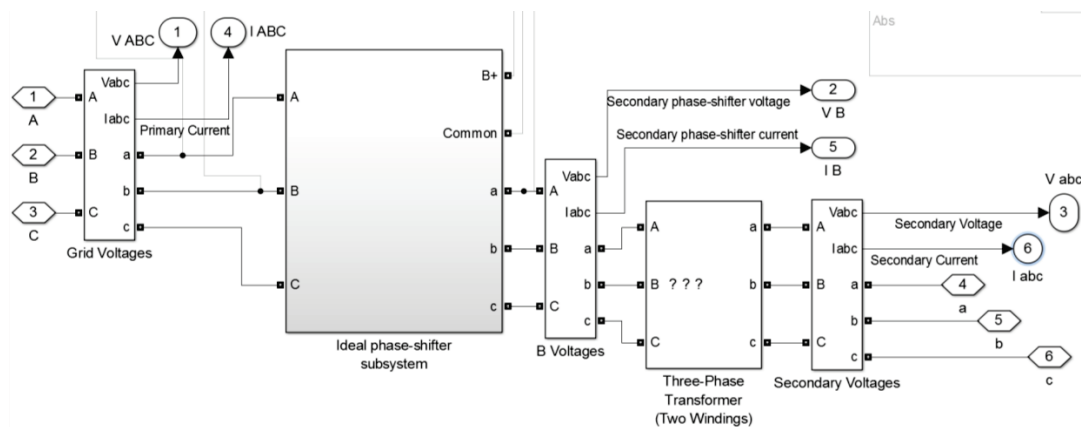


Figure 4.15: Extended-delta/delta subsystem connections

Within the subsystem there are also same ancillary blocks that are commented out (and appears in light grey): this blocks have been used for the measurement of the **B** phasor phase-shift and magnitude.

All the elements are connected together and masked under a subsystem, with an edited mask as described in Chapter 4.2.1. This subsystem has as input the three line voltages \mathbf{V} and as output the three secondary voltages \mathbf{V}' and it has six terminals for the measurements of voltages and currents in the different branches (Figure 4.16).

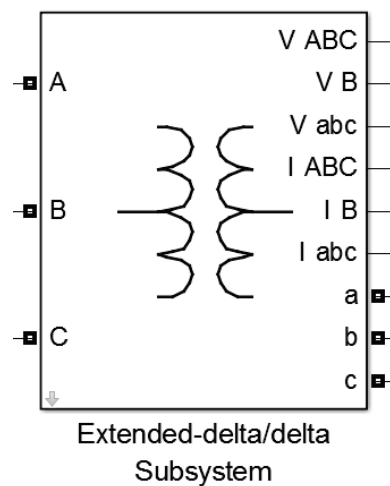


Figure 4.16: Extended-delta/delta subsystem mask

4.3 Real extended-delta/delta transformer's model

The model described in previous Chapters is valid from an electrical point of view and, neglecting the losses of the transformer, can represent an extended-delta/delta transformer with custom phase shift. To consider the dissipation, it is necessary to calculate the correct value of windings and magnetic impedance [15] and the saturation curve of the specific transformer under analysis.

The datasheet parameters and test data (like no-load losses, load losses, short circuit impedance, no-load current, etc.) of the ITER CCS converter transformer presented in Chapter 4.1 were used for calculations. All the value of the needed parameters has been calculated in p.u.

4.3.1 Model in per units

The simple mono-phase equivalent circuit of the extended-delta/delta transformer under analysis (Figure 4.17⁴) is here considered.

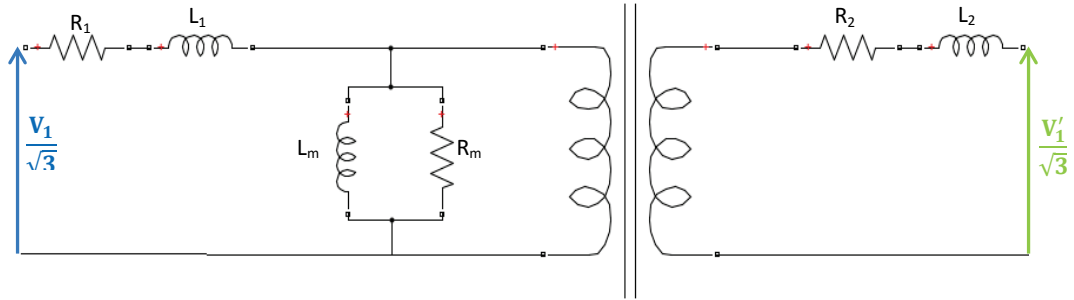


Figure 4.17: Mono-phase equivalent circuit

The per-units system is the expression of system quantities as fractions of a defined base unit quantity. To adopt a per-units system, a base power and base voltages for each side of transformer have to be defined [13], [15]. Then it is possible to define all resistances and inductances in the per-units system referring to the base voltages and to the base power. The mono-phase equivalent circuit in per-units becomes the one in the Figure 4.18.

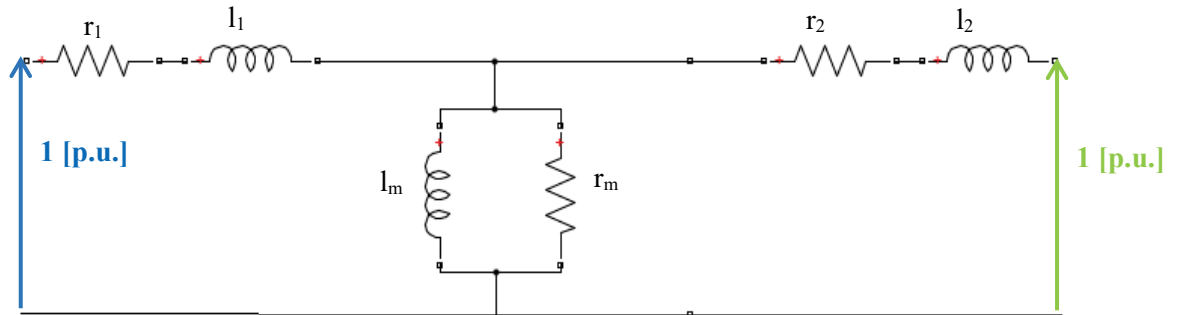


Figure 4.18: Mono-phase equivalent circuit in per units

Calculations in per-units system are simplified because quantities expressed as per-units do not change when they are referred from one side of a transformer to the other [16]. Therefore, the values of resistance r_l , inductance l_l , resistance r_m and inductance l_m in per-units can be

⁴ Capital letters refer to the quantity expressed in SI, lowercase letters in per-units system.

attributed, in the presented model, to the three-phase delta/delta transformer, as anticipated in Chapter 4.2.3.

The mono-phase equivalent circuit of the SPS ST built model is shown in the Figure 4.19 (where all the values are expressed in SI).

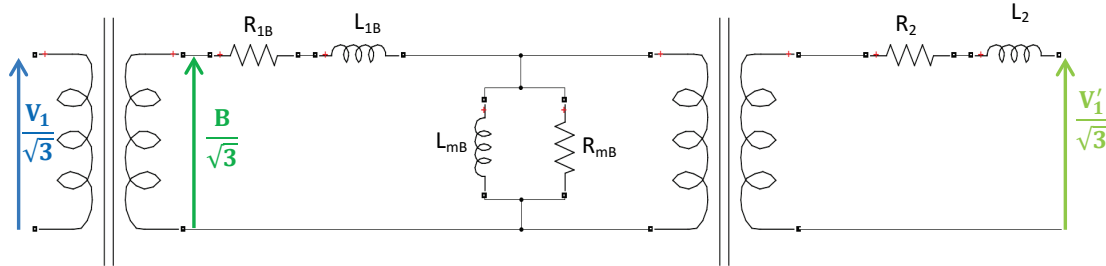


Figure 4.19: Mono-phase equivalent circuit of extended-delta/delta created model

Since in model of the extended-delta/delta transformer the values have to be typed in p.u., R_{1B} , L_{1B} , L_{mB} and R_{mB} are automatically calculated by SPS ST basing on the voltage B . In other words, the values of R_{1B} , L_{1B} , L_{mB} and R_{mB} have the same values of R_1 , L_1 , L_m and R_m when they are converted in per-units. Also the circuit in Figure 4.19 once converted in p.u. becomes the one in Figure 4.18.

Similarly, in this model the zero-sequence inductance $L0$ of the transformer is set in the extended-delta/delta subsystem dialog box and it is considered in the three-phase transformer block.

4.3.2 Needed parameters' script

In order to model the behaviour of CCS transformer of Chapter 4.1 with the built SPS Specialized Technology model, it is needed to know the values of the parameters of the mono-phase delta-equivalent electric circuit of the transformer under analysis [13], [15]. A MatLab script has been built to calculate these values (Figure 4.20).

```

1 - % data sheet
2 - f=50;
3 - Sn=2.209e6;
4 - V1n=22e3;
5 - V2n=0.327e3;
6 - P0=5.6e3/2;
7 - i0pc=1.23;
8 - Pcc=79.2e3/2;
9 - vccpc=16;
10 - % load parameters calculus
11 - cosficc=(Pcc/Sn)*100/vccpc;
12 - I1n=Sn/(V1n*sqrt(3));
13 - V1cc=V1n*vccpc/100;
14 - Z1cc=sqrt(3)*V1cc/I1n;
15 - R=Z1cc*cosficc;
16 - X=Z1cc*sin(acos(cosficc));
17 - L=X/(2*pi*f);
18 - % no-load parameters calculus
19 - cosfi0=P0/(Sn*i0pc)*100;
20 - R0=3*V1n^2/P0;
21 - X0=R0/tan(acos(cosfi0));
22 - L0=X0/(2*pi*f);
23 - % per unit values calculus
24 - vb1=V1n;
25 - vb2=V2n;
26 - Sb=Sn/3;
27 - zb1=vb1^2/Sb;
28 - zb2=vb2^2/Sb;
29 - lb1=zb1/(2*pi*f);
30 - lb2=zb2/(2*pi*f);
31 - format longE;
32 - r=R/zb1;
33 - l=L/lb1;
34 - % output
35 - r1=r/2
36 - l1=l/2
37 - rm=R0/zb1
38 - lm=L0/lb1
39 - format shortG;

```

Figure 4.20: Script for calculus of transformers parameters

Referring to Figure 4.20, from line 2 to line 9 there is the declaration of the datasheet parameters, which are:

- Nominal frequency f ;
- Three-phase nominal power S_n ;
- Nominal primary phase-to-phase voltage V_{1n} ;
- Nominal secondary phase-to-phase voltage V_{2n} ;
- No-load losses P_0 ;
- No-load current percentage i_{0pc} ;
- Load losses P_{cc} ;
- Impedance voltage percentage v_{ccpc} ;

Starting from the datasheet parameters that are here set, the script calculates and saves as variables the transformer’s parameters of interest.

From line 11 to line 17 the on-load parameters are calculated and in particular longitudinal resistance R and inductance L for the single-phase equivalent circuit:

11 -	$\cos \varphi_{cc} = \frac{P_{cc}}{S_n} * \frac{100}{v_{cc\%}}$	
12 -	$I_{1n} = \frac{S_n}{(\sqrt{3} \cdot V_{1n})}$	Nominal primary Current
13 -	$V_{1cc} = V_{1n} * \frac{v_{ccpc}}{100}$	Primary impedance voltage
14 -	$Z_{1cc} = \sqrt{3} * \frac{V_{1cc}}{I_{1n}}$	Primary short-circuit impedance
15 -	$R = Z_{cc} * \cos \varphi_{cc}$	Longitudinal resistance
16 -	$X = Z_{cc} * \sin \varphi_{cc}$	Longitudinal reactance
17 -	$L = \frac{X}{2\pi \cdot f}$	Longitudinal inductance

In the same way, from line 19 to line 22, the no-load parameters are calculated, in particular magnetic resistance R0 and inductance L0.

19 -	$\cos \varphi_0 = \frac{P_0}{S_n \cdot i_{0\%}} \cdot 100$	
20 -	$R_0 = 3 \cdot \frac{V_{1n}^2}{P_0}$	Magnetic resistance
21 -	$X_0 = \frac{R_0}{\tan(\cos^{-1} \varphi_0)}$	Magnetic reactance
22 -	$L_0 = \frac{X_0}{2\pi \cdot f}$	Magnetic inductance

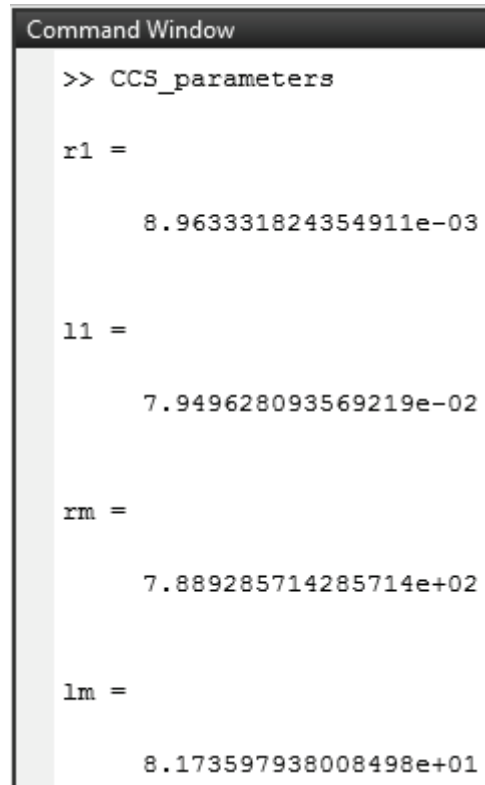
In the subsequent lines the per-units values of the mentioned parameters are calculated. Note that in line 26 the base power is the mono-phase nominal machines power (note 2, page 15).

In lines 32 and 33 the longitudinal resistance and inductance values are calculated in p.u. This impedance can be attributed to either windings, is split in half, at lines 35 and 36, with the aim of attributing it to both the primary and secondary windings, as it commonly done [15]. In the subsequent lines the magnetic resistance and inductance in p.u. are then calculated.

At lines 31 and 39 there are format indications:

- The command *format longE* set the long scientific notation: with 15 digits after the decimal point for double values and 7 digits after the decimal point for single values.
- The command *format shortG* brings back the settings of format at the default.

By running this script, the variables defined within it are saved in the workspace and in the command window the values in p.u. of magnetic resistance and inductance and resistance and inductance of each winding appear (Figure 4.21).



```
Command Window

>> CCS_parameters

r1 =

    8.963331824354911e-03

l1 =

    7.949628093569219e-02

rm =

    7.889285714285714e+02

lm =

    8.173597938008498e+01
```

Figure 4.21: Example of script output in MatLab command window

These numerical values can be manually put in the extended-delta/delta subsystem’s dialog box (Figure 4.22) or, as SPS ST is toolbox of MatLab/Simulink®, we can type the variable names in the dialog box (Figure 4.23).

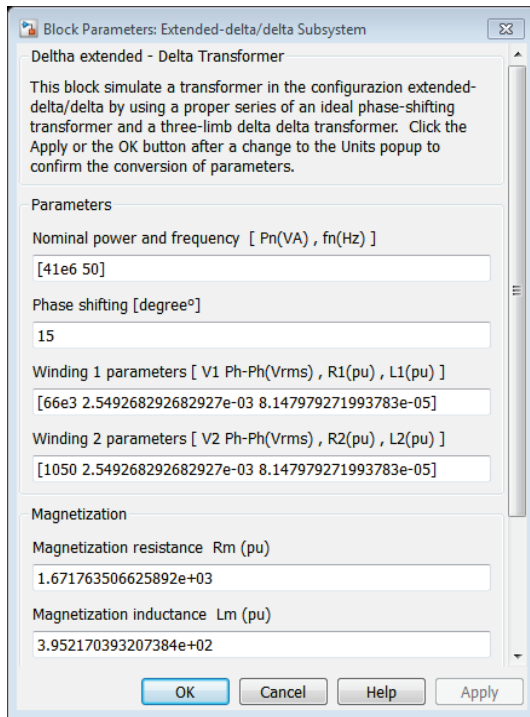


Figure 4.22: Numerical parameters editing (illustrative values)

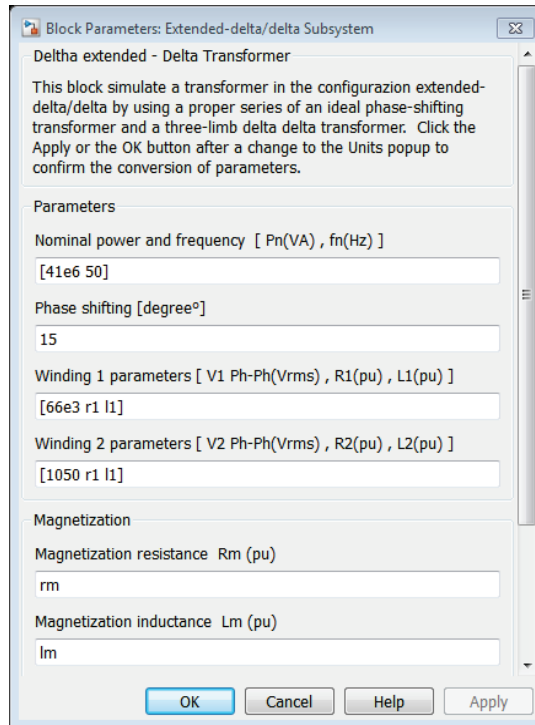


Figure 4.23: Name variables editing (illustrative values)

4.3.3 Model of core saturation

Until now the saturation of the transformer’s core has not been mentioned, but it is a fundamental aspect to consider in order to have a good transformer’s model, especially if some kind of fault has to be studied.

As when the saturation was neglected, the mono-phase equivalent electric circuit of Figure 4.18 can be studied putting, instead of the magnetization inductance L_m , a nonlinear inductance L_{SAT} (Figure 4.24).

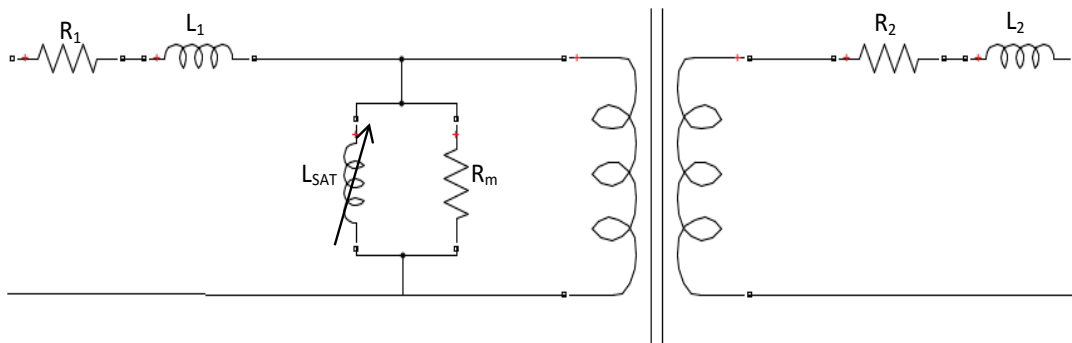


Figure 4.24: Saturable mono-phase equivalent circuit

SPS ST transformer blocks can simulate, as seen in Chapter 3.1.2, core saturation enabling this feature from dialog box of the block (Figure 4.25).

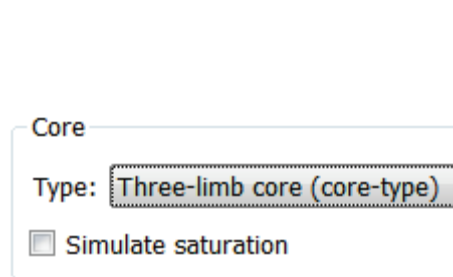


Figure 4.25: Transformer dialog box without saturation settings

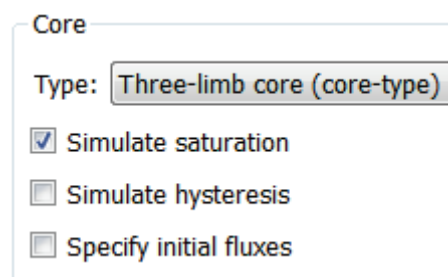


Figure 4.26: Transformer dialog box with saturation settings

Once enabled the simulation of saturation, it can be chosen to simulate also hysteresis (a proper magnetic characteristic has to be edited with a SPS ST tool) and to edit the initial flux values (Figure 4.26).

It can be observed that enabling core saturation, in the parameters tab the possibility to input the magnetization characteristic appears and the magnetic inductance becomes a useless parameter (Figure 4.27). Thus magnetization characteristic set in the dialog box of the transformer actually is the characteristic of the nonlinear inductance in the equivalent circuit.

Configuration	Parameters	Advanced
Units pu		
Nominal power and frequency [Pn(VA) , fn(Hz)] [250e6 , 60]		
Winding 1 parameters [V1 Ph-Ph(Vrms) , R1(pu) , L1(pu)] [735e3 , 0.002 , 0.08]		
Winding 2 parameters [V2 Ph-Ph(Vrms) , R2(pu) , L2(pu)] [315e3 , 0.002 , 0.08]		
Magnetization resistance Rm (pu) 500		
Magnetization inductance Lm (pu) 500		
Inductance L0 of zero-sequence flux path return (pu) 0.5		
Saturation characteristic [i1 , phi1 ; i2 , phi2 ; ...] (pu) [0,0 ; 0.0024,1.2 ; 1.0,1.52]		
Initial fluxes [phi0A , phi0B , phi0C] (pu): [0.8 , -0.8 , 0.7]		

Figure 4.27: Saturation characteristic setting

Since the magnetization characteristic is in p.u., it can be imputed to any transformer of the model, as seen in Chapter 4.3.1. In this model the core magnetic saturation is considered in the three-phase transformer block.

4.3.3.1 Computation of saturation characteristic of CCS transformer

In SPS ST, to model a nonlinear transformer, a saturation characteristic has to be set by specifying a series of magnetization current/ flux pairs (in p.u.) starting from the pair (0,0) [12]. It has to be underlined the magnetization current is the current that is passing through the magnetic inductance not in all the magnetic impedance.

The Korean manufacturer did not provide magnetizing curve of CCS converter transformer with that pair, but with the pair B-H (see Chapter 4.1), so some calculations are needed to obtain the correct pair.

The flux is proportional to the B induction field:

$$\Phi = B \cdot S$$

In per-units, since S is simplified, the value of the flux and the value of the B field are the same:

$$B_{[pu]} = \frac{B}{B_b} = \frac{B \cdot S}{\Phi_b} = \frac{\Phi \cdot S}{\Phi_b \cdot S} = \Phi_{[pu]}$$

Moreover the magnetization current is proportional to the magnetization force and can be calculated from the relation:

$$H \cdot N = I \cdot l$$

Where N is the number of turns and l is the length of the pathway of the flux in the magnetic circuit.

Then the value in per units is obtained dividing the magnetization current for the base current of one side of the transformer. In particular, in order to simplify the calculation of the magnetization current from magnetization force, the secondary side parameters have been chosen, because it has only one winding per phase and not two winding as the primary side (the extended and the main, see Chapter 2). Since the length l is unknown, in the calculation it has been approximated, introducing an error in the model, to the length of the column of the transformer. In other words, as can be seen in Chapter 4.1:

- $N=N_2=17$
- $l=695$ [mm]

So from B-H pairs (extracted by Figure 4.2) the Φ - i_μ pairs are calculated in per-units:

H (A/m)	B (T)
0	0
6,6	0,3
8	0,5
11,5	0,99
16	1,32
42	1,65
4200	1,98

**Table 4: B-H
magnetization pairs of
CCS transformer**



i_μ (pu)	Φ (pu)
0	0
6,92E-05	0,181818
8,39E-05	0,30303
0,000121	0,6
0,000168	0,8
0,00044	1
0,044025	1,2

**Table 5: Φ - i_μ
magnetization pairs of
CCS transformer**

The pairs of Table 5 are input to the saturation characteristic parameters of the delta/delta transformer described in Chapter 4.2.3.

The Φ - i_μ pairs can also be plotted to see the magnetization characteristic behavior.

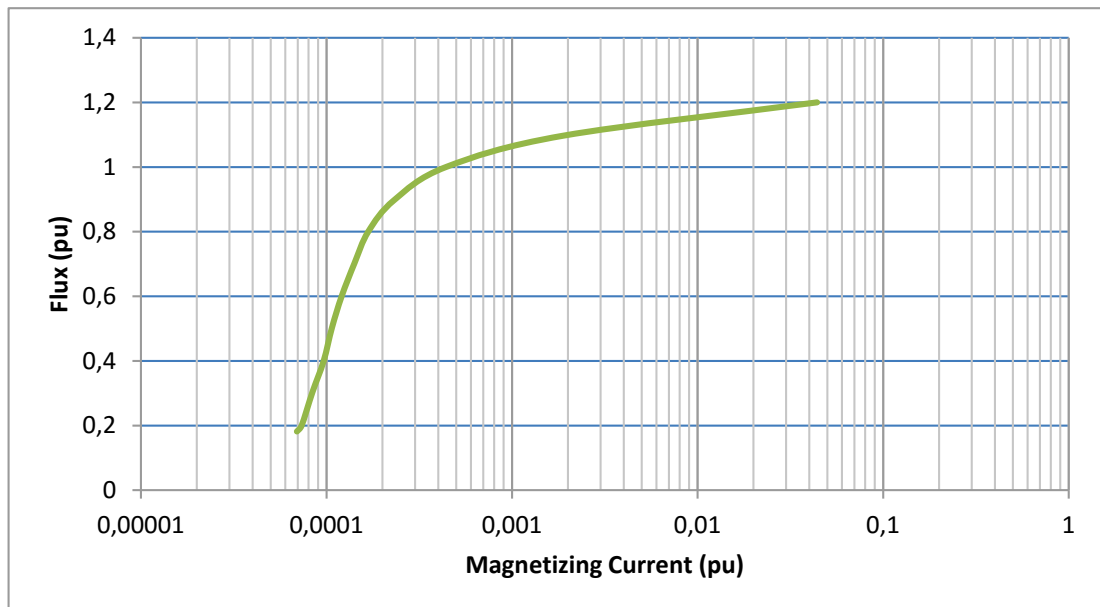


Figure 4.28: Magnetization characteristic with the Φ - i_μ pairs

5. Model’s first validation: comparison with actual datasheets

A first validation of the proposed model consists of a comparison between the result of simulations in typical situations and the values reported in the datasheet of the real transformer. In particular, the comparison occurs between the power values calculated using the actual impedance values and the power values as they appear from the circuit simulation performed using SPS ST.

The parameters based on the datasheet of the CCS Rectifier Transformer presented in Chapter 4.1 (Table 1) are used. These values regard the entire transformer, composed as already mentioned of two units. For this reason, the losses shown in the table are divided by two.

The values of the input parameters in the extended-delta/delta subsystem’s dialog box have been calculated using the script presented in Chapter 4.3.2.

Three different situations have been simulated:

1. No load: considering at the secondary a resistance of $10^{10}[\Omega]$;
2. Short circuit: considering at the secondary a resistance of $10^{-5}[\Omega]$;
3. On load: considering at the secondary a load of 2.209 [MW] (transformer’s nominal power).

5.1 Verification circuit

The SPS ST verification circuit includes a three-phase voltage source which supplies the transformer in the different load conditions (Figure 5.1).

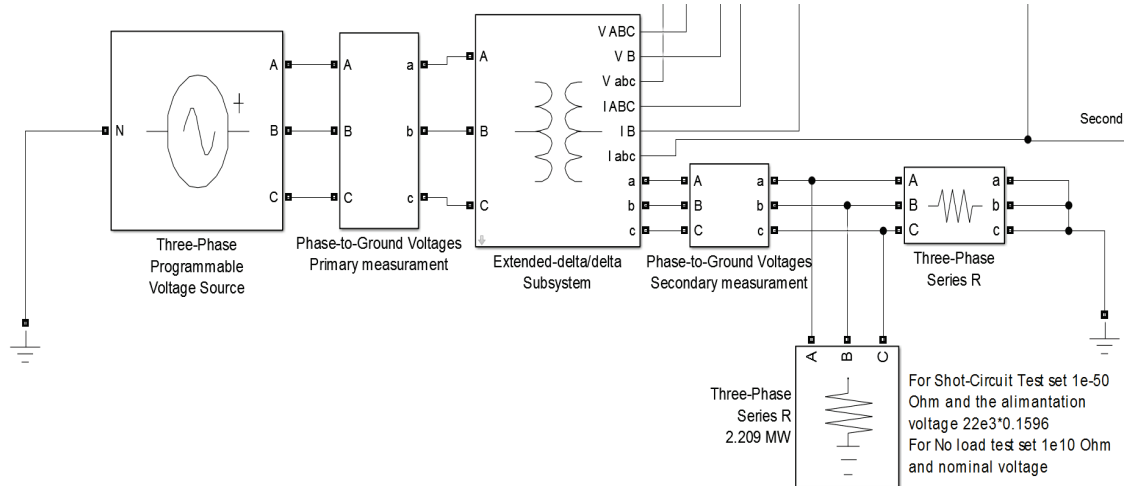


Figure 5.1: SPS's verification circuit

The three-phase source produces a 22 [kV] RMS three-phase voltage that supplies the transformer block, passing through a phase-to-ground voltage measurement block. The load is connected at the secondary side of the transformer block and it is changed in the different test situations. Also at the secondary side there is a phase-to-ground voltage measurement block: this two measurement blocks are used to have the phase reference and to calculate the powers exchanged.

The following values are calculated with the Simulink® signals as output of the extended-delta/delta subsystem and with the two additional voltage measurements. They are displayed in some Simulink®'s scopes or in display blocks (Figure 5.2) and consist of:

- Primary and secondary voltages and currents values;
- RMS primary and secondary voltages and currents values;
- Voltage and current phase-shift of each phase;
- Power at the primary;
- Power at the secondary;
- Losses: as difference between the values of power at primary and secondary.



5.2 Phase shift measurement

The principal purpose of an extended-delta/delta transformer is to produce secondary voltages with a phase shift. So first it is important to verification whether the primary voltages and the secondary voltages have the chosen phase shift.

To do this a subsystem called *Tern Shift* has been built using the Simulink® *Fourier* block that provides in output the magnitude and the phase of the signal in input. The signals of the primary and secondary voltages pass through these blocks and their phase is calculated; then, phase per phase, the phase shift as the difference of the two phases is calculated (Figure 5.3).

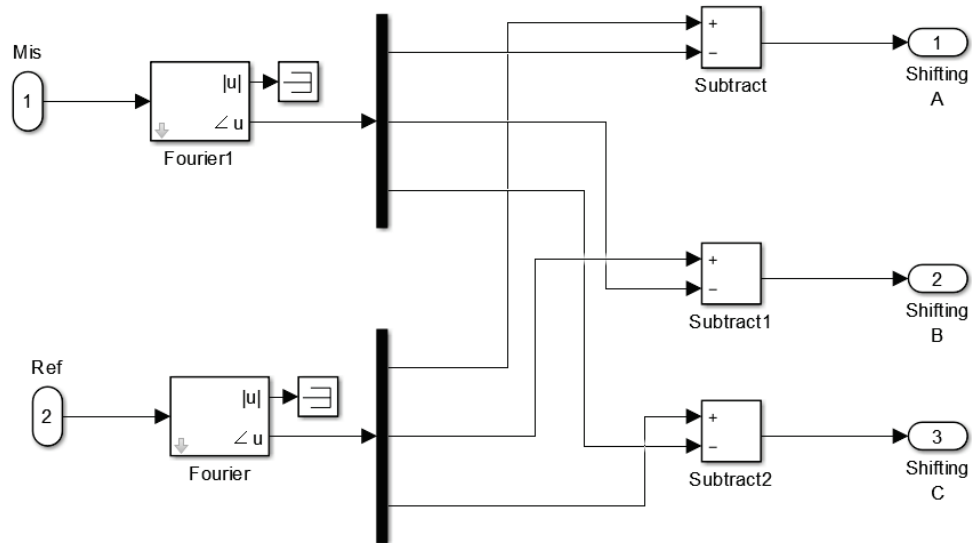


Figure 5.3: Triplet Shift subsystem

The nominal phase shift has to be measured in no-load condition [8] and at steady state, so after to the transitory behavior caused by the saturation of the transformer. Otherwise the impedance of the load and the short-circuit impedance are the dominant impedances of the circuit and the phase shift is determined by their phase angles.

In no-load situation the phase shift measured was the one set in the transformer dialog box, so the phase shift can be considered well described by the built model. An example is given in the Figure 5.4 where the phase shift in the case of the CCS converter transformer is measured.

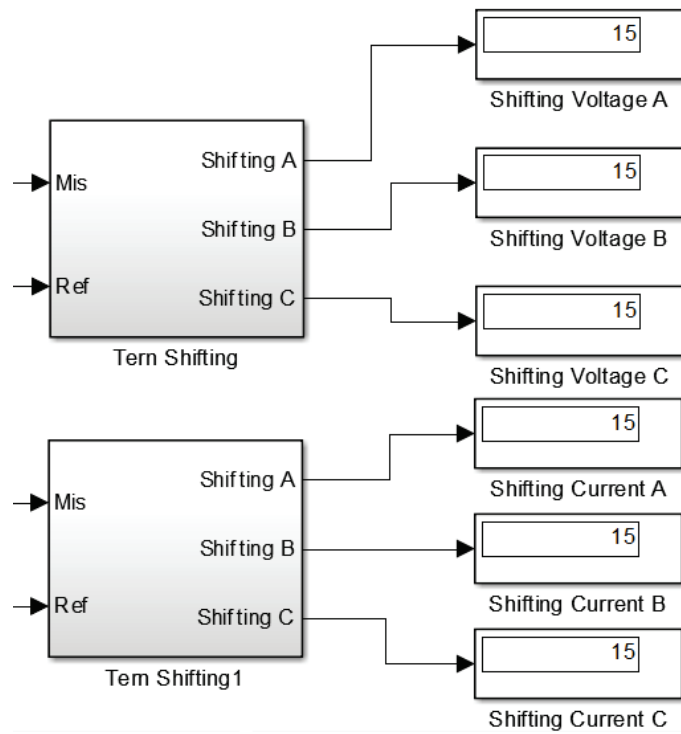


Figure 5.4: Measured phase-shift, an example with 15° set

5.3 No load simulation

The purpose of this simulation is to verify that, with no load at secondary, the power at primary side of the subsystem modelling the extended-delta/delta transformer correspond to the datasheet value. Moreover, it is possible to check whether the current measured match with the no-load current written in the datasheet.

Since at the secondary side there is the phase-to-ground voltage measurement block, it cannot be an open circuit. So to do this simulation at the secondary side, as previously said, a very high resistance ($10^{10}[\Omega]$) is connected, that is like an open circuit (Figure 5.5).

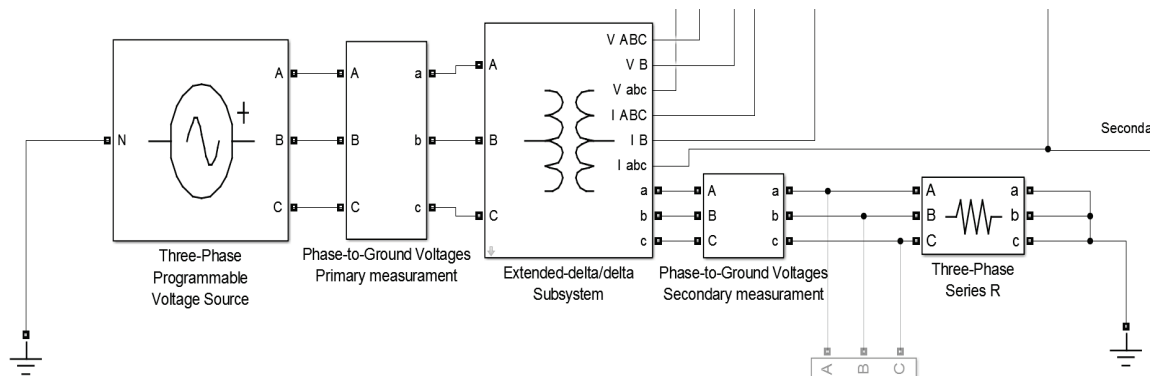


Figure 5.5: Circuit for no-load and short-circuit verification

After changing the topology, the simulation has been run and the displays of the power are shown in Figure 5.6.

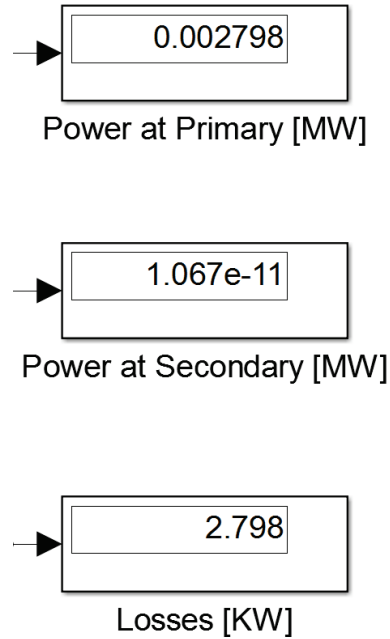


Figure 5.6: Measured power in no-load simulation

It can be observed that the no-load loss, shown in the primary power display block, is 0,002798 [MW] and is almost the no-load loss in datasheet of 2,8 [kW].

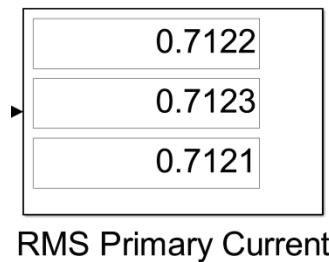


Figure 5.7: No-load RMS primary currents

The measured RMS primary current is, in this condition, 0,712 [A]. Taking as nominal current the one measured in the on-load verification (see Chapter 5.5) 60,08 [A] the no-load current percentage is:

$$i_{\%} = \frac{I_0}{I_{1N}} * 100 = \frac{0,7123}{60,08} * 100 = 1,22\%$$

The calculated no-load current percentage is almost the same as the one given in the data sheet of 1,23%.

5.4 Short circuit simulation

The purpose of this simulation is to verify that the winding resistances and inductances calculated for the model well represent the transformer’s behavior in short-circuit. To do this it is necessary to supply the transformer with the impedance voltage percentage of the nominal voltage [13]. If the power registered at the primary side of the model has the same value of the load loss in the datasheet, then the model well represents the CCS converter transformer in this condition.

The topology of the simulation circuit remains the same as the one presented in no-load simulation (Figure 5.5), but some settings of the blocks need to be changed. First the voltage of source has to be set, in dialog box (Figure 5.8), to the impedance voltage and then the resistance at the secondary side has to be small enough to resemble a short circuit (Figure 5.9).

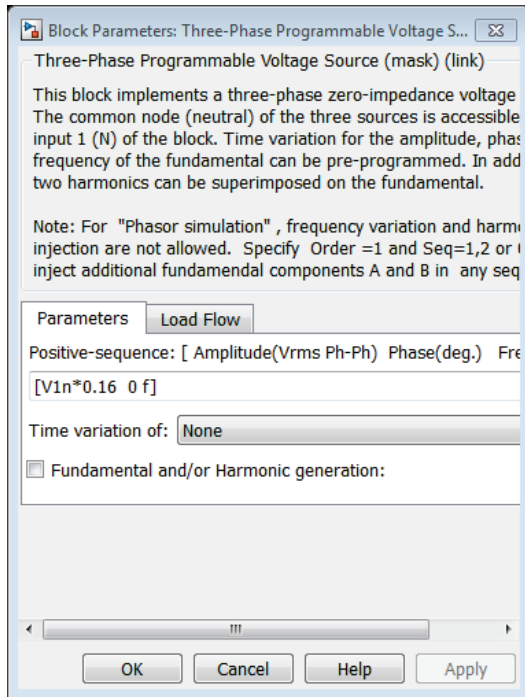


Figure 5.8: Voltage source dialog box

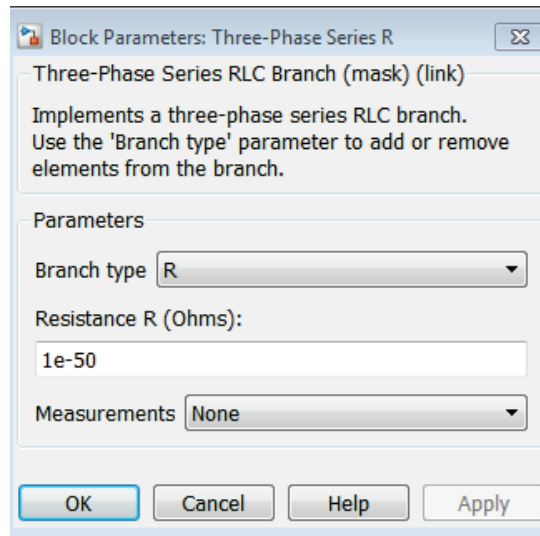


Figure 5.9: Secondary resistance dialog box

Finally, the simulation can be run and in the Figure 5.10 the resulting power values are shown.

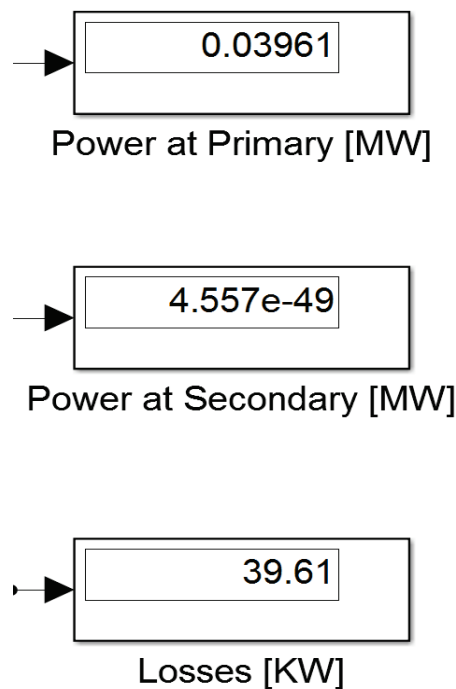


Figure 5.10: Measured power in short-circuit simulation

Note that a short-circuit power of 0,03961 [MW] results, as was expected, since 39,6 [kW] is half of the datasheet load loss. Also this simulation verifies the validity of the model.

5.5 On load simulation

The purpose of this simulation is to verify that, at nominal conditions, the total loss calculated in the model is the same as the total loss in the datasheet. As should be noticed from Table 1, the value of the total loss include the harmonic losses and so it is different from the sum of load and no-load losses:

$$2,8 + 39,6 = 42,4 \neq 49,9$$

Since the circuit parameters have been calculated from the values of load and no-load losses, one can assume that the total losses are the sum of this two values. In other words, this simulation can be actually considered as another proof of the validity of the previous verifications.

As mentioned before, to do this verification a load block, set as a pure resistance and for absorb the nominal power 2,209 [MW], has been connected to the transformer’s secondary side (Figure 5.11).

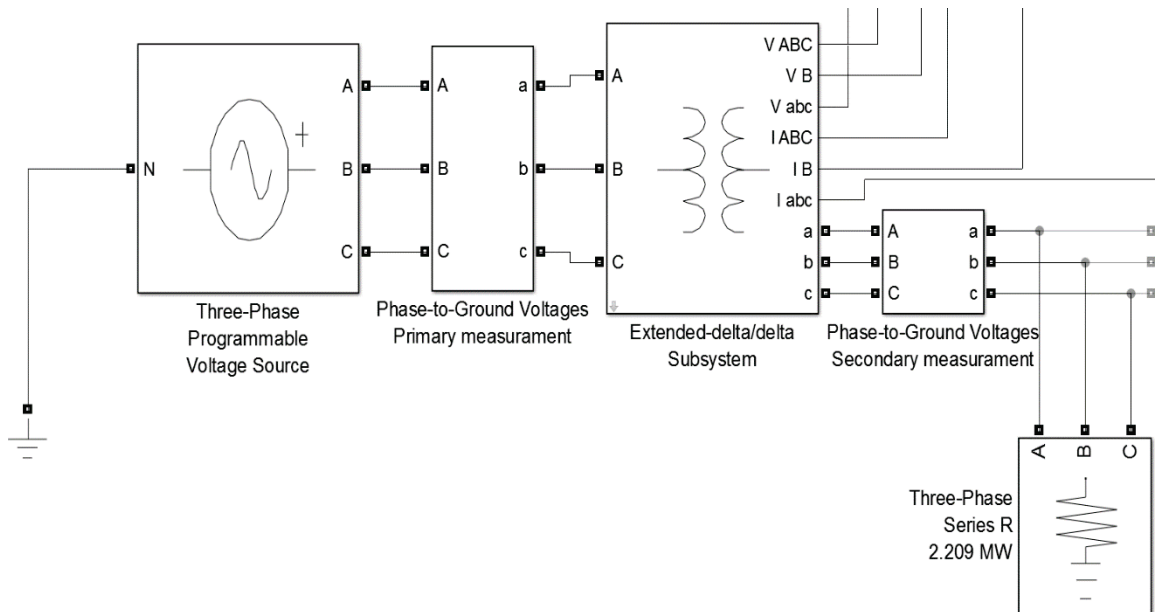


Figure 5.11: On load verification circuit

In these conditions, the simulation has been run and the power measurements shown in Figure 5.12 were registered.

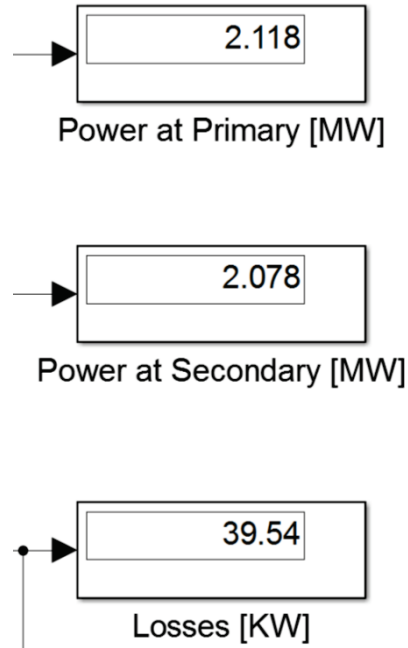


Figure 5.12: Measured power with a resistance load of S_n

As it can be observed from the Figure 5.12, the measured losses in this situation are smaller than expected. This occurs because the load block at the secondary side is set to work at the secondary nominal voltage, but the voltage at the secondary side is not the nominal one due to the internal voltage drop of the transformer. This is also evident from the display block of the secondary power: indeed the power is not the chosen one. To solve this issue, the load voltage has to be changed considering the voltage drop. So:

$$V_{2load} = V_{2N} - \Delta V$$

The value of ΔV has been estimated in order to see on the secondary power display the adsorption of 2,209 [MW] and then the losses are calculated again.

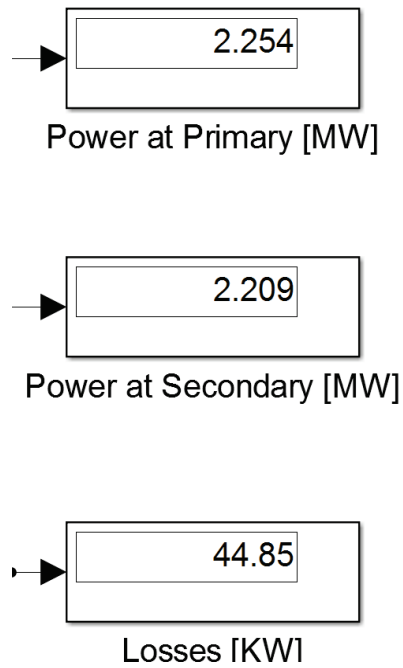


Figure 5.13: Power losses with nominal power adsorption

As it can be observed, the losses calculated in this situation are 44,85 [kW] that is near to the expected value of 42,4 [kW].

In this simulation, it can be appreciated (Figure 5.14) that the measured RMS current value at primary is 60.08 [A], which is very near to the nominal primary current value of 63 [A] obtained from the datasheet as:

$$I_{1N} = \frac{P_N}{\sqrt{3} * V_{1N}}$$

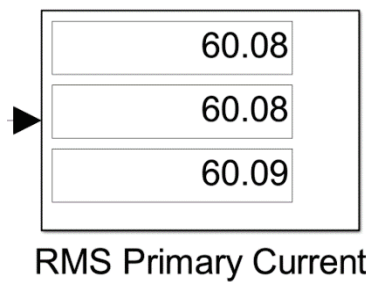


Figure 5.14: Primary on-load current

5.6 Results comparison in brief

The results of the previous verification results are reported in brief in Table 6.

Test	SPS ST Model	Datasheet values
Phase Shift	15°	15°
No-load Loss	2.798 [kW]	2.8 [kW]
No-load current	1.22 %	1.23 %
Short circuit Loss	39.61 [kW]	39.6 [kW]
Impedance voltage	16 %	16 %
On load Loss	44.85 [kW]	42.4 [kW]

Table 6: results comparison

It can be observed that the values here reported are almost the same so the transformer is properly represented.

6. Model’s second validation: a different approach

The SPS Specialized Technology model developed in Chapter 4 has been verified in comparison with the typical transformer’s tests, because they were the only available in the actual datasheet of a real transformer. To validate the SPS ST model in other uncommon conditions (i.e. in some specific fault conditions), the comparison with other experimental measurements should be performed. However, these kinds of tests might have a deep impact on the transformer integrity and it would have been difficult and expensive to find a transformer to perform experimental tests. Finally, considering also time constraints, performing real tests is clearly not in the scope of this thesis.

For these reasons, another simulation model of CCS transformer has been built, using SPS *Simscape Components*. This MatLab/Simulink® toolbox gives the possibility to “physically” model the transformer, i.e. including magnetic circuits.

This second model has been used in the same simulations of Chapter 5 and the results compared.

In addition, some extreme conditions of interest for ITER applications have been simulated using both approaches (SPS SC and SPS ST), achieving similar results

Actually the two models behaved in a similar way, providing a substantial validation for both and a significant robustness indication for the first SPS ST model, which is the main aim of the present thesis work.

6.1 SPS Simscape Components model

With the blocks presented in Chapter 3.2 has been built a subsystem that represent an extended-delta/delta transformer. This subsystem has been composed starting from a Simscape example, that can be found in reference [17], where the same traditional transformer is modelled with both the SC and the ST Simscape Power Systems™ libraries. The SC part of that example has been modified to represent an extended-delta/delta transformer.

The created subsystem (Figure 6.1) can be divided in two parts: the electric circuit (blue) and the magnetic circuit (pink). These two parts interact with each other in the *Electromagnetic Converter* blocks and will be analysed separately.



6.1.1 Turns of electromagnetic converter blocks

The *Electromagnetic Converter* block is presented in Chapter 3.2.2 and plays a very important role in this model. Since the blocks represent the transformer windings, the number of turns of the different blocks have to respect the relation presented in Chapter 2.1.1. In particular, defining the number of turns of one winding, the others are uniquely established. The number of turns of all the blocks is so calculated in the parameter initialization of the subsystem.

In the Figure 6.1, and zoomed in the Figure 6.2, can be observed that all the *Electromagnetic Converters* blocks have a linear reluctance in parallel at the magnetic side.

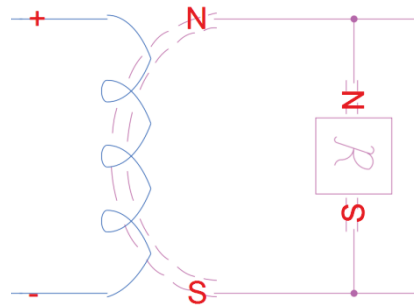


Figure 6.2: Zoom of reluctance in parallel with Electromagnetic converters

This reluctance, if correctly set, could be set to model the winding dissipations of flux. However, this aspect is already considered with the leakage inductance in the electric circuit that is an easier parameter to calculate. Consequently, this reluctance should be removed; but, removing it, some numerical errors occur and the model cannot converge. For this reason, these reluctances are present in the model and they are set to have very high value so that their effect can be neglected.

6.1.2 Electrical Circuit

Figure 6.1 can be observed that the electric circuit is divided in two parts: one represents the primary windings side and the other the secondary windings side, with their impedances.

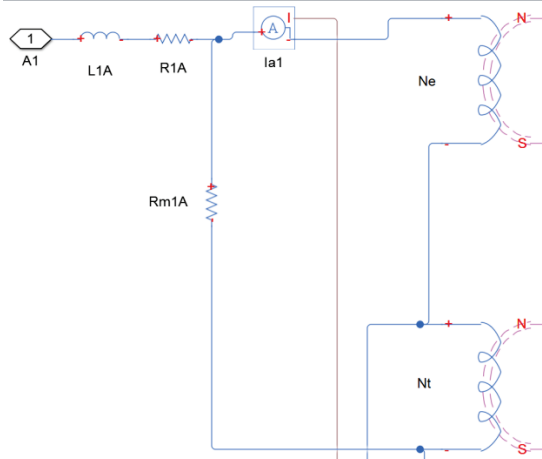


Figure 6.3: Zoom on one phase of primary winding

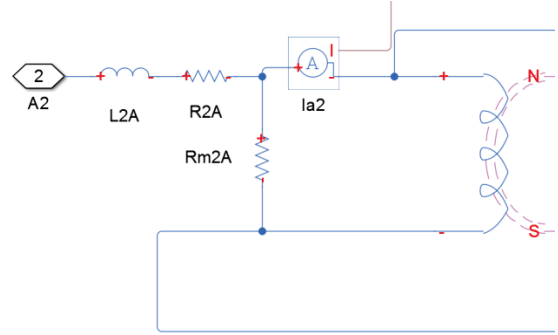


Figure 6.4: Zoom on one phase of secondary winding

The resistances **R1** and **R2** are the wye-equivalent resistances of the primary windings and secondary windings. It has to be underlined that these are wye-connected and so their value is one third of the delta-equivalent resistance (that has to be input in the SPS ST model). The same is for the winding inductances leakage **L1** and **L2**.

The resistances **Rm1** and **Rm2** are the magnetic resistances that represents the iron core losses of the transformer from an electrical point of view. Note that here there are not the frequently seen magnetic inductances in parallel with these resistances; this is because their effect is considered within the magnetic circuit.

In the Figure 6.1 and in the Figure 6.3 it is possible to see that the primary side has two *Electromagnetic Converter* blocks: one is the extended winding and the other is the main winding (as reported in Chapter 2). All the primary *Electromagnetic Converter* blocks are electrically connected together to realize the extended-delta windings connection: the main windings are connected in a delta configuration and the extended winding are connected to the corners of the triangle.

In the Figure 6.1 and in the Figure 6.4 it is possible to observe that the secondary *Electromagnetic Converter* block are electrically connected in a delta configuration.

Each primary winding couple and secondary winding has also one single-phase current sensor per phase, to measure the current flowing in the two sides of the transformer.

6.1.3 Magnetic circuit

The magnetic circuit, pink in Figure 6.1, represents the core of a three-limb transformer with an extended-delta connection. With this kind of connection there are two magneto motive force generators at the primary and one at the secondary per limb, from magnetic point of view. The electric equivalent scheme of the magnetic circuit is shown in Figure 6.5.

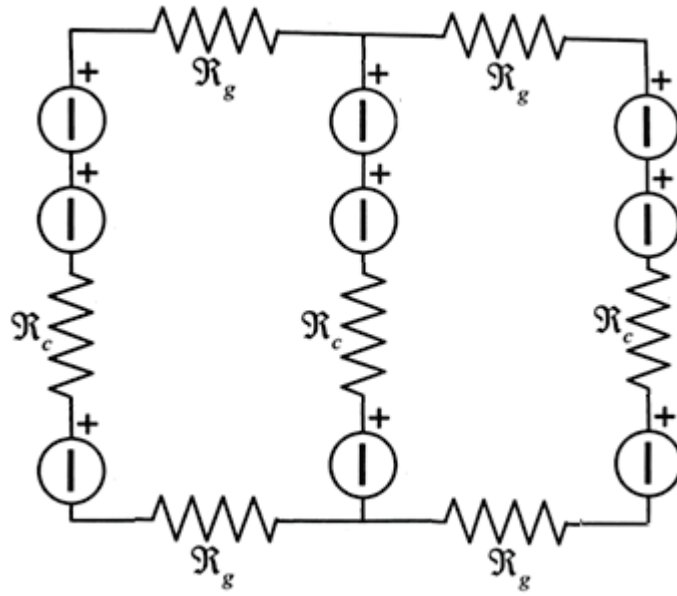


Figure 6.5: Electric equivalent scheme of the magnetic circuit

Comparing the Figure 6.1 with the Figure 6.5 it can be seen that the blue blocks in the magnetic circuit of first figure represent the iron reluctance of a column or of a yoke. These reluctances are variable reluctances, modelled with a *Controlled MMF Source* and with a feedback of flux.

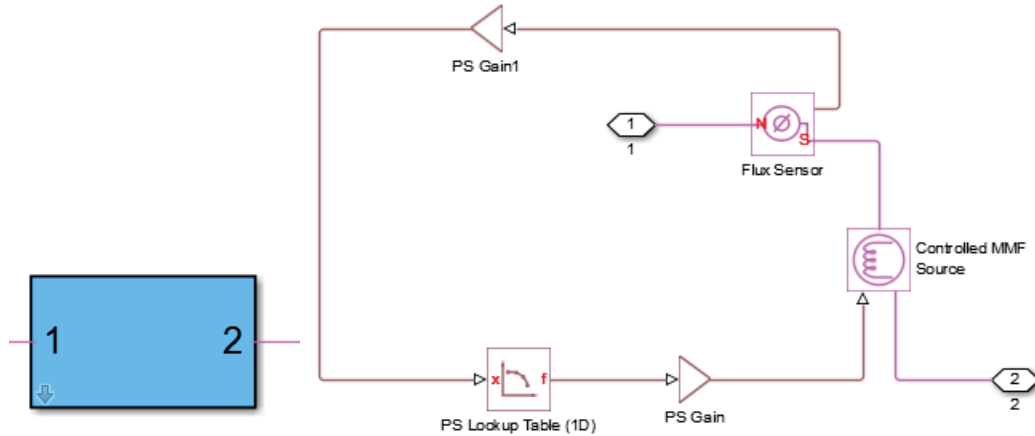


Figure 6.6: Iron reluctance model subsystem (left) and expanded (right)

The feedback signal is created starting by a measurement of flux. Then the value of the flux is divided by the cross section of the iron core transformer in the branch to obtain the induction, in fact:

$$\Phi = B \cdot S \rightarrow B = \frac{\Phi}{S}$$

Then the value of induction is sent to a block where the B-H characteristic is modelled and gives as output the correct H value for the B in input.

Finally, the value of the magnetization force H is multiplied by the branch's length of the magnetic circuit the reluctance is representing, for having the signal of control for the mmf source.

Please note that this block can represent the magnetic characteristic of the transformer just having the B-H curve, so it isn't necessary to do the calculation done (see Chapter 4.3.3.1) to model CCS transformer's saturation with the presented SPS ST model.

6.1.4 Subsystem mask

The physical system presented is masked under an edited subsystem to make it easier to use in a SPS Simscape Components' circuit (Figure 6.7). In the block A1, B1 and C1 are the primary terminals and A2, B2 and C2 are the secondary. Moreover the block has 2 measurement output: one is the vector of fluxes in each column and the other is currents' vector.

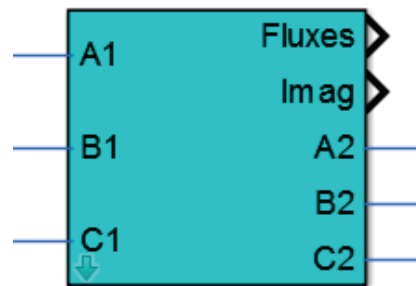


Figure 6.7: Mask of the SPS Simscape Component transformer's model

The block has an edited dialog box where all the typical parameters of a transformer can be set. In the dialog box have to be also set the dimensions of the transformer's core and the secondary winding's number of turns (Figure 6.8). In order to simulate the CCS converter transformer, the parameters calculated in Chapter 4.3.2 has been considered as input, reminding that in this model the windings' impedences have to be divided by a factor 3.

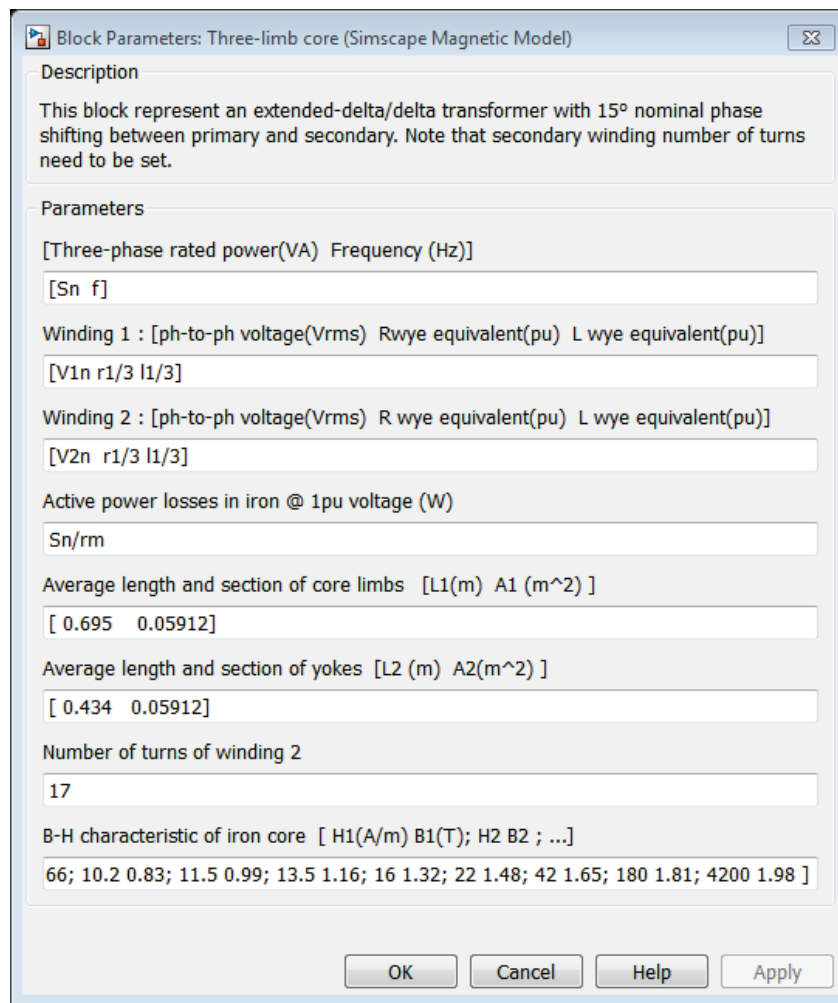


Figure 6.8: Dialog box of built block

The dimensional data of the core acts in the variable reluctance blocks together with the B-H characteristic of the core (see Chapter 6.1.3).

In the initialization tab of the editing parameters, many parameters are calculated from the one input in the dialog box (Figure 6.9).

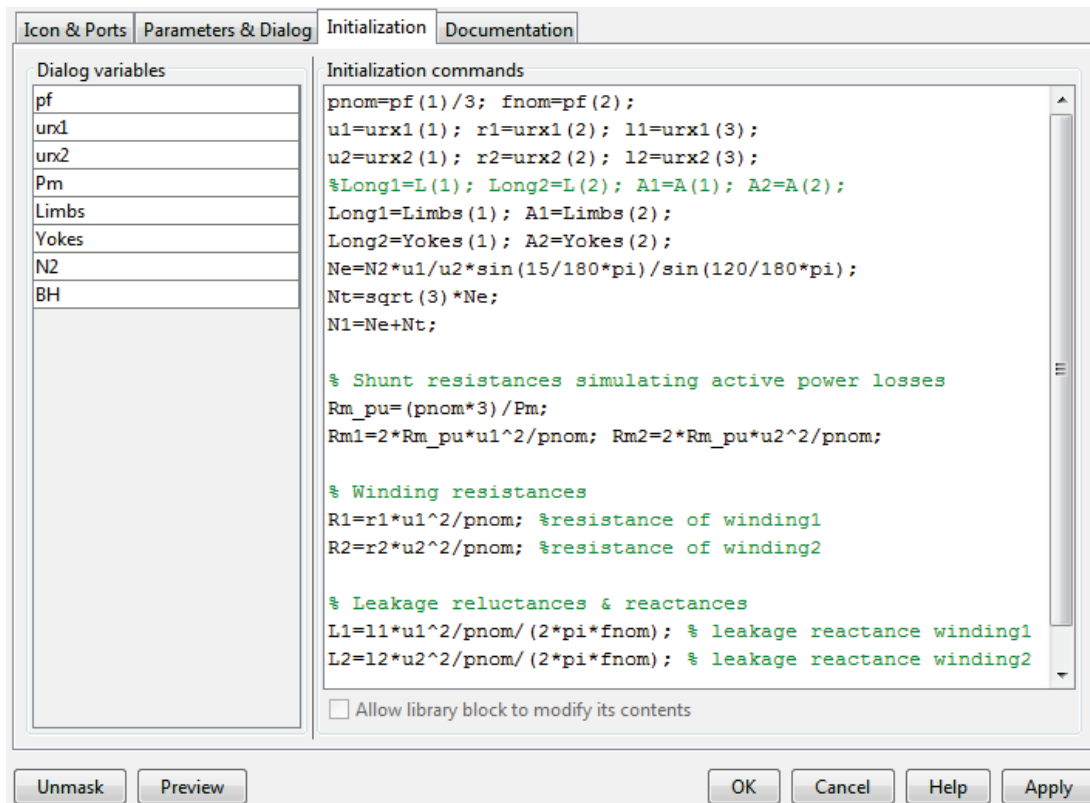


Figure 6.9: SPS Simscape components transformer's block initialization parameters tab

In particular it can be noted that are calculated the number of turns of the *Electromagnetic Converter* blocks using the formulas of Chapter 2.1.1 for a transformer which has 15° as nominal phase shift (as the CCS transformer).

6.2 Validation of two models

In this Chapter is presented the comparison between the results coming from the simulation of two models in typical work situation. In particular the same verifications described in Chapter 5, done for the SPS Specialized Technology model, has been repeated for the SPS Simscape Components model and here is reported a results’ comparison.

6.2.1 SPS Simscape Components verification circuit

In order to validate the SPS ST model with the SPS SC model, a verification circuit for the latter has been built (Figure 6.10), as it was done for SPS ST model in Chapter 5.1.

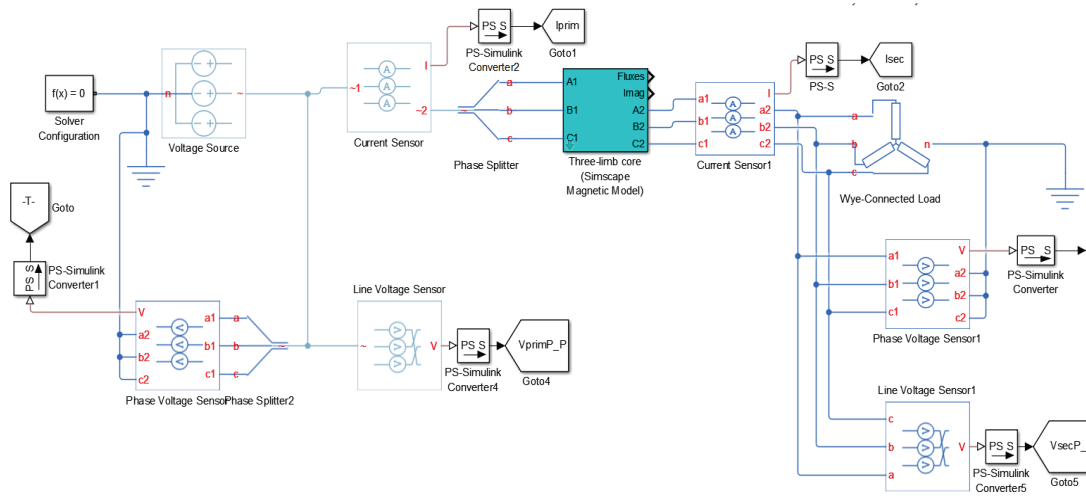


Figure 6.10: SPS Simscape Components verification circuit

In the verification circuit, the transformer is feed by a three-phase *Voltage Source* block set to be ideal and to give the a 22 [kV] RMS three-phase voltage. At the secondary the transformer has a *Wye-Connected Load* block that is grounded and can be set to absorb different power in the different verification situation.

Between the transformer and these blocks are present some current and voltage (phase-to-phase and phase-to-ground) measurements block; the output of these blocks is then converted in Simulink® language to be analyzed. With these Simulink® signals are calculated and displayed (Figure 6.11), in some Simulink®’s scopes or in display blocks, following values which are in all similar to those described in Chapter 5.1:

- Primary and secondary phase to phase voltages and currents values;
- RMS primary and secondary phase to phase voltages and currents values;
- Voltage phase-shift of each phase;
- Power at the primary;
- Power at the secondary;
- Losses: as difference between the values of power at primary and secondary.

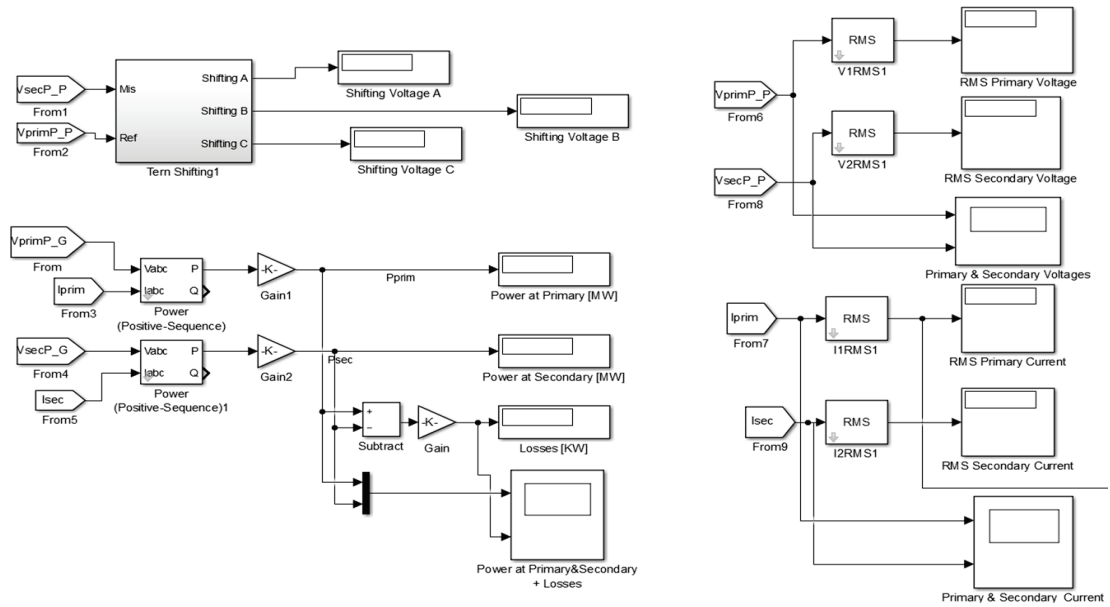


Figure 6.11: Simulink® measurement circuit for physical model

6.2.2 Phase-shift and no-load verifications

The propose of the no-load verification is to verify if the losses measured in the transformer’s SPS SC model, with an almost null load on secondary ($10^{10}[\Omega]$), are the same to those in the datasheet of Chapter 4.1 and with the one measured on SPS ST presented in Chapter 5.3.

In this condition of the secondary, can be also measured the nominal phase-shift of the transformer’s SPS SC model, to see if it’s 15° as it’s wanted. The phase shift has been measured with the same measuring circuit used in Chapter 5.2. In this case has been measured only the voltages’ phase shift.

It has to be reminded that this two verifications have to be done in steady state, so after the transitory regime of the in-rush of the transformer.

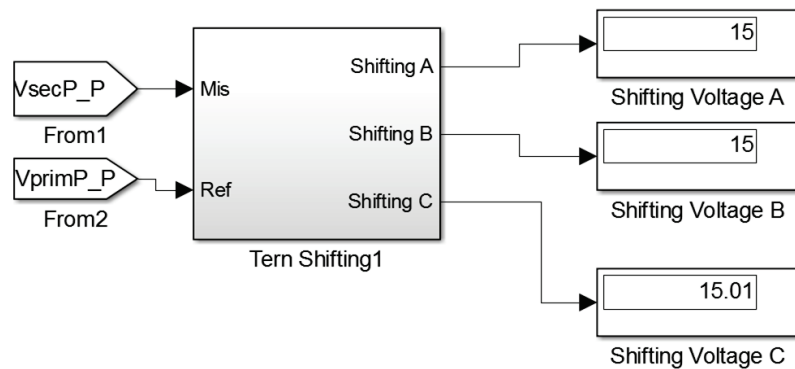


Figure 6.12: Physical model voltages phase-shift

In the Figure 6.12 the measured phase shift can be observed that is 15° as it is set, as is for SPS ST model and as is in data sheet.

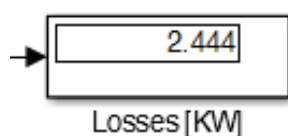


Figure 6.13: Physical model measured no-load losses

In the Figure 6.13 it can be seen that in the physical model the no load losses are 2,44 [kW], that is less than the 2,78 [kW] measured in the SPS ST model and also less than the data sheet no-load losses of 2,8 [kW]. The difference is probably due to a numerical oscillation problem and in any case the difference between the two measures is 340 [W] that can be neglect since it is about 0.15‰ of the nominal power of the transformer. It can be so assumed that the two models behave in the same way in no-load conditions.

6.2.3 Short Circuit verification

The purpose of this verification is to see if the physical model has the same short-circuit losses measured in the verifications on the SPS Specialized Technology model and with what reported in datasheet.

In order to simulate a short circuit test, a small resistance (of $10^{-50}[\Omega]$) is posed at the secondary of the transformer's model and, as done for the simulation of Chapter 5.4, the voltage source is set to give the impedance voltage of 16% of the nominal.

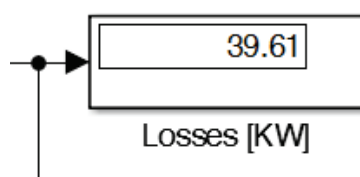


Figure 6.14: Physical model short-circuit losses

As can be observed in the Figure 6.14, the measured power losses are in this situation of 39,61 [kW]. This is the same value of losses measured in the short circuit verification done on SPS ST model and it's also the same that can be found in datasheet short-circuit test.

The two model so behave at the same way also in short circuit situation.

6.2.4 On load verification

The on load verification is done to verify whether the transformer's losses in the load condition are the same for the two model. As explained in Chapter 5.5, if the load is set to have as nominal power the transformer's one and as nominal voltage the transformer's secondary nominal voltage, then the losses registered won't be the sum of the no load and short circuit losses because of the internal voltage drop of the transformer.

However, in this verification it is not necessary to have the exact nominal load, but it is just needed to compare the results of the two models when they have same load at the transformer's secondary side. For this reason, and for simplicity, the load in the two models is set to have nominal power the transformer's one and the nominal voltage of 327 [V], that is transformer's secondary nominal voltage.

As can be seen in Figure 6.15 and in Figure 6.16 the results of the on-load verification are perfectly coherent in the two models. In particular, note that the RMS value of currents, the on load phase shift (that is not the nominal), the power and the power losses are practically the same in the two models.

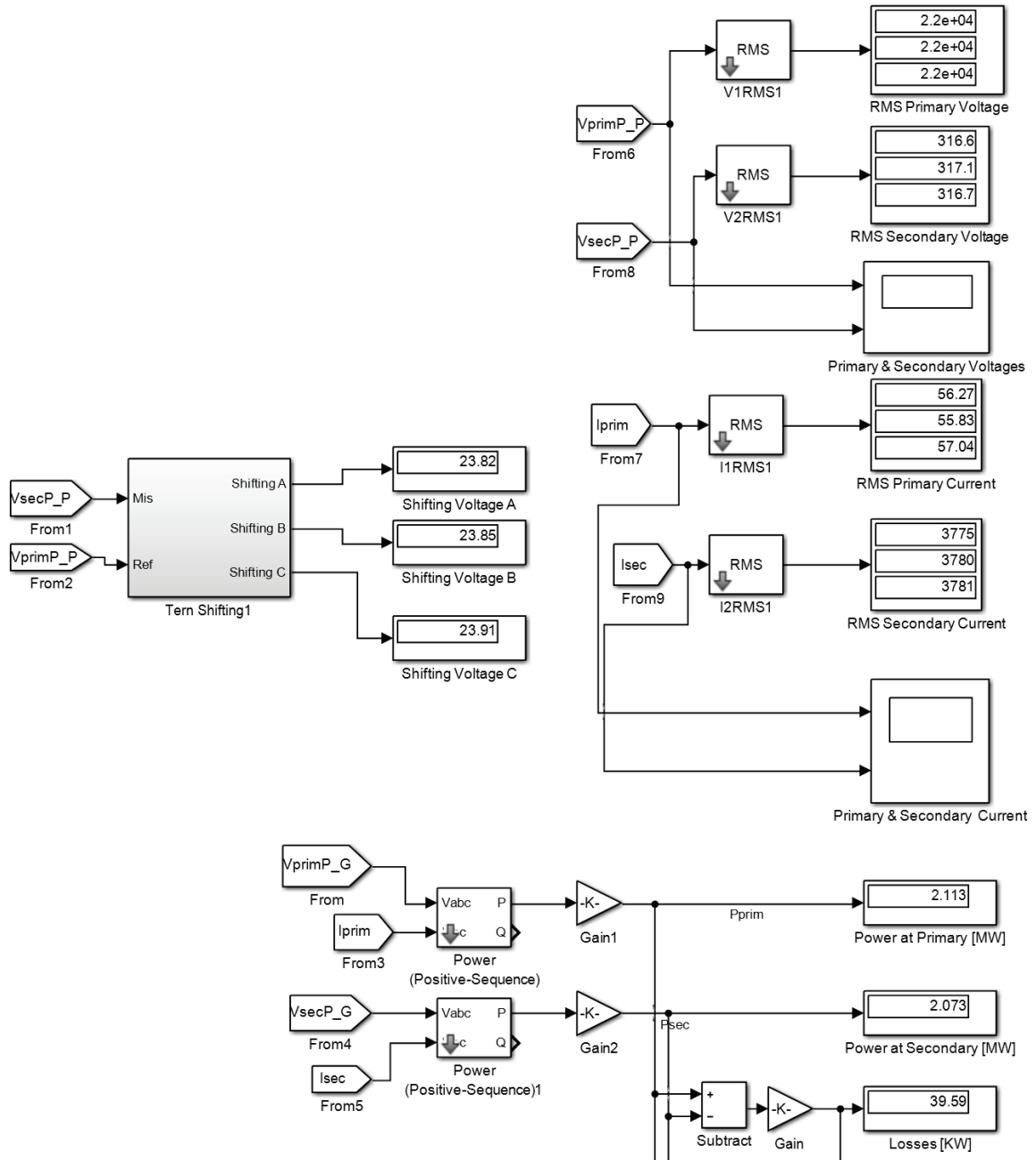


Figure 6.15: Physical model on-load verification results

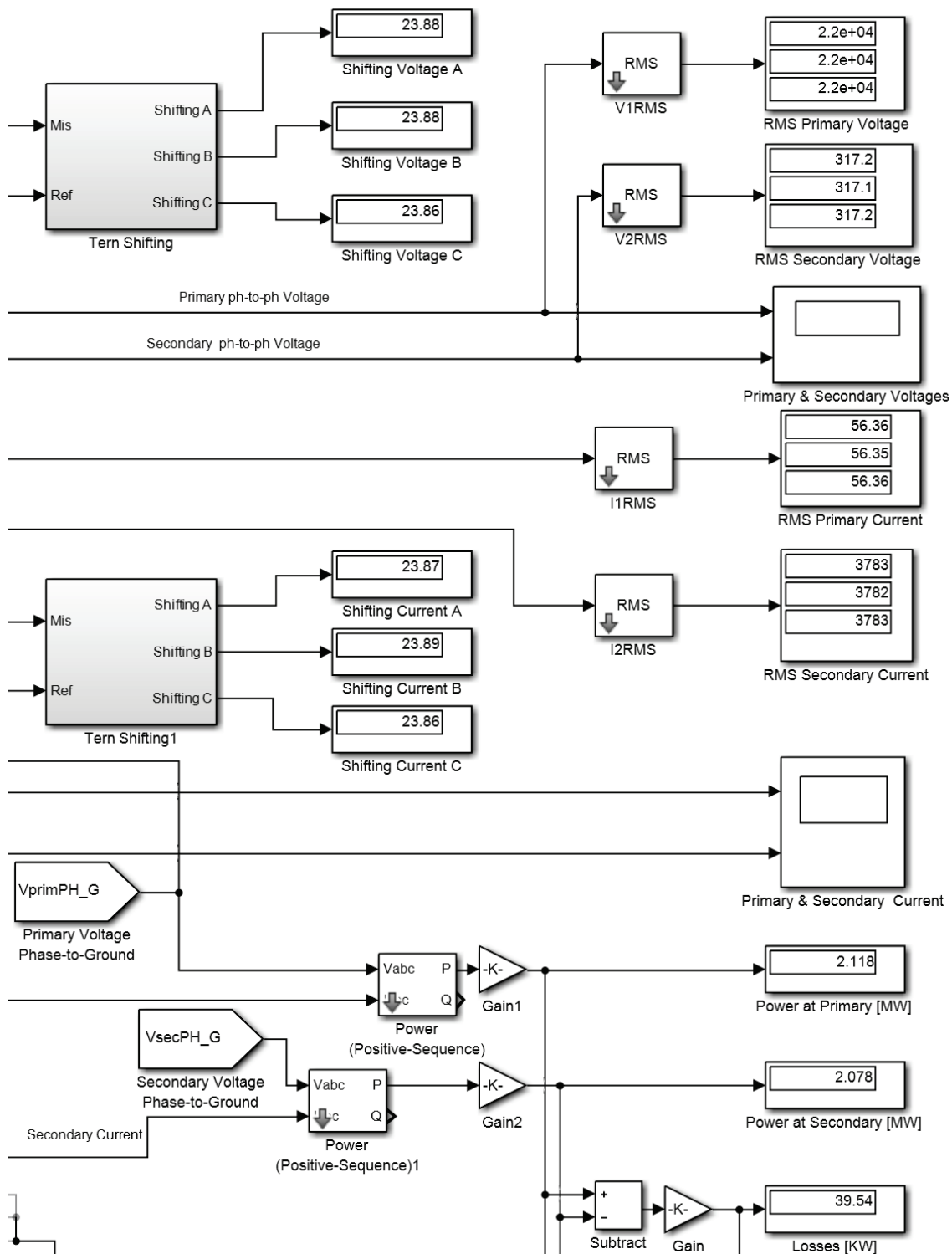


Figure 6.16: SPS Specialized Technology model on-load verification results

Since the primary voltages in two model are imposed by the voltage source, the more relevant thing to study from the primary side is the current in the three phases in the two models. For this reason, the primary currents are compared, instant by instant, in scopes where their time

variation can be observed. The Figure 6.17 shows the primary current of phase A, the other phases behave in very similar way.

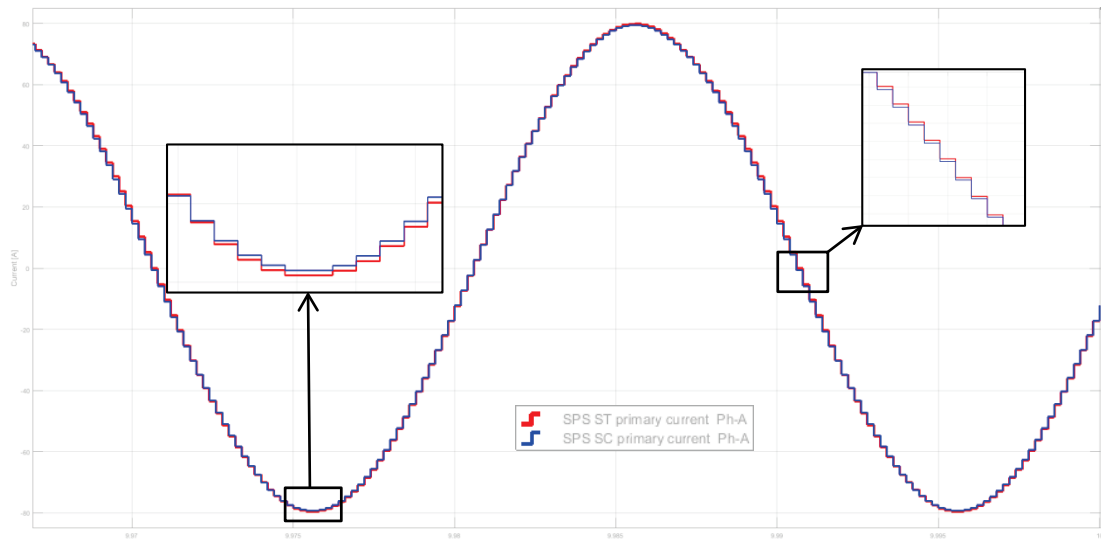


Figure 6.17: Primary currents in phase A for SPS Specialized Technology model (red) and for physical model (blue) in discrete time mode

In the Figure 6.17 can be observed that two current have the same andament and, intant per instant, they have about the same value with very little differences. In this figure can be also noticed that the two currents are measured in discrete mode, so this little differences can be attribute also to the Simulink® solver that was used.

After this verification we can say that, also in on-load condition, the two models behave in the same way and this could be cosidered as a relevant proof of the robust validity of the built SPS ST model.

6.2.5 In-rush current comparison

There are not many data about the in-rush current of the CCS transformer, but this is an aspect of central importance in the transformers' core saturation study [18].

For this reason, the two model has been compared for the in-rush current, so in the transitory event that occur when the transformer is energized and the worst case is when it is in no-load conditions.

The two model has been set for simulate the no-load in the same way they are set in Chapter 5.3 for the SPS ST model and in Chapter 6.2.2 for the SPS SC model and with the parameters of the CCS transformer's datasheet. The simulation on the two models has been done in discrete mode and for a time long enough to see all the transitory event.

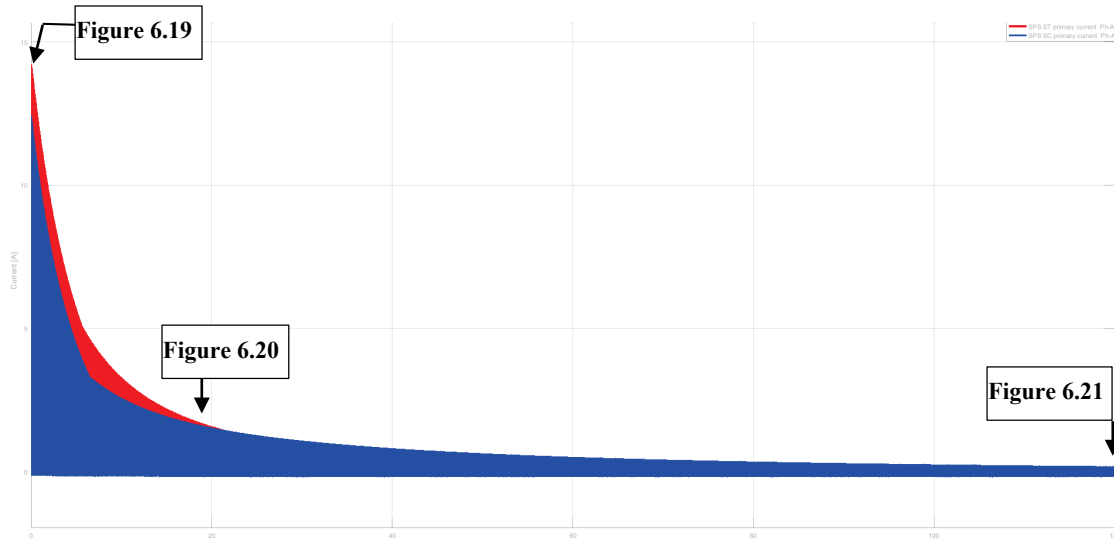


Figure 6.18: 120 seconds of in-rush current in the physical model (blue) and in the SPS ST model (red)

Macroscopically it can be seen that the two models differs at the beginning of the transitory and they begin to behave at the same way after about twenty seconds. This macroscopic difference can be explained by the approximation done in the calculus of the magnetization curve for the SPS ST model. In fact remind that in the calculus of Chapter 4.3.3.1, done to obtain the magnetization curve Φ -I, cannot consider the presence of the yokes in the circuit and so thier effect of saturation.

The difference is maximum at the beginning of the simulation and the pitches difference is about 2 [A].

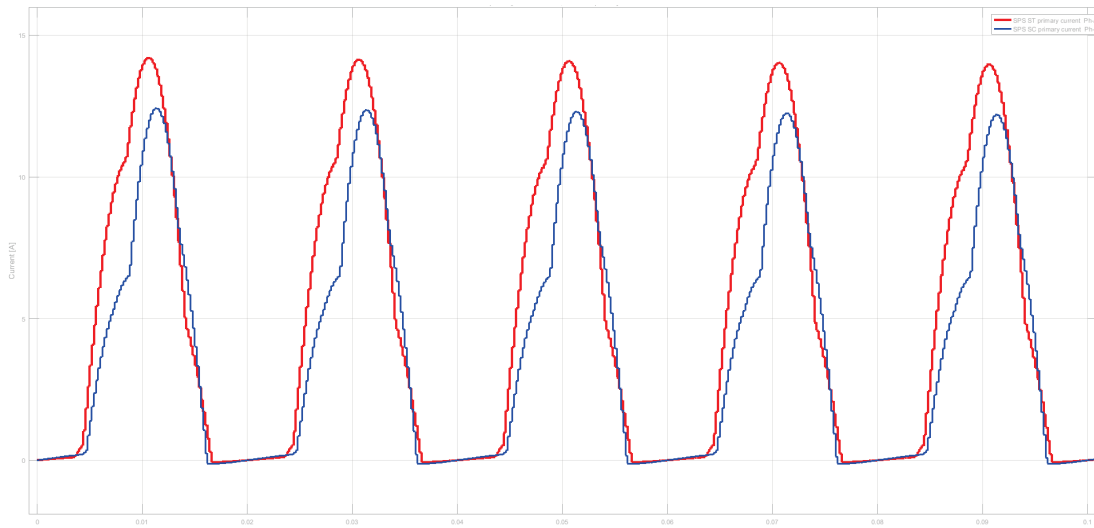


Figure 6.19: In-rush current in the interval 0-0,1 [s]

This difference progressively decreases and the pitches difference at 5 [s] is about 1 [A], that is relatively smaller than at the beginning.

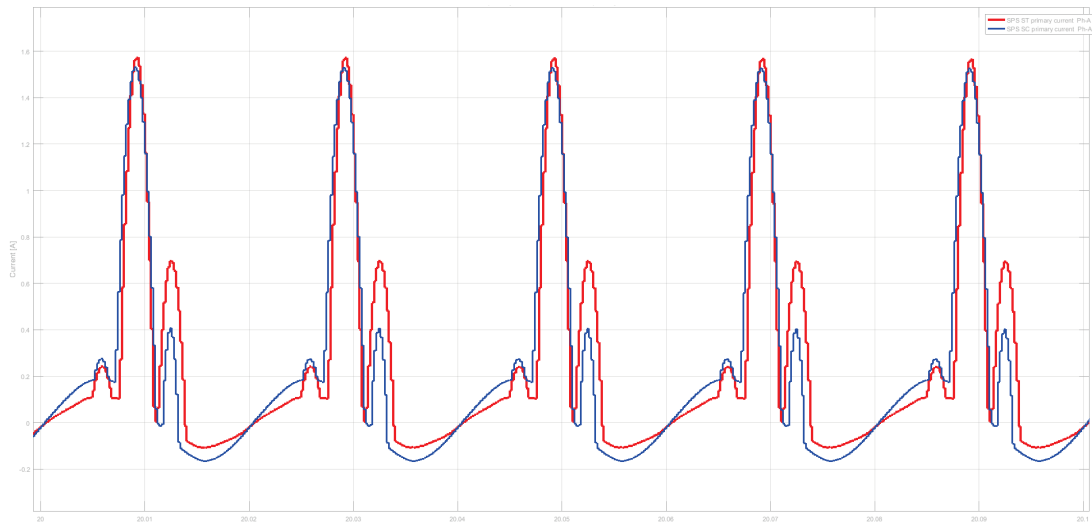


Figure 6.20: In-rush current in the interval 20-20,1 [s]

After twenty seconds the pitches difference of the transient currents is almost null, even if the two currents are not exactly the same, instant per instant (Figure 6.20).

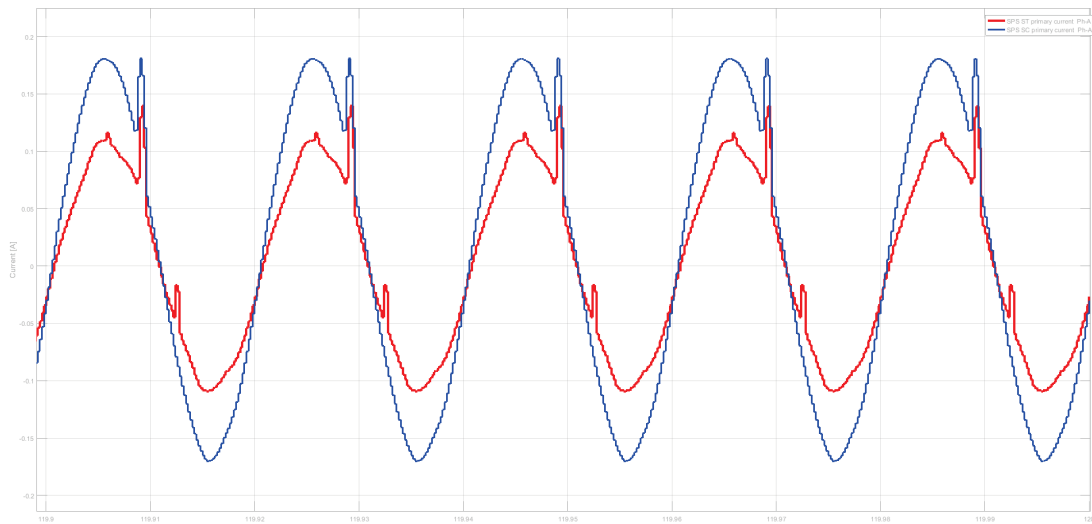


Figure 6.21: In-rush current in the interval 119.9-120 [s]

After a long time (120 [s]), when the steady state is nearly reached, the currents have the same value of in no-load verification ($\sim 0,712$ [A] RMS). The two currents still not equal but arise a pitch difference between the currents in SPS SC and the SPS ST models. However, as can be observed in the Figure 6.21, the difference between the two pitches is about 50 [mA]. This difference can be neglected considering that the nominal current of the transformer is about one thousand time bigger.

6.3 Specific verifications for ITER

Due to the nature of the transformer’s usage in ITER, it could be subjected to unbalanced or, in general, to non-common fault conditions. For this reason, the SPS ST model robustness has been verified also in these peculiar situation of stress, comparing it with the SPS SC model in the same situation.

In order to do this validation is needed a study of the model at the sequences. Since until now no unbalanced loads were used in the simulations, the model has been validated for the positive-sequence. For this reason, it is also valid for the inverse-sequence, because they are symmetric triplets [19]. Therefore, last validation to be done is for the zero-sequence (z-sequence).

After this verification, some specific analyses on the models have been performed:

1. A direct current injection among two secondary phases;
2. A phase-to-phase fault at the secondary.

6.3.1 Zero-sequence verification

The purpose of this verification is to verify whether the effect of the core saturation due to a zero-sequence component can be observed in the two models. In fact, since the transformer delta connected (even if extended), it cannot have neutral terminal and it has infinite zero-sequence impedance [7], [19]. So no zero-sequence current can pass through the transformer, but the zero-sequence current circulating in one side of the transformer can saturate the core. In this case, on the other side of the transformer, the current increases due to this saturation effect.

In order to compare the two models for the zero-sequence, a zero-sequence injection from the secondary side has been simulated in both models and the primary currents has been measured. To do this, a subsystem simulating a zero-sequence generator has been built for the two models (Figure 6.22 and Figure 6.23).

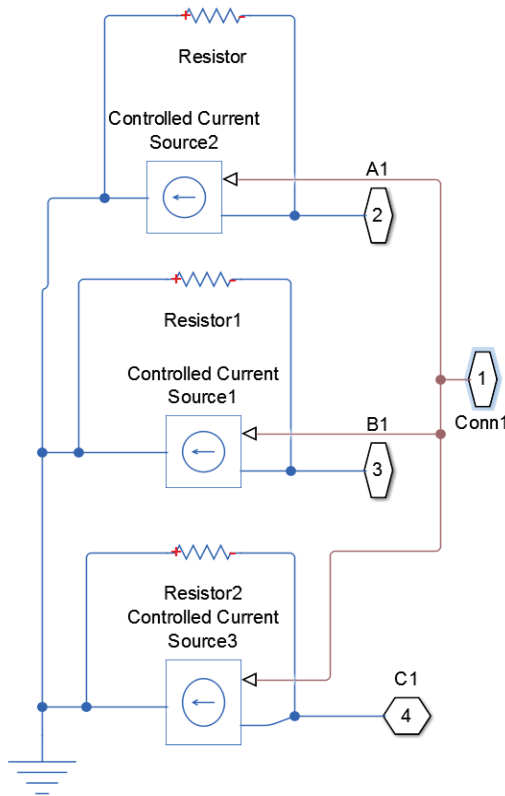


Figure 6.22: SPS SC z-sequence generator

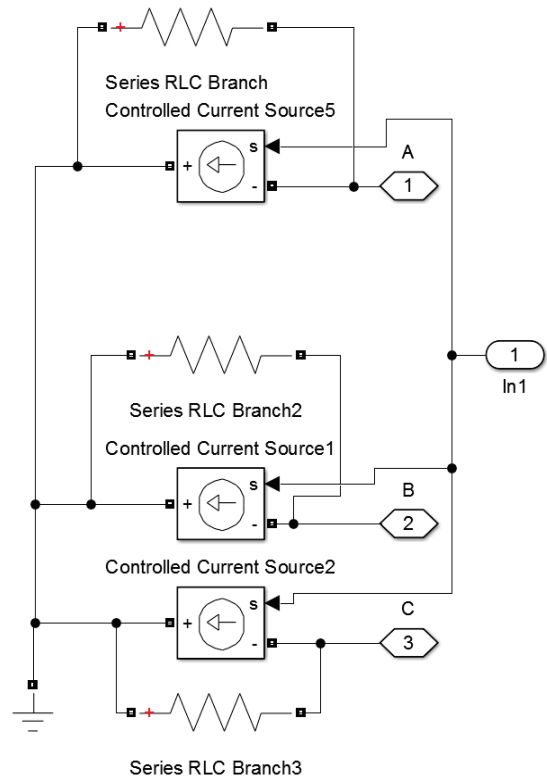


Figure 6.23: SPS ST z-sequence generator

Each z-sequence generator is composed by three current source, controlled by the same signal, with one side grounded and the other connected to one phase. The control signal is an input of the subsystem. It can be noted that each of them has in parallel a resistance: they are there because of convergence problems (see Chapter 3.1.1.1) so they have a very high value and can be neglected.

The two z-sequence generators are controlled with the same Simulink® signal, that is a sine wave multiplied by a step signal. The step signal has the amplitude of 1 and the sine signal has the amplitude of 10^9 in order to exalt the saturation effect.

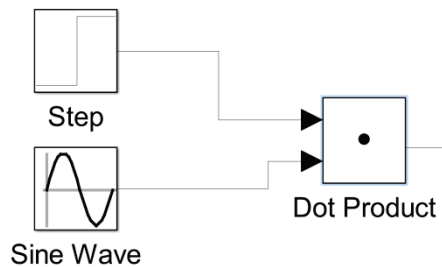


Figure 6.24: Signal of control of z-sequence generators

Since the z-sequence has to pass through the secondary windings, the load at the secondary cannot be grounded. This can introduce some convergence errors since the neutral at the secondary side would be floating. For this reason, in both models a high wye-connected grounded resistance of $10^{10}[\Omega]$ is connected in parallel with a consistent delta-connected load (Figure 6.25). In this way the secondary can be considered as having only the delta-connected

load. The delta-load is set to have nominal voltage equal to the secondary nominal voltage and the nominal power the transformer’s nominal one.

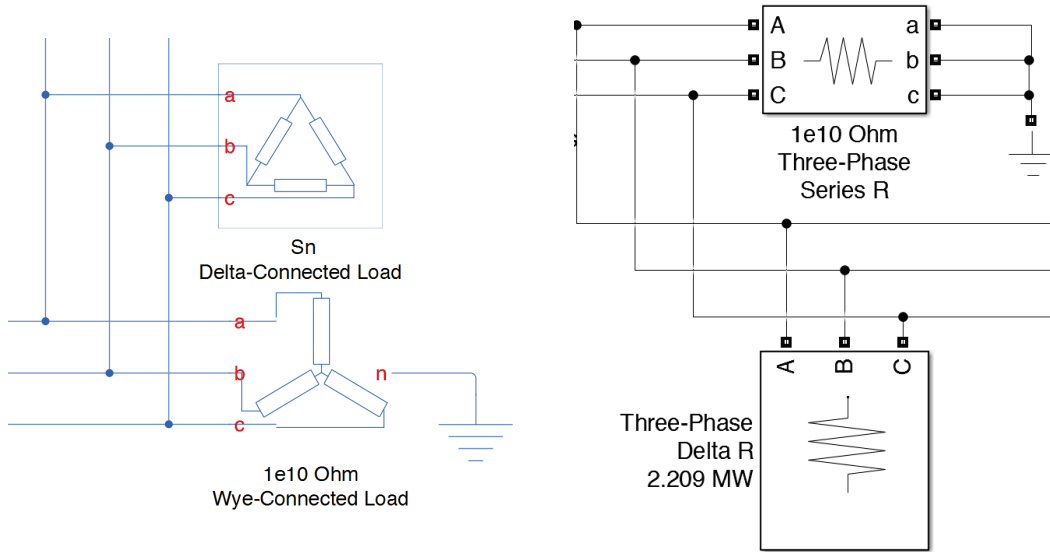


Figure 6.25: Z-sequence verification loads in the two models

Taking as example the phase A (the other behave similarly), before the zero-sequence is injected the two primary current are almost equal as can be observed in Figure 6.26.

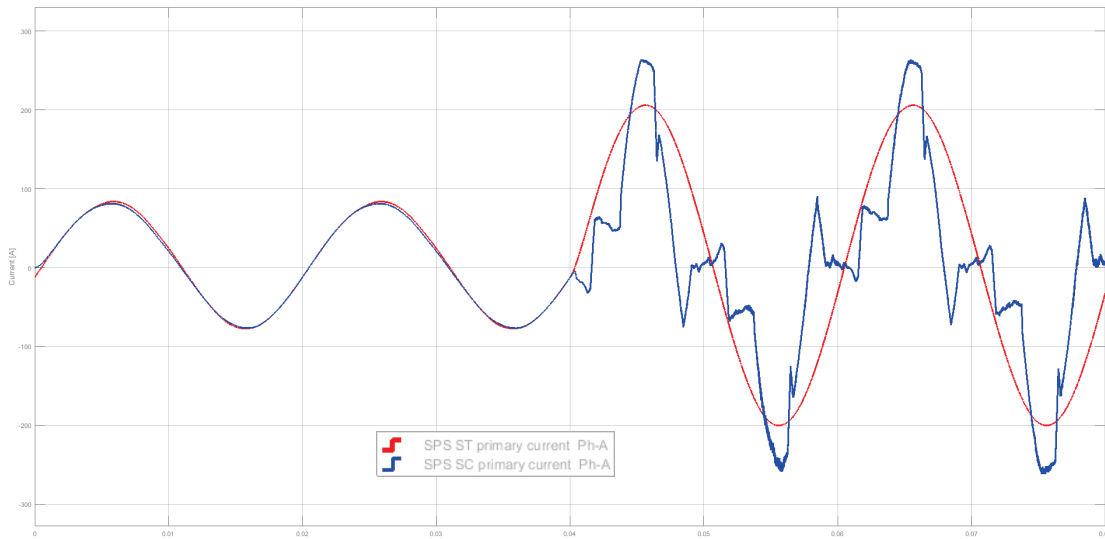


Figure 6.26: Primary current of phase A in z-sequence verification of physical model (blue) and of SPS ST model (red).

At the time of 0.04 [s], when the z-sequence generators start, it can be noted that the current of the SPS ST model (red) increases its amplitude as expected and it has not any other distortion in magnitude or phase. Otherwise the current in SPS SC model (blue) has spikes and ripples.

This effect can be studied a little more deeply analyzing the magnitude of the current.

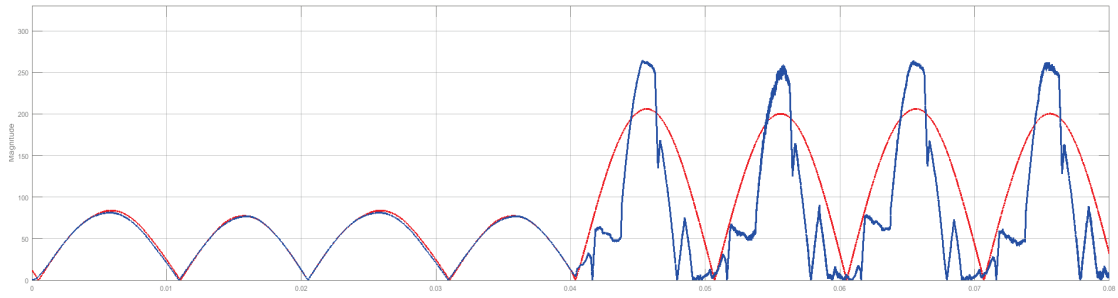


Figure 6.27: Magnitude of current in z-sequence verification

In the Figure 6.27 can be observed that the magnitude of current in the physical model is periodically the same and its mean value it is the same as in the SPS ST model.

The strange trend of the current in the SPS SC model is due to some Simscape numerical problems. Indeed it has to be underlined that these results can be obtained only with very high precision and for simulations that takes only few milliseconds. Otherwise the simulation could not start or the physical model lose the convergence stability.

This is still an open question for a future work, that would probably go on in collaboration with MathWorks Inc. Although, by the obtained results, the robustness of the SPS ST model of the delta-extended/delta transformer can be considered proved for the zero-sequence and it is even stronger than the SPS SC model one.

6.3.2 DC fault among two phases

In specific fault situation that can occur to the AC/DC converters in ITER, currents, that can be approximate to direct currents, can be injected among two secondary terminals of the transformer. In this case at the primary side, even if the DC cannot be seen, the current increases its magnitude if the current injected at the secondary side is considerable. This happen because the secondary direct current moves the working point on the magnetic characteristic in higher flux zone, thus the primary current has to be higher to transmit the same power from primary to secondary.

In order to simulate this specific condition in the two models, a *Controlled Current Source* block has been connected to two secondary terminals and it has been commanded to inject the established direct current at a certain point (Figure 6.28). The direct current is injected from the phase B to the phase A of the secondary. Then the primary currents in all the three primary phases has been measured and, phase per phase, the results of the two models has been compared.

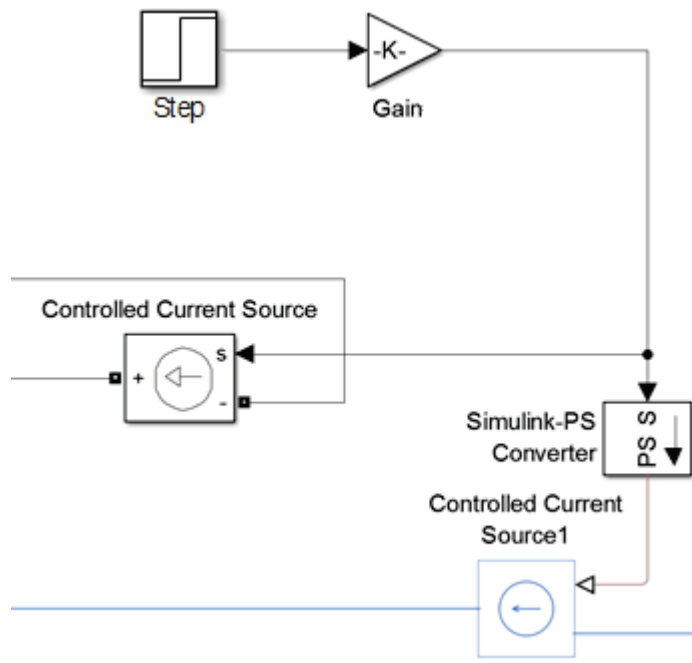


Figure 6.28: Controlled DC source in the two models

Since this kind of fault occurs during the normal work of the transformer, this situation has been simulated with the same load of the on-load verification, that is a three-phase pure resistance load set to have as nominal power the transformer's one and as nominal voltage the secondary nominal voltage of the transformer.

The simulation has been done in three cases:

1. With an extremely high value of direct current injected;
2. With a value near to the short-circuit secondary current RMS value;
3. With a value near to the nominal secondary current RMS value.

To change the value of the injected current is sufficient to change the value of the *Gain* block. Since this signal is referring to a secondary current, it is divided to the nominal transformation ratio ($V1n/V2n$) to be converted to an equivalent primary current, so it can be compared with the measured primary currents.

6.3.2.1 Very high direct current

In order to have a qualitative idea on how the models work when there is a DC injection into two phases of the transformer's secondary, it has begun controlling the current source to produce a current of 2 [MA].

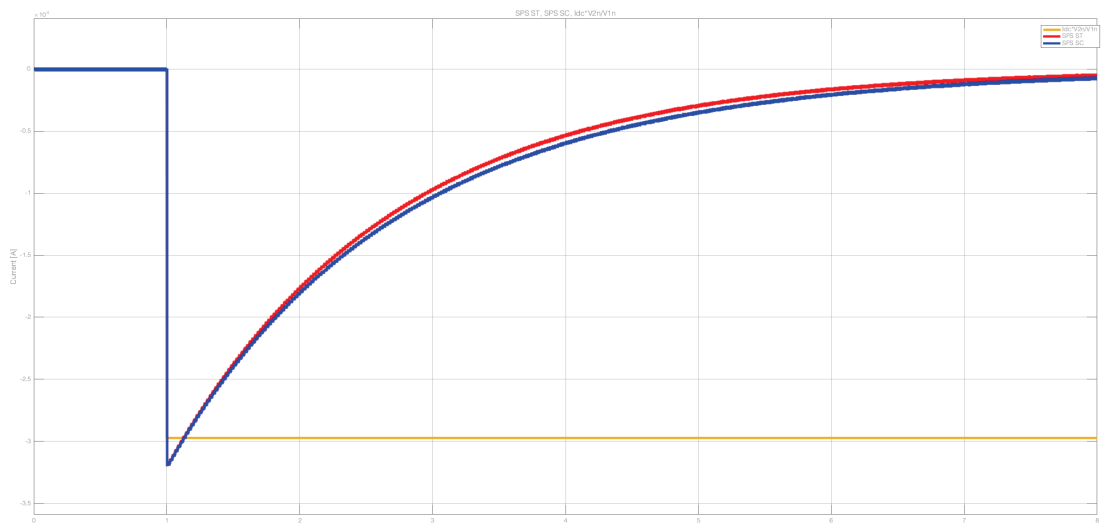


Figure 6.29: Primary current of phase A with 2 [MA] direct current

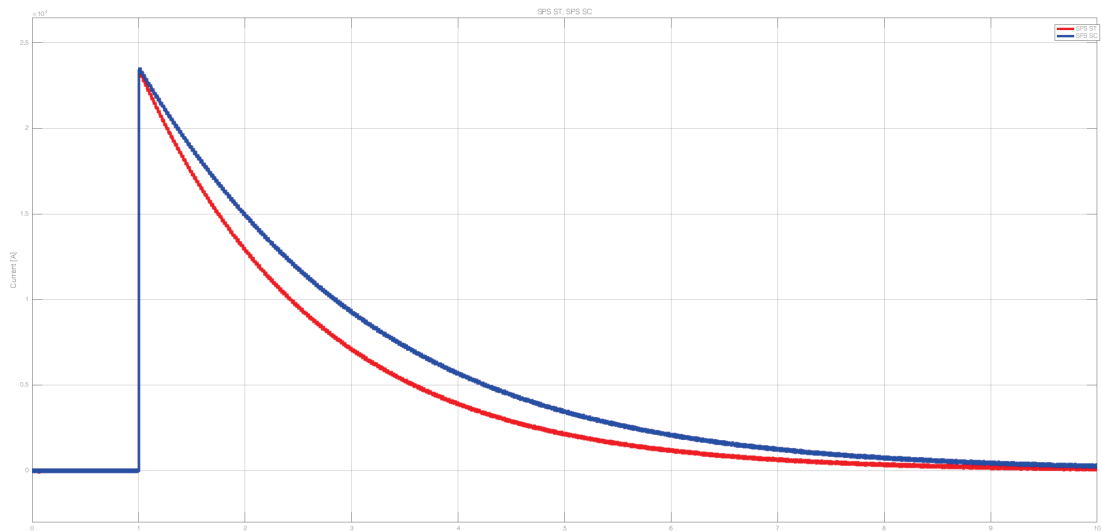


Figure 6.30: Primary current of phase B with 2 [MA] direct current

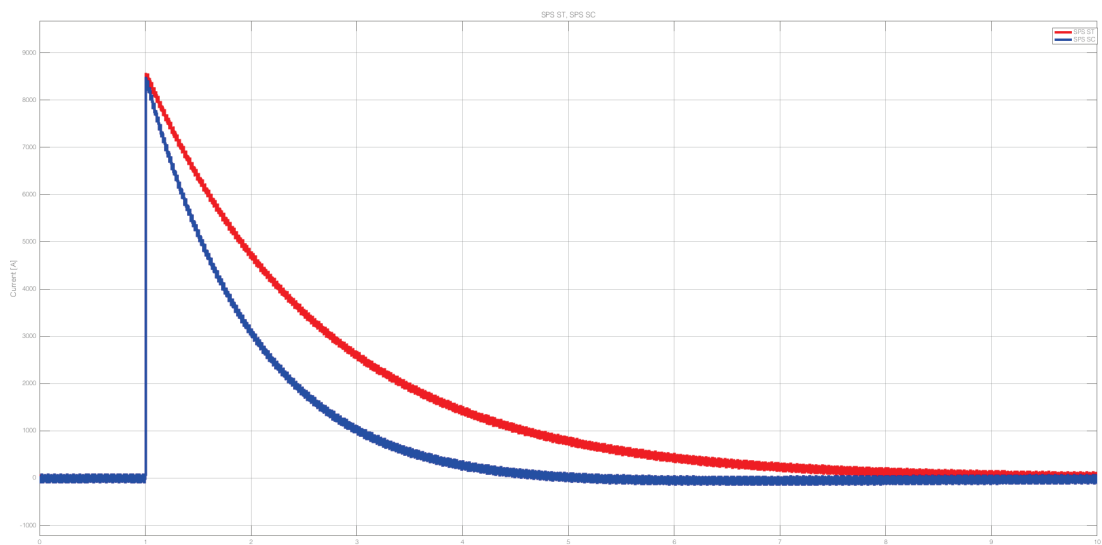


Figure 6.31: Primary current of phase C with 2 [MA] direct current

In all the figures can be notice an effect of core saturation, but it can also be observed that the two models do not behave exactly at the same way. This difference is because of the different model of saturation characteristic in the two model: in one is modelled with the B-H curve and the other with the I- Φ (see Chapter 6.2.5). Neglecting this difference, we can see that the trend of the currents in the two model are the same.

However, the important aspect of this verification is that a direct current injected among two secondary terminals have effect on all the three primary phases, because it makes the core saturate.

6.3.2.2 Short-circuit direct current

The value of the short-circuit current, at transformer’s secondary said, can be calculated from the value of the magnitude of the short-circuit impedance, referred to the secondary, Z_{2SC} that can be calculated as:

$$Z_{2SC} = \frac{Z_{1SC}}{z_{b1}} \cdot z_{b2}$$

Where Z_{1SC} is the short circuit impedance calculated in Chapter 4.3.3.1 and z_{b1} and z_{b2} are the base impedance of the two transformer sides in the per-unit system.

The short circuit current is then calculated as:

$$I_{2SC} = \sqrt{3} \cdot \frac{V_{2n}}{Z_{2SC}}$$

That, for the CCS transformer, is about 24 [kA].

The value is set in the *Gain* block of the signal that controls the currents sources and the simulation is run.

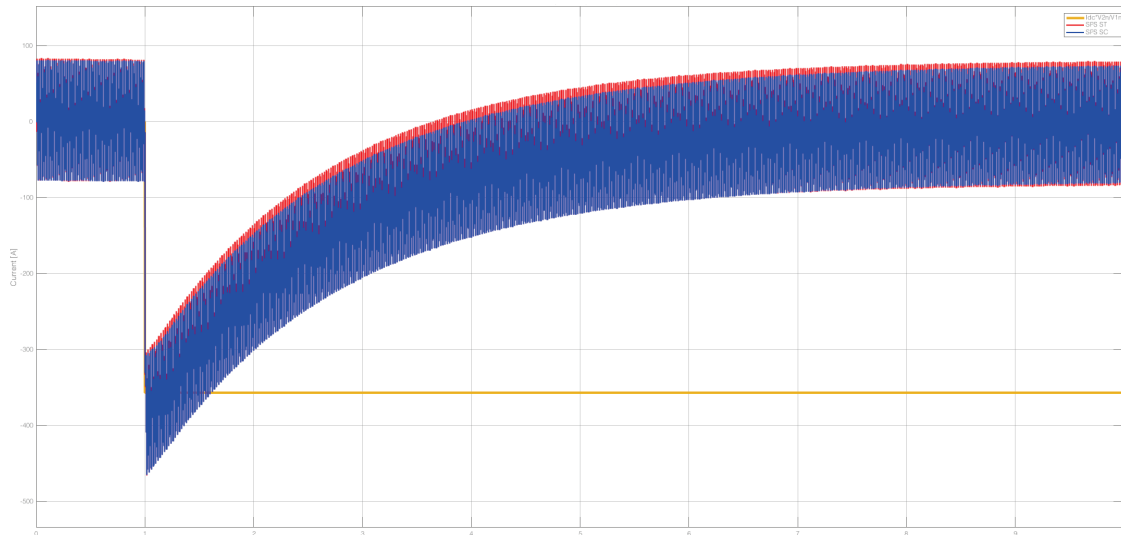


Figure 6.32: Primary current of phase A with 24 [kA] direct current

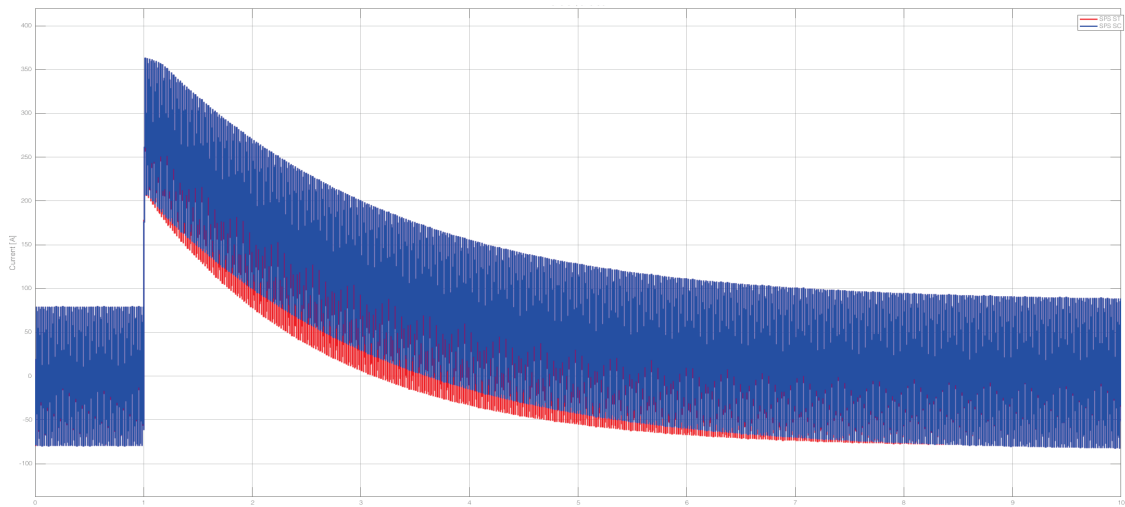


Figure 6.33: Primary current of phase B with 24 [kA] direct current

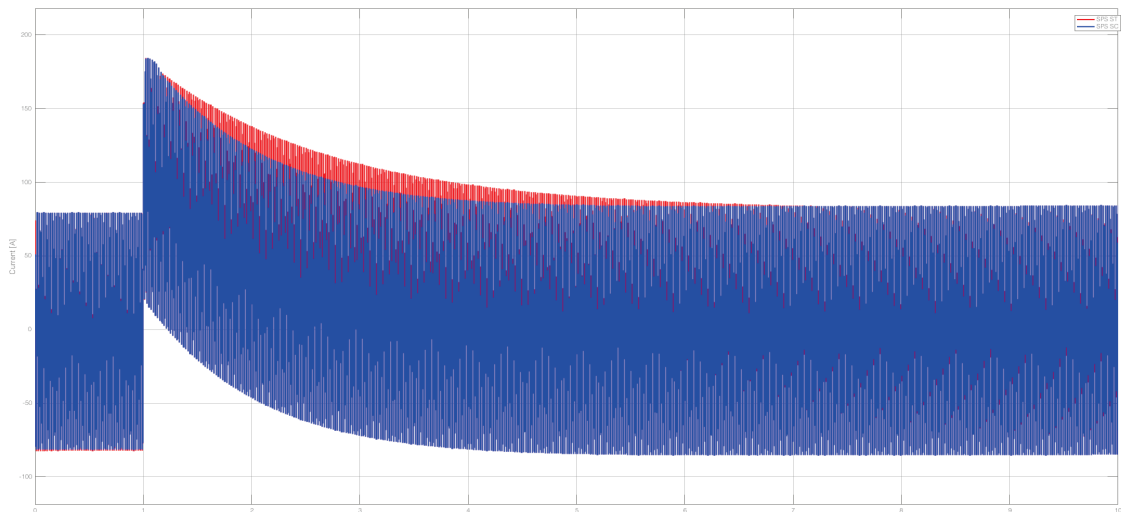


Figure 6.34: Primary current of phase C with 24 [kA] direct current

As it can be seen in the previous figures, the currents in the two models are almost the same, and the difference can be observed just is during the transient.

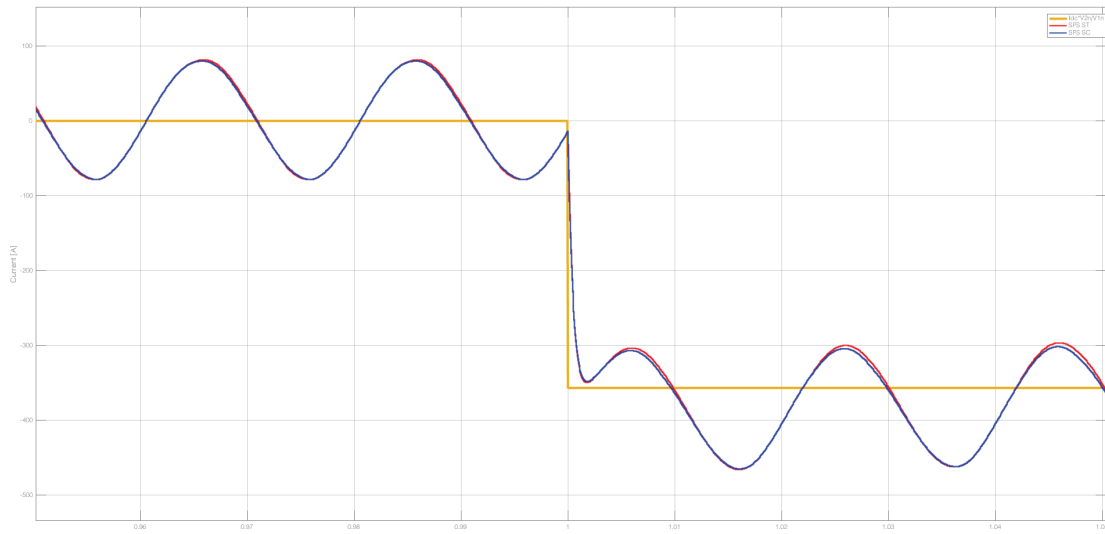


Figure 6.35: Phase A zoom at 1[s] with 24 [kA] DC fault

Taking the phase A as example, when the direct current injection begin (Figure 6.35) the primary currents change rapidly its mean value to the value of the DC (referred to the primary). The two currents in the two model are still instant per instant almost the same.

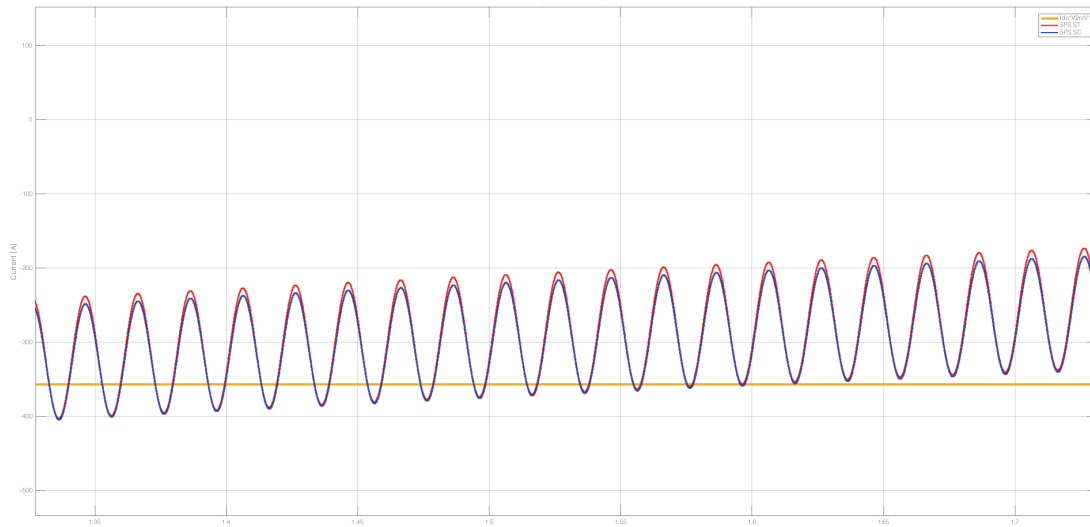


Figure 6.36: Phase A zoom at 1.5 [s] with 24 [kA] DC fault

After 0,5 [s] from the step of direct current, the mean value of the primary current changes slowly but it remains almost the same in the two models, even if a difference begins to be viewable.

In the Figure 6.32 it seems that the maximum difference of the two current measured is around 6 [s].

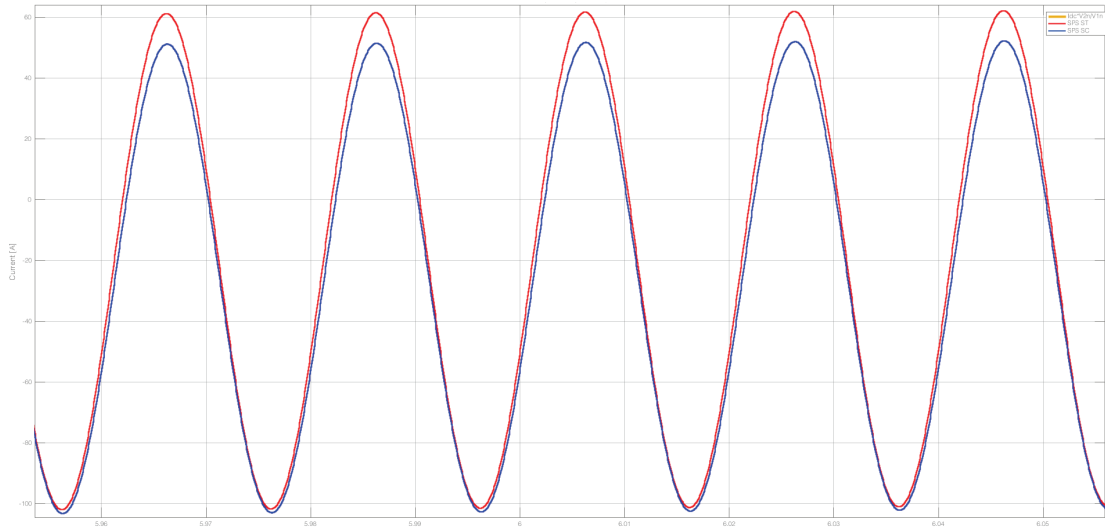


Figure 6.37: Phase A zoom at 6 [s] with 24 [kA] DC fault

In the Figure 6.37 can be observed that the difference at 6 [s] between the mean values of the two currents it is about 5 [A]. This difference can be explained again considering that the SPS ST model do not consider the saturation of yokes, but in any case this difference can be neglected considering that at primary the current is about 160 [A] pitch-to-pitch.

In the other phases can be done the same considerations, and the difference in the two models has the same explanation and so can be neglected also in this case. Thus the two models under this kind of unbalanced fault behave almost at the same way.

This result is one of the most important result of this part of the work. Indeed, what done in Chapter 6.3.1 is affect to numerical errors so could be tax to be wrong and what done in Chapter 6.3.2.1 can give only qualitative ideas but has no physical sense. What done in this Chapter has instead physical sense, since the short circuit current is a physical datum of the transformer.

6.3.2.3 Direct current of nominal secondary value

The nominal secondary current is 4082.5 [A], so we set the *Gain* block of the command signal to 4000. With this setting and with the same configurations of the circuit in the preceded verification the simulation of two models has been run.

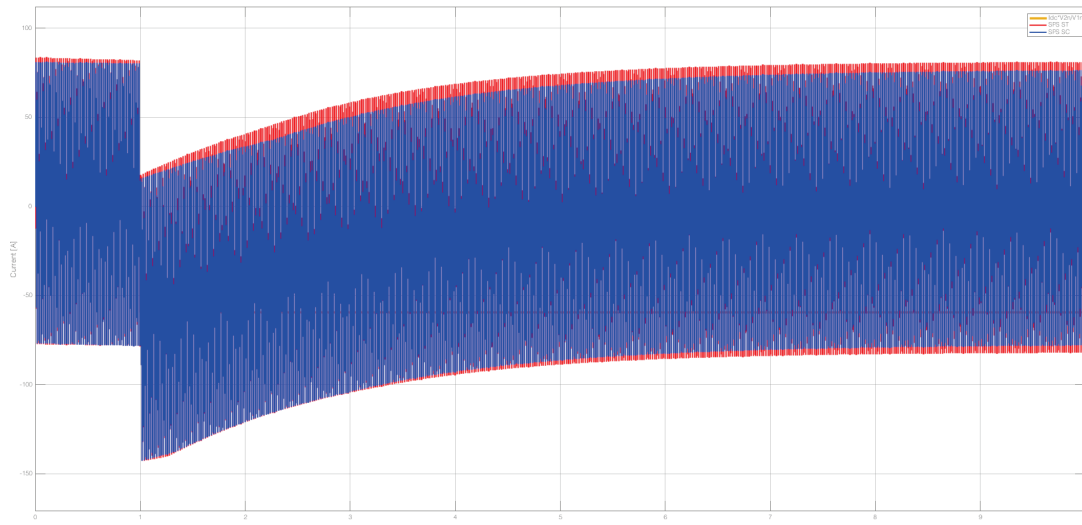


Figure 6.38: Primary current of phase A with 0.4 [kA] direct current

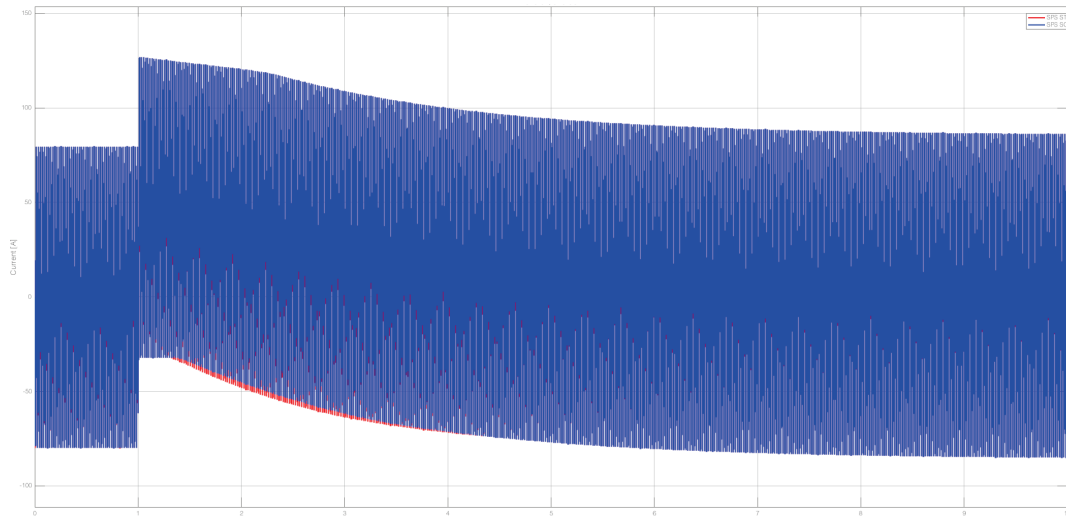


Figure 6.39: Primary current of phase B with 0.4 [kA] direct current

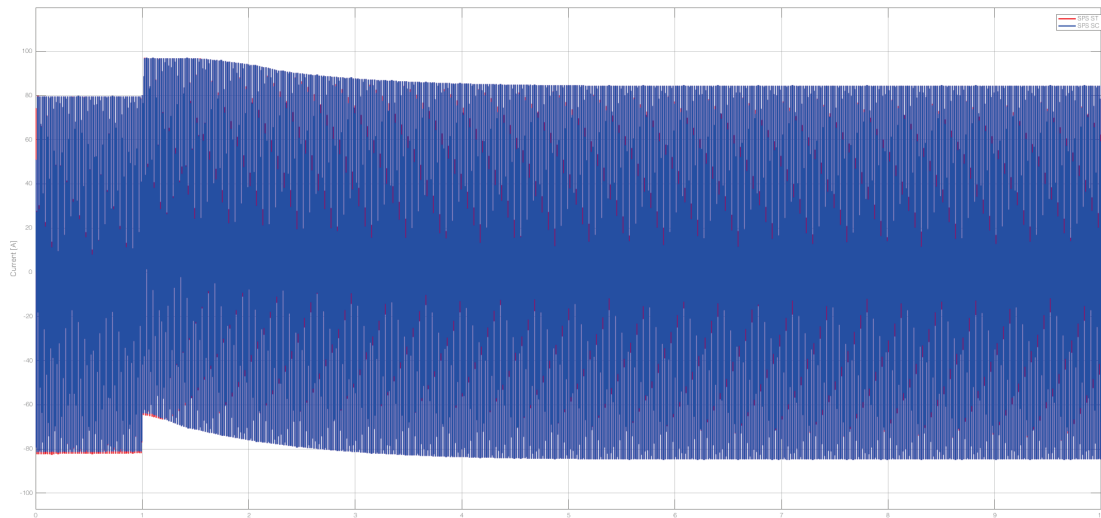


Figure 6.40: Primary current of phase C with 0.4 [kA] direct current

In this simulation the difference between the currents in the two models is relatively smaller respect to in previous simulations. This can be explained thinking that the injected direct current moves the working point, but it remains almost in the linear zone of the magnetic characteristic so the presence of core saturation is not considerable yet. The phase where major difference can be see is the phase A.

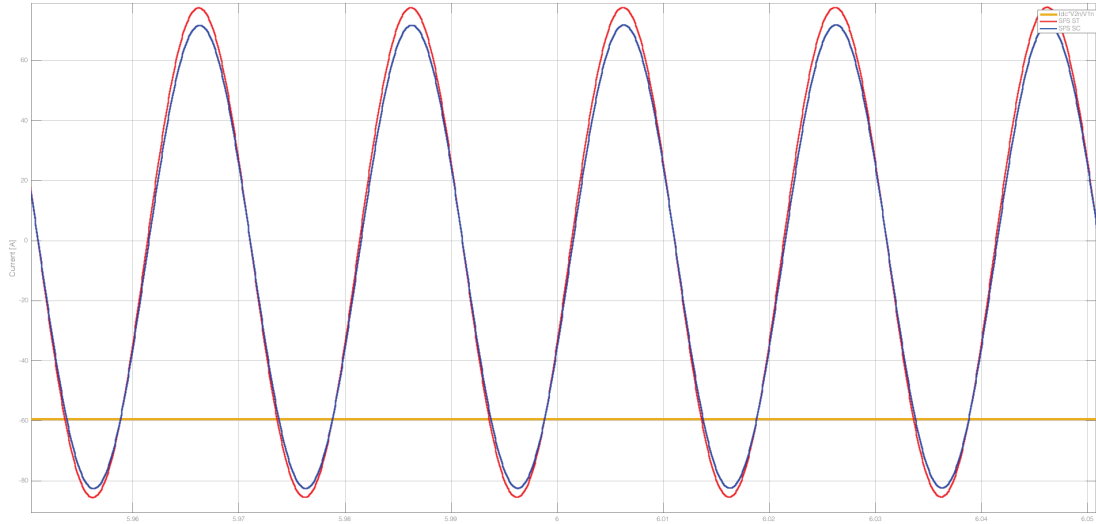


Figure 6.41: Phase A zoom at 6 [s] with 0.4 [kA] DC fault

Almost at 6 [s] from the beginning of the simulation there is qualitatively the higher difference between the two mensuration. As can be observed in Figure 6.41 the difference between the two pitches is once again about 5 [A]. Since at 6 [s] the pitch-to-pitch value of the current is about 140 [A] the difference can be neglected.

Also in this verification the two models reproof their equivalence and, since the SPS Simscape Components represent a physical model of the transformer, the robustness of the SPS Specialized Technology model is proved again.

6.3.3 Phase-to-phase fault verification

In this simulation has been verified the two models in the condition of phase-to-phase fault at the secondary side of the transformer. In order to do this, a controlled breaker is poised between the phase A and phase B of the secondary of each model and, to make the two breakers close at the same time, they are commanded with the same step signal (Figure 6.42).

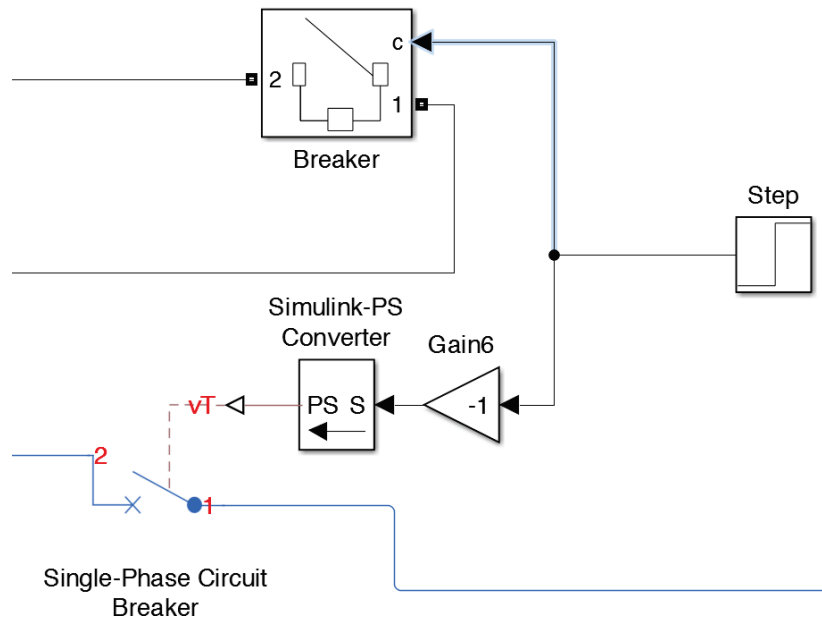


Figure 6.42: Breaker blocks in the two models

In order to exalt the effect of the phase-to-phase fault the simulation has been done in the same conditions of the no-load verifications, so with a very big resistance at the secondary. Then the simulation has been run and the currents at the primary side are compared phase per phase.

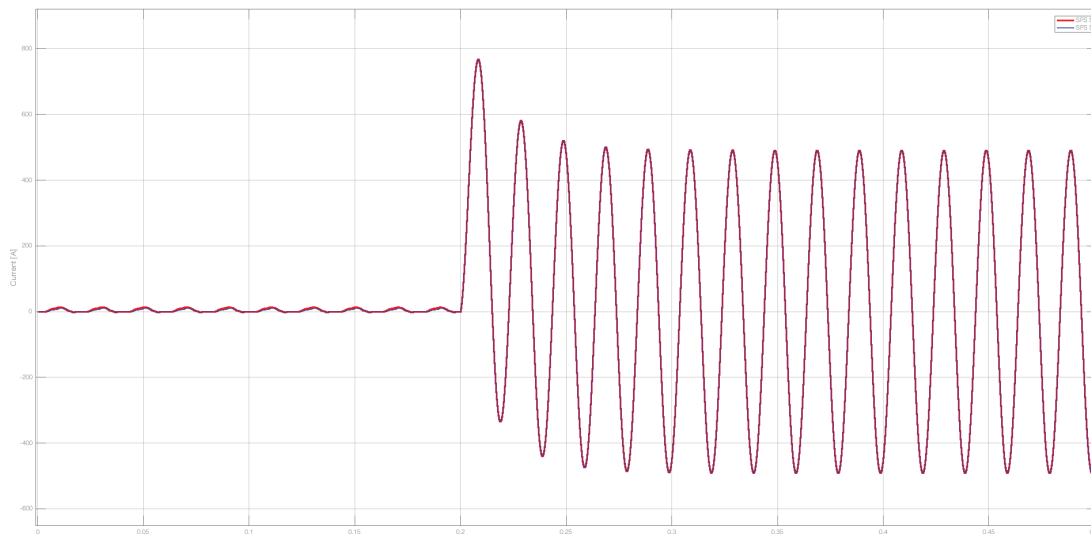


Figure 6.43: Current in the phase A during phase-to-phase fault

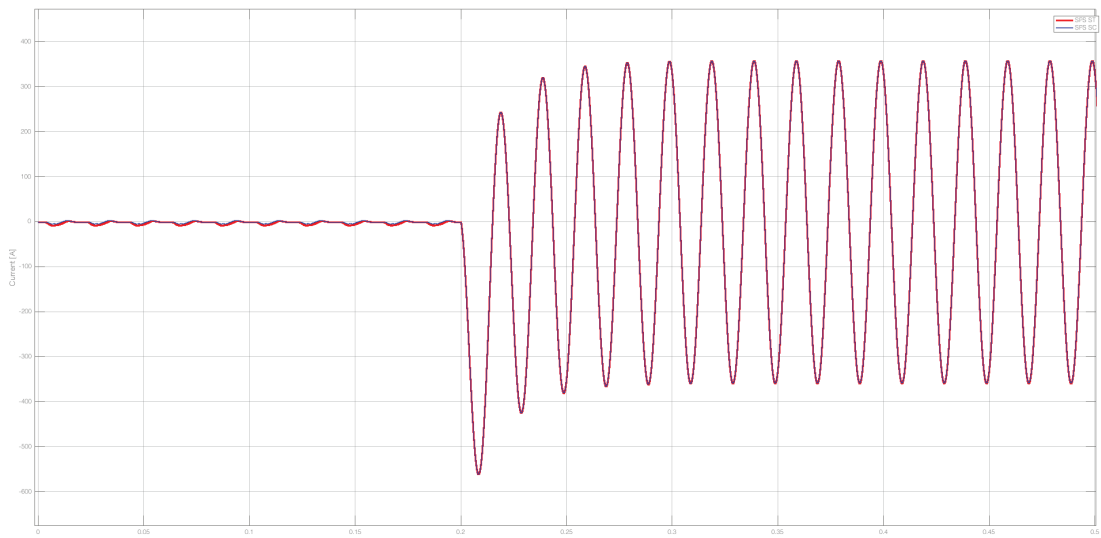


Figure 6.44: Current in the phase B during phase-to-phase fault

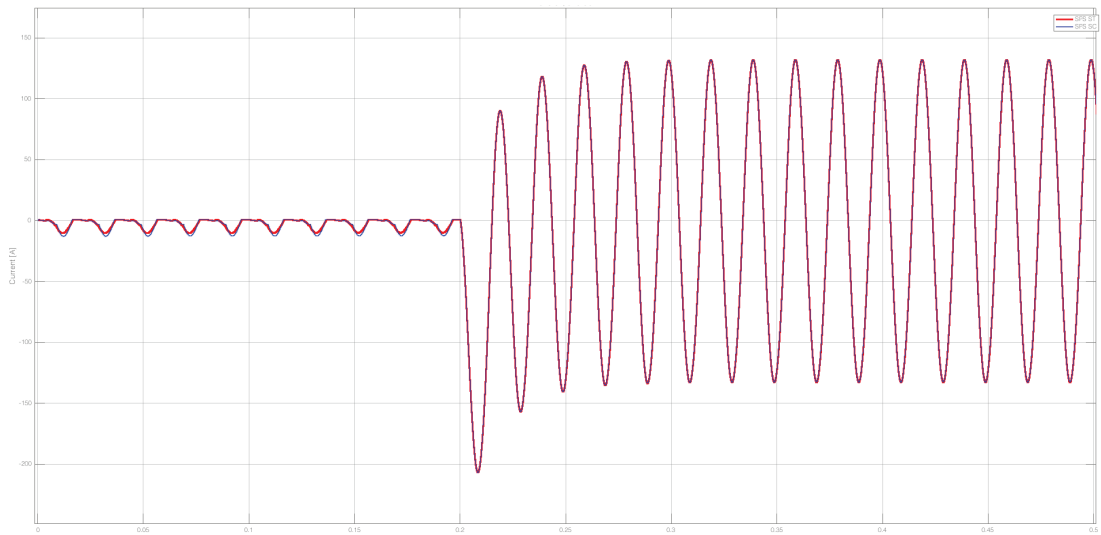


Figure 6.45: Current in the phase C during phase-to-phase fault

As it can be seen in the figures above, also in this case the two models have the same behaviour: when the phase-to-phase fault occurs in all the phases of the primary the current has a little transitory, but then the short circuit is supplied by all the three phases together in balanced mode as expected.

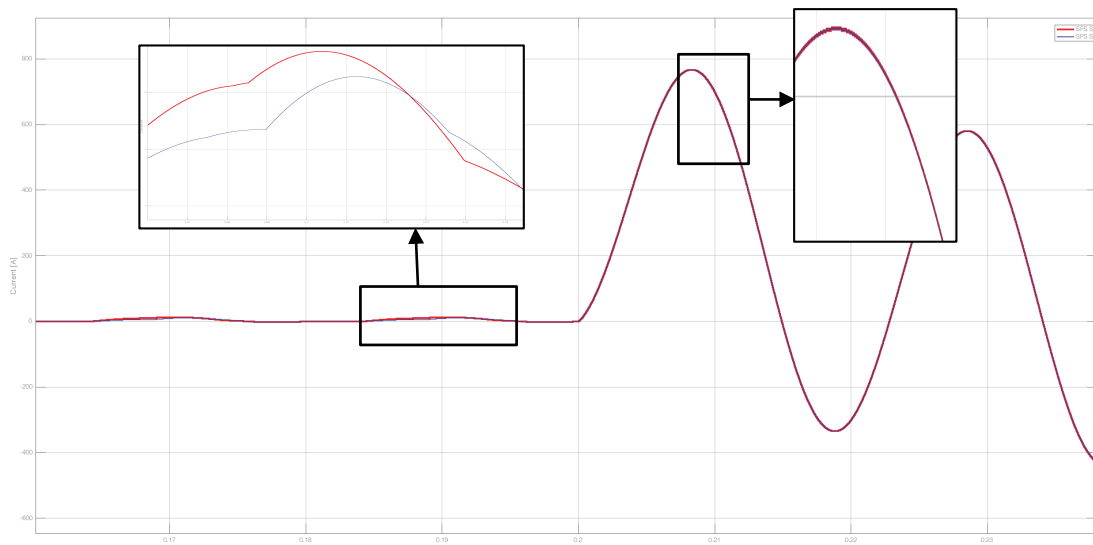


Figure 6.46: Zoom of the current in the phase A at the moment of the fault

In the Figure 6.46 is reported as an example the current in phase A around the moment when the fault begins. Before the fault, the currents in the models are the same as the currents measured at the beginning of the in-rush verification, indeed the circuital situation is the same, and their difference is explained in Chapter 6.2.5. It can be notice that after the fault the primary currents assumes exactly the same values during the transitory and when the steady state is reached.

In this verification the SPS ST model of CCS extended-delta/delta transformer behave once again in the same way of the physical model simulated with SPS SC library. This validate SPS ST model robustness.

7. Conclusions

In this work of thesis has been realized a model of a transformer with windings connected in extended-delta configuration. In particular, a subsystem that models the transformer’s electrical behavior was built with SPS ST MatLab/Simulink® toolbox.

In order to develop this model, the study started from a theoretical analysis of the voltage phasors that are present on this kind of windings configuration. In this analysis the focus was on the voltage phasor that is directly proportional and in phase with the flux into the magnetic circuit. A way to express this phasor by the sum of two voltages in phase with the grid phase-to-phase voltage has been found. The originality of the work stays in this achievement: it is no more necessary to have a magnetic model of the of the transformer’s core using this technique. Furthermore, this approach has a general validity and any kind of transformer can be modelled.

The model realized with SPS ST was verified when it is simulating the CCS converter transformer used by ITER. Initially it was submit to verifications that model some of the typical tests for transformers (like no-load and short-circuit test). The results of these verifications have been compared with the datasheet results of the corresponding tests. The comparison reveals that the model well represent this transformer in several balanced load conditions.

Then, in order to verify the robustness of SPS ST model in situations different from the reported in the datasheet, a model of the same transformer was built using SPS SC software. The behavior of this model was firstly verified with same the verifications already done for the previous SPS ST model and comparing the results. Subsequently the two models were submit to other non-usual load conditions and the resulting currents has been compared. In these comparisons the two models are very similar even if some time they do not act exactly in some way. The emerging difference is due to some essential approximations done to calculate the input data of the magnetic characteristic for SPS ST model. However it is usually very small with respect to the total quantity of the two measurement and often is negligible.

Since the results in the verifications done on the SPS ST model are coherent respect to the expected one, then the realized model has a validity. Moreover, during some verifications the model reveals itself stronger than the SPS SC model. This justifies and confirms the choice of using SPS ST to build the transformer’s model.

In order to be more sure about the value of the model, some other studies need to be done. Surely one of them is a deep analysis of Simscape settings. As a matter of fact, the numerical errors that some time occurs are probably due to a not too much precise setting of the Simulink® solver. After this detailed study, if this kind of problem remains, developing a work in collaboration with The MatWorks Inc. would be useful to solve this issue. Another possible study development would be some physical tests on a real transformer. Indeed, it is possible to verify the numerical data coming from the comparison of the SPS ST and SPS SC models. Moreover, with these real tests it is possible to improve the approximations of the magnetic characteristic and thus in the two models differences should not be present anymore.

Finally another way to develop and to improve the model is to introduce the core magnetic hysteresis loops consideration. Indeed in this thesis this aspect is marginally considered because the data about it were leaking or were not precise. Introducing the hysteresis in the transformer’s model, it could be possible to better analyze the saturation phenomena and the

electric behavior of the transformer. To do this it should just be necessary to have the hysteresis characteristic curve of the transformer’s core and to elaborate it with the Hysteresis Designer tool of SPS ST. Then the designed curve can be used in the model inputting it the block where the saturation is considered.

Acknowledgments

I would like to thank the Hyosung Corporation (www.hyosung.com) for granting permission to use the manufacturing data of a HYOSUNG transformer to verify the validity of the approach described in this thesis.

In addition, I would like to thank the team of the ITER Electrical Engineering Division, for the suggestions and the evaluation received during the development of my work.

I would also like to thank Dr Antonio De Lorenzi of IGI-CNR for the indications received about the delta-extended winding connection and for reviewing my manuscript.

Finally, I wish to express my warm thanks for their helpful welcoming in the laboratory to all the members of the Electric Power Systems group of the Department of Industrial Engineering of the Padova University, in particular dr Massimiliano Coppo and Andrea Savio.

References

- [1] ITER Organization, “About ITER,” [Online]. Available: <http://www.iter.org/proj/inafewlines>. [Accessed 28 06 2016].
- [2] I. B. J. Tao, J. K. Goff, A. Mankani, F. Milani, I. Song, H. Tan and J. Thomsen, “ITER Coil Power Supply and Distribution System,” in *2011 IEEE/NPSS 24th Symposium*, 2011.
- [3] ITER, “Design and modeling of main components, A79DNG,” 2012.
- [4] N. Mohan, T. M. Undeland and W. P. Robbins, "Elettronica di Potenza. . Convertitori e applicazioni", Hoepli, 2005.
- [5] C. Sewan, L. Bang Sup and N. E. Prasad, “New 24-Pulse Diode Rectifier Systems for Utility Interface of High-Power AC Motor Drives,” *IEEE TRANSACTIONS ON INDUSTRY APPLICATIONS*, VOL. 33, NO. 2, 1997.
- [6] M. Olivier, "*Development of a Model for Simulating the Transformer Saturation Effect on the Voltage Transients at ITER*", Padova, 2016.
- [7] W. Jiaopu, Q. Haihong, W. Shishan and Z. Bo, “Basic Connections and Strategies of Isolated Phase-Shifting Transformers for Multipulse Rectifiers: A Review,” 2012.
- [8] IEC, IEC 60076-1:2011 "Power Transformers".
- [9] B. Wu, High-power converters and AC drivers, Wiley-Interscience.
- [10] Private communication from the ITER Organization
- [11] The MathWorks, Inc., Simscape Power System User's Guide (Simscape Components), 2016.
- [12] Hydro-Québec, Simscape Power Systems Reference (Specialized Technology), The MathWorks, Inc., 2016.
- [13] M. Andriollo, G. Martinelli e A. Morini, "Trasformari, teoria ed esercizi", Padova: Libreria Cortina, 2010.
- [14] Hydro-Quebec, Simscape Power System User's Guide (Specialized Technology), The MathWorks Inc, 2016.
- [15] Teshmont Consultants LP, Transformer Modelling Guide, Calgary, Alberta, 2014.
- [16] “Wikipedia,” [Online]. Available: https://en.wikipedia.org/wiki/Per-unit_system. [Accessed 6 May 2016].
- [17] MathWorks, "Three-Phase Three-Limb (Core-Type) Two-Winding Transformer," [Online]. Available: <http://it.mathworks.com/help/phymod/sps/examples/three-phase-three-limb-core-type-two-winding-transformer.html>. [Accessed 14 June 2016].

- [18] A. D. Theocharis, J. Miliias-Argitis and T. Zacharias, “Three-Phase Transformer Model Including Magnetic Hysteresis and Eddy Currents Effects,” *IEEE Transaction on power delivery*, vol. 24, 2009.
- [19] R. Benato e L. Fellin, *Impianti Elettrici*, Padova: Utet Scienze Tecniche, 2011.
- [20] Xi'an XD Transformer Co., Ltd., “Manufacture Readiness Review for PF Rectifier Transformer”.
- [21] J. Hurng-Liahns, J.-C. Wu and W. Kuen-Der, "*Analysis of Zig-Zag Transformer Applying in the Three-Phase Four-Wire Distribution Power System*", IEEE, 2005.
- [22] F. de Leòn and J. Martinetz, ““Dual Three-Winding Transformer Equivalent Circuit Matching Leakage Measurements”,” in *IEEE TRANSACTIONS ON POWER DELIVERY*, VOL. 24, IEEE, 2009, pp. 160-165.
- [23] C. E. Lin, J.-B. Wei and C.-J. Huang, *New Model for Transformer Saturation Characteristics by Including Hysteresis Loops*, IEEE, 1989.
- [24] F. de Leòn, P. Gòmez, J. Martinetz and M. Rioual, “Transformers,” in *Power System Transients: Parameter Determination*, pp. 177-247.
- [25] J. Wang and R. Lascu, "Zero Sequence Circuit of Three-legged Core Type Transformers".
- [26] I. Harlow and J. Harlow, "Electric Power Transformer Engeneering", James H. Harlow, 2004.
- [27] J. Martinez-Velasco, *Power System Transient*, 2010.

Figures

Figure 1.1: Conventional 12-pulse system	3
Figure 1.2: Scheme of a 12-pulse converter with ED-d transformer.....	4
Figure 2.1: Extended-delta windings on a three-limb transformer.....	6
Figure 2.2: Phasor voltage diagram.....	7
Figure 2.3: Shifted primary phasor diagram.....	8
Figure 2.4: B phasor as sum of phasors D and E.....	10
Figure 2.5: Negative phase-shift phasor diagram.....	11
Figure 2.6: Phasor diagram with phase connection exchanging	12
Figure 3.1: Linear Transformer block parameters.....	14
Figure 3.2: Three-Phase Transformer block parameters	14
Figure 3.3: mono-phase equivalent electric circuit of a transformer (with two secondary)...	15
Figure 3.4: Error with 2 ideal transformer connected together	15
Figure 3.5: Configuration tab of Three-Phase Transformer block	16
Figure 3.6: Simscape Foundation Library Electromagnetic Converter block	17
Figure 3.7: Electromagnetic converter dialog box	18
Figure 3.8: Simscape Foundation Library Controlled MMF Source.....	18
Figure 3.9: Un-masked resistance dialog control.....	19
Figure 3.10: Masked resistance with custom dialog control	19
Figure 3.11: Parameters Mask Editor.....	19
Figure 3.12: Initialization parameters in Mask Editor.....	20
Figure 4.1: Simplified circuit scheme of Correction Coil supply system	22
Figure 4.2: Magnetizing characteristic of CCS transformer as given by the manufacturer, courtesy of the Hyosung Corporation (A Korean company supplying products to the ITER Project.)	24
Figure 4.3: Extended-delta/delta subsystem dialog control parameters (illustrative values) .	25
Figure 4.4: Mask parameters name of extended-delta/delta subsystem	26
Figure 4.5: Parameter initialization syntax in extended-delta/delta subsystem.....	27
Figure 4.6: Mono-phase ideal B former transformer.....	27
Figure 4.7: Transformer D parameters	28
Figure 4.8: Transformer E parameters.....	29
Figure 4.9: B former transformer subsystem.....	30
Figure 4.10: Three B former transformers	30
Figure 4.11: Connection of the three B former transformers	31
Figure 4.12: Ideal phase-shifter subsystem	31
Figure 4.13: Delta/delta configuration of three-phase transformer block	32
Figure 4.14: Delta/delta transformer block parameters	33
Figure 4.15: Extended-delta/delta subsystem connections.....	34
Figure 4.16: Extended-delta/delta subsystem mask	34
Figure 4.17: Mono-phase equivalent circuit.....	35
Figure 4.18: Mono-phase equivalent circuit in per units.....	35
Figure 4.19: Mono-phase equivalent circuit of extended-delta/delta created model.....	36
Figure 4.20: Script for calculus of transformers parameters	37

Figure 4.21: Example of script output in MatLab command window	39
Figure 4.22: Numerical parameters editing (illustrative values).....	40
Figure 4.23: Name variables editing (illustrative values)	40
Figure 4.24: Saturable mono-phase equivalent circuit.....	40
Figure 4.25: Transformer dialog box without saturation settings	41
Figure 4.26: Transformer dialog box with saturation settings	41
Figure 4.27: Saturation characteristic setting.....	41
Figure 4.28: Magnetization characteristic with the Φ - i_μ pairs	43
Figure 5.1: SPS's verification circuit	45
Figure 5.2: Measurements' blocks	46
Figure 5.3: Triplet Shift subsystem.....	47
Figure 5.4: Measured phase-shift, an example with 15° set	48
Figure 5.5: Circuit for no-load and short-circuit verification.....	48
Figure 5.6: Measured power in no-load simulation	49
Figure 5.7: No-load RMS primary currents	49
Figure 5.8: Voltage source dialog box	50
Figure 5.9: Secondary resistance dialog box	50
Figure 5.10: Measured power in short-circuit simulation.....	50
Figure 5.11: On load verification circuit.....	51
Figure 5.12: Measured power with a resistance load of S_n	52
Figure 5.13: Power losses with nominal power adsorption	53
Figure 5.14: Primary on-load current.....	53
Figure 6.1: Extended-delta/delta physical magnetic (pink) and electrical (blue) circuit	57
Figure 6.2: Zoom of reluctance in parallel with Electromagnetic converters.....	58
Figure 6.3: Zoom on one phase of primary winding.....	59
Figure 6.4: Zoom on one phase of secondary winding	59
Figure 6.5: Electric equivalent scheme of the magnetic circuit	60
Figure 6.6: Iron reluctance model subsystem (left) and expanded (right)	60
Figure 6.7: Mask of the SPS Simscape Component transformer's model.....	61
Figure 6.8: Dialog box of built block.....	62
Figure 6.9: SPS Simscape components transformer's block initialization parameters tab.....	63
Figure 6.10: SPS Simscape Components verification circuit	64
Figure 6.11: Simulink® measurement circuit for physical model.....	65
Figure 6.12: Physical model voltages phase-shift.....	65
Figure 6.13: Physical model measured no-load losses.....	66
Figure 6.14: Physical model short-circuit losses	66
Figure 6.15: Physical model on-load verification results.....	67
Figure 6.16: SPS Specialized Technology model on-load verification results	68
Figure 6.17: Primary currents in phase A for SPS Specialized Technology model (red) and for physical model (blue) in discrete time mode	69
Figure 6.18: 120 seconds of in-rush current in the physical model (blue) and in the SPS ST model (red).....	70
Figure 6.19: In-rush current in the interval 0-0,1 [s].....	70
Figure 6.20: In-rush current in the interval 20-20,1 [s].....	71
Figure 6.21: In-rush current in the interval 119.9-120 [s].....	71
Figure 6.22: SPS SC z-sequence generator.....	73

Figure 6.23:SPS ST z-sequence generator	73
Figure 6.24: Signal of control of z-sequence generators	73
Figure 6.25: Z-sequence verification loads in the two models.....	74
Figure 6.26: Primary current of phase A in z-sequence verification of physical model (blue) and of SPS ST model (red).....	74
Figure 6.27: Magnitude of current in z-sequence verification	75
Figure 6.28: Controlled DC surge in the two models	76
Figure 6.29: Primary current of phase A with 2 [MA] direct current	77
Figure 6.30: Primary current of phase B with 2 [MA] direct current.....	77
Figure 6.31: Primary current of phase C with 2 [MA] direct current.....	77
Figure 6.32: Primary current of phase A with 24 [kA] direct current	78
Figure 6.33: Primary current of phase B with 24 [kA] direct current	79
Figure 6.34: Primary current of phase C with 24 [kA] direct current	79
Figure 6.35: Phase A zoom at 1[s] with 24 [kA] DC fault.....	80
Figure 6.36: Phase A zoom at 1.5 [s] with 24 [kA] DC fault.....	80
Figure 6.37: Phase A zoom at 6 [s] with 24 [kA] DC fault.....	81
Figure 6.38: Primary current of phase A with 0.4 [kA] direct current	82
Figure 6.39: Primary current of phase B with 0.4 [kA] direct current	82
Figure 6.40: Primary current of phase C with 0.4 [kA] direct current	82
Figure 6.41: Phase A zoom at 6 [s] with 0.4 [kA] DC fault.....	83
Figure 6.42: Breaker blocks in the two models	84
Figure 6.43: Current in the phase A during phase-to-phase fault.....	84
Figure 6.44: Current in the phase B during phase-to-phase fault.....	85
Figure 6.45: Current in the phase C during phase-to-phase fault.....	85
Figure 6.46: Zoom of the current in the phase A at the moment of the fault	86